University of Alberta

A Lab and Field Scale Evaluation of Reducing Landfill Greenhouse Gas Emissions with a Methane Oxidizing Biofilter

by

Andrew Philopoulos 

A thesis submitted to the Faculty of Graduate Studies and Research in partial fulfillment of the

requirements for the degree of Master of Science

in

Environmental Engineering

Department of Civil and Environmental Engineering

Edmonton, Alberta
Fall 2006

Your file Votre référence
ISBN: 978-0-494-22344-4
Our file Notre référence
ISBN: 978-0-494-22344-4

Abstract

Landfills are a significant contributor to global methane emissions, with many sites emitting un-treated landfill gas (LFG) into the atmosphere. A treatment approach is to passively vent landfill gas through a methane oxidizing biofilter, which contains a porous medium that facilitates the growth of methanotrophic bacteria. In a lab-scale experiment, two substrates, yard-waste compost and a sand-compost-perlite mixture were evaluated as potential biofilter mediums. The long-term (218 days) removal rates showed that both mediums were capable of removing 100% of the methane influent flux (134 $gCH_4 \cdot m^{-2} \cdot d^{-1}$). A field-scale trial was undertaken by installing three biofilters at the Leduc and District Regional Landfill (AB). Yard-waste compost was used as the biofilter medium. The results showed that two sites performed well, as low surface emissions (< 15 $gCH_4 \cdot m^{-2} \cdot d^{-1}$) were generally observed. The third site showed low calculated methane influent flows (< 5 $gCH_4 \cdot m^{-2} \cdot d^{-1}$), and therefore observations of performance were limited.

Acknowledgement

The study has been produced with the assistance of the Green Municipal Enabling Fund and the Leduc and District Regional Waste Management Authority. The Green Fund is financed by the Government of Canada and administered by the Federation of Canadian Municipalities. Nothwithstanding this support, the points of view expressed are those of the author(s) and in no way incur liability of the Federation of Canadian Municipalities nor the Government of Canada.

Special thanks to my supervisors: Dr. Daryl McCartney and Dr. Christian Felske.

For Chapter 2, the lab-scale experiment, special thanks to Juliane Ruck, who initially setup the experiment. Thanks to the technical staff in the Environmental Engineering Department at the University of Alberta: Nick Chernuka, Maria Demeter, and Gary Solonynko. Thanks to Dr. Patrick Hettiaratchi and Dinishi Jayasinghe, from the University of Calgary, for conducting the methane oxidation potential test.

For Chapter 3, the field-scale experiment, special thanks to Ulf Raesfeld for his assistance in constructing the pilot biofilters. Also thanks to the Alberta Research Council technical staff: Frances De Jong and Darrel Reid.

Table of Contents

List of Tables

List of Figures

List of Symbols

BD – Bulk Density

CN – Total Carbon to Total Nitrogen Ratio

D-Glucose – Dextrose Glucose

DI – Deionized Water

dS – Deci Siemens

EPS – Expolymeric Substance

ER – Evolution Rate

GC – Gas Chromatography

GS – Garden Sand

ID – Inter Diameter

IR – Infrared Radiation

LDPE – Low Density Polyethylene

LFG – Landfill Gas

MC –Moisture Content

MOP – Methane Oxidation Potential

MSW – Municipal Solid Waste

OM –Organic Matter

PD - Particle Density

PPMV – Parts Per Million Volumetric Basis

PSD – Particle Size Distribution

PVC – Poly Vinyl Chloride

RuMp – Ribulose Monophosphate

SAR – Surface Area Ration

SCP – Sand Compost Perlite

SE – Standard Error

TAS – Total Air Space

TDR – Time Domain Reflectometry

TMECC – Test Methods for the Evaluation of Compost and Composting

USGA – United States Gold Association

UWS – Un-Washed Sand

Vol. - Volumetric

WS – Washed Sand

1 Introduction

1.0 Methane as a Greenhouse Gas

Ultraviolet light, produced from the sun, is absorbed and reflected from the earth's surface as longer wave infrared radiation (IR) (VanLoon and Duffy 2000). Greenhouse gases that are in the earth's atmosphere, such as water, carbon dioxide (CO_2), ozone, nitrous oxide, and methane (CH_4), absorb and reflect the IR back towards the earth's surface, thus playing an important role in planetary temperature and climate change. In particular, CH_4 is a potent greenhouse gas, and when compared to CO_2 has 21 times the global warming potential over a 100 year horizon. Table 1.1 shows the worldwide CH_4 emissions from natural and anthropogenic sources. The largest source is from natural wetlands, while ruminants (methane producing livestock) and energy related (seepage from natural gas operations) are major anthropogenic contributors. A major sink of methane emissions is tropospheric oxidation by the hydroxyl radical, which accounts for the removal of 510 $TgCH_4 \cdot a^{-1}$ (Whalen 2005).

Table 1.1. Global Sources of Methane Emissions (Whalen 2005)

Natural	Emissions ($TgCH_4 \cdot a^{-1}$)
Wetlands	145
Termites	20
Oceans	15
Hydrates	10
Total natural	**190**

Anthropogenic	Emissions ($TgCH_4 \cdot a^{-1}$)
Rice	80
Ruminants	115
Landfills	40
Wastewater treatment	25
Biomass burning	40
Energy-related	110
Total anthropogenic	**410**

2.0 Landfill Gas Generation

Landfills are also a major contributor of methane emissions, accounting for 10 (as shown in Table 1.1) to 17 % (Wuebbles and Hayhoe 2002) of global anthropogenic emissions. Landfills produce methane as a result of the anaerobic biodegradation of the organic fraction of the waste. After oxygen has been consumed in the buried waste, a reducing environment initiates a three stage breakdown process (Tchobanoglous et al. 1993). First, large complex compounds such as proteins, carbohydrates, and lipids, are broken down by enzyme mediated hydrolysis to monomer units, such as amino acids and glucose. Second, the monomer unit compounds are fermented by bacteria into short-chain fatty acids (propionate, butyrate, and acetic acid), hydrogen, and carbon dioxide. Third, methanogenic bacteria reduce the carbon dioxide (Eq. 1) and acetic acid (Eq. 2) into methane, utilizing hydrogen and water as the electron donors (Brock and Madigan 1991):

[1] $4H_2 + CO_2 + H_2O \longrightarrow CH_4 + 3H_2O$

[2] $CH_3COOH + H_2O \longrightarrow CH_4 + CO_2 + H^+$

Theoretically, landfill gas (LFG) is mainly composed of CO_2 (88%) and smaller concentrations of CH_4 and N_2 in the first three months after the closure of a landfill cell (Tchobanoglous et al. 1993). After 1.5 years, the gas is composed mainly of equal volumes of CH_4 and CO_2. In practice this will vary considerably as a result of several factors, including the distribution of the organic waste, available nutrients, moisture content, and the degree of compaction.

3.0 Methane Oxidation

Methane oxidizing bacteria have been found in landfill cover soils as a result of migrating LFG. These methanotrophic bacteria, a subset of one-carbon oxidizing methylotrophs, are ubiquitous in aerobic soils as a result of global CH_4 concentrations of 1.75 ppmV (Whalen 2005). Methane oxidation can be shown as:

[3] $CH_4 + 2O_2 \longrightarrow CO_2 + 2H_2O$ + biomass + heat

In practice the stoichiometric coefficients for O_2 and CO_2 have been found to range between 0.2-1.8 and 0.2-0.9 respectively (Stepniewski and Pawlowska 1996). The biochemical transformation of methane is shown (Brock and Madigan 1991):

[4] CH_4 (Methane) $\longrightarrow$ CH_3OH (Methanol) $\longrightarrow$ HCHO (Formaldehyde) $\longrightarrow$ HCOOH (Formate) $\longrightarrow$ CO_2 (Carbon Dioxide)

Methanotrophs are differentiated from other methylotrophic bacteria by their ability to oxidize methane, using the methane monooxygenase enzyme. This enzyme introduces oxygen into the CH_4 molecule to produce methanol. The production of formaldehyde is used for carbon assimilation via two pathways. Type I methanotrophs use the more energetically favorable ribulose monophosphate pathway (RuMP), while type II use the serine pathway. Another subset, type X, are known to use primarily the RuMP pathway, but also possess small concentrations of enzymes used in the serine pathway.

4.0 Current Research

Traditionally, flaring and energy conversion technologies have been employed to treat methane. For smaller landfills these options can be both technically and economically un-feasible as a result of lower LFG generation and concentrations. The application of a biofilter presents a cost-effective alternative to treat LFG. Hilger and Humer (2003) reported that 10 to 100 % of migrating methane emissions through landfill cover soils have been oxidized by methanotrophic bacteria (not by design). Therefore, the possibility exists to integrate a biofilter into the landfill cover to enhance the methane oxidation process and treat LFG. A biofilter consists of several components, including a mechanism to trap the LFG (such as a geomembrane, or gas collection system), a gas distribution layer, and a medium. The biofilter medium is a porous medium that facilitates the movement of the LFG and supports the growth of the methane oxidizing bacteria. The current investigation, as will be seen in Chapters 2 and 3, was focused on developing an approach to integrate a methane oxidizing biofilter into a landfill cover. Chapter 2 will present the results from a lab-scale experiment, where two substrates, compost and a sand-compost-perlite mixture, were evaluated as potential biofilter mediums. The research questions were:

1. Can a sand based medium, developed with a turfgrass standard, be as effective as compost at treating methane?

2. Will using a sand based medium reduce settlement when compared to compost? How will this affect the results?

3. Will the formation of exopolymeric substance, by the methanotrophic bacteria, have an effect on methane removal rates?

Chapter 3 will present the results from a field installation of three pilot biofilters at the Leduc and District Regional Landfill (AB). The scope of the investigation was to evaluate the biofilter design used and the research questions were:

1. Can 80 % of CH_4 emissions be removed by the pilot biofilters?

2. Can temperature (>20°) and moisture (>0.25 $L \cdot L^{-1}$) levels be adequate to support the methane oxidizing bacteria?

Chapter 4 summarizes the results from the two experiments.

5.0 References

Brock, T. D., and Madigan, M. T. 1991. Biology of microorganisms. Englewood Cliffs, NJ.

Hilger, H., and Humer, M. 2003. Biotic landfill cover treatments for mitigating methane emissions. Environmental Monitoring and Assesment **84:** 71-84.

Stepniewski, W., and Pawlowska, M. 1996. Chemistry for the protection of the environment 2. Plenum Press, New York, NY.

Tchobanoglous, G., Theisen, H., and Vigil, S. 1993. Disposal of solid wastes and residual matter. Irwin McGraw-Hill, USA.

VanLoon, G. W., and Duffy, S. J. 2000. Environmental chemistry. Oxford University Press, New York, NY.

Whalen, S. C. 2005. Biogeochemistry of methane exchange between natural wetlands and the atmosphere. Environ. Eng. Sci. **22:** 73-87.

Wuebbles, D. J., and Hayhoe, K. 2002. Atmospheric methane and global change. Earth-Science Reviews **57:** 177-210.

2 Lab-Scale Comparison of Compost and Sand-Compost-Perlite as Methane Oxidizing Biofilter Mediums

1.0 Introduction

Methane (CH_4) is a greenhouse gas that is 21 times more effective than carbon dioxide (CO_2) at influencing climate change (Whalen 2005). Global atmospheric methane concentrations (1.75 ppmV) have increased by a factor of 2.5 over the last 200 years (Whalen 2005). Methane gas is generated mostly from worldwide anthropogenic sources (68 %) such as natural gas production, rice fields, and landfills. The latter has been reported to account for 10 (Whalen 2005) to 17 % (Wuebbles and Hayhoe 2002) of worldwide anthropogenic methane emissions. Municipal solid waste (MSW) landfills produce gas, in the methanogenic phase, that is composed of equal volumes of CH_4 and CO_2, as a result of the anaerobic degradation of the organic fraction of the waste.

Methanotrophic bacteria, ubiquitous in aerobic soils including landfill covers, oxidize CH_4 as a source of energy and carbon. Methanotrophs are characterized by their carbon assimilation pathways. Type I use the ribulose monophosphate (RuMp) pathway, while type II use the serine pathway (Hanson and Hanson 1996). Type X methanotophs have also been identified and use primarily the same carbon assimilation pathway as type I, but also posses small concentrations of enzymes that are part of the serine pathway. The methane oxidation reaction can be described as:

[1] $CH_4 + 2O_2 \longrightarrow CO_2 + 2H_2O + \text{biomass} + \text{heat}$

The role methanotrophs play in reducing methane emissions in landfill cover soils has been examined. Current attention has been focused on enhancing this process to further reduce CH_4 emissions. One approach is to passively vent landfill gas (LFG) through a biofilter. A biofilter is a system in which the main component consists of a medium that hosts the methanotrophs, with the aim to provide the best physical, chemical, and biological conditions for a high level of activity. Other components of a biofilter depend on the approach to passively vent the LFG through the medium. For example, the medium could be integrated into the landfill cover, or could be connected to a LFG collection system.

Many lab-scale experiments have been conducted to determine the effect of environmental conditions such as temperature, moisture content (MC), pH, and electrical conductivity (EC) on methane oxidation rates. Optimal temperatures of 15-30°C have been reported for a garden waste compost (Mor et al. 2006), and 25-30°C for a sandy loam (Boeckx and Van Cleemput 1996). The respective optimum MC values of those mediums were 0.45-0.85 $g \cdot g^{-1}$ and 0.15 $g \cdot g^{-1}$ (dry basis). The optimal MC has been observed to increase with higher soil organic matter (Christophersen et al. 2000; Mor et al. 2006), since the water holding capacity was also assumed to increase. Gebert et al. (2003) reported that salt concentrations resulting in EC greater than 6 $dS \cdot m^{-1}$ caused a decrease in oxidation rates in an expanded clay medium. Bender and Conrad (1995) found pH values between 6.7-8.1 yielded the highest oxidation rates in four soils from agricultural and forest origins.

The focus of the current investigation was to develop a suitable biofilter medium. Table 2.1 shows several biofilter mediums that have been evaluated, and the removal rates that have been achieved. The mineral based mediums follow the textural classification outlined by Edmonds (2000). In many cases an initial peak oxidation rate was observed, followed by a lower steady state value (Table 2.1). In three cases the authors (Hilger et al. 2000; Streese and Stegmann 2003; Wilshusen et al. 2004a) attributed the decline to the formation of exopolymeric substance (EPS). EPS is a slime layer produced by methanotrophs, and is mainly composed of polysaccharides. The formation of EPS was thought to reduce the mass transfer of O_2 and CH_4 as a result of coating the microbes and the surrounding pore space (Hilger et al. 2000). It has been demonstrated that increasing the ratio of O_2 to CH_4 increases the quantity of EPS produced, while lowering the oxidations rates (Chiemchaisri et al. 2001; Wilshusen et al. 2004b). Chiemchaisri et al. (2001) attributes the production of EPS as a defense mechanism to reduce oxygen concentrations. Wilshusen et al. (2004b) attribute the majority of the EPS production to type I methanotrophs, which are more dominant in aerobic environments (O_2 concentrations of 0.105 $L \cdot L^{-1}$), as a mechanism to cycle carbon to synthesize biomass with less nitrogen (as it becomes limiting). Type II methanotrophs were reported to be able to fix atmospheric nitrogen. They further demonstrated that peak oxidation rates were re-achieved by mixing the leaf and manure compost. They found mixing the biofilter medium every 30 days allowed for the breakage of EPS agglomerates, and improved the removal rates.

Table 2.1. Biofilter Mediums and Removal Rates

Author	Medium	Duration (d)	Influent Flux ($gCH_4?m^{-2}?d^{-1}$)	CH_4 Removal (% of Influent Flux)	
				Peak	End of Experiment
Gebert and Grongroft (2006)	Crushed Expanded Clay	480	1920	100%	N/A
Felske and Widmann (2004)	Silt	250	144	100%	100%
Wilshusen et al. (2004a)	Leaf and Manure Compost	220	400	100%	28%
Streese and Stegman (2003)	Mixture of Yard Compost, Peat and Wood Fibres (equal volumes)	340	1040	31%	18%
Hilger et al.(2000)	Sandy Loam	40	281	38%	21%
Humer and Lechner (1999b)	MSW Compost	59	166	100%	100%
Kightley et al. (1995)	Sand	180	273	72%	61%

Gebert and Grongroft (2006) have shown the highest methane removal rates (1920 $gCH_4 \cdot m^{-2} \cdot d^{-1}$) in the literature thus far (Table 2.1). They attributed the high removal rates to favorable conditions such as non-limiting mass transfer, adequate moisture and nutrient content, as well as non-degradable filter material. The expanded clay used was a porous medium, with 0.83 $L \cdot L^{-1}$ porosity, in which 71% of the pore volume consisted of pores that were larger than 50 μm. Kightley et al. (1995) found higher removal rates (with the same influent flux shown in Table 2.1) with sand (166 $gCH_4 \cdot m^{-2} \cdot d^{-1}$), than with loamy sand (112 $gCH_4 \cdot m^{-2} \cdot d^{-1}$), and a sandy loam (109 $gCH_4 \cdot m^{-2} \cdot d^{-1}$). They attributed the better removal rates to the coarser texture of the sand, which would result in better gas transport, and to the nutrient supply of each medium. Wilshusen et al. (2004a) found better long-term oxidation rates (110 $gCH_4 \cdot m^{-2} \cdot d^{-1}$), using the same influent flux as

shown Table 2.1, in a leaf and manure compost (< 5 mm), than in woodchip compost (< 25 mm), and MSW compost (< 10 mm). They attributed the better performance in the leaf and manure compost to the finer and more homogeneous particle sizes, resulting in more porosity and surface area for mass transfer and reactive sites.

Several studies have compared mineral and organic soils respectively, as well as mineral and organic soil mixtures as biofilter mediums. Humer and Lechner (1999a) found better removal rates with MSW compost, than with a mixture of sewage sludge compost (0.70 $g \cdot g^{-1}$, dry basis) and sand (0.30 $g \cdot g^{-1}$, dry basis), using the same influent flux as shown in Table 2.1. However, the sewage sludge compost and sand mixture did achieve the same removal rate (166 $gCH_4 \cdot m^{-2} \cdot d^{-1}$) as the compost at the end of the experiment. Felske and Widmann (2004) found better long-term removal rates with a silty soil (shown in Table 2.1), than with a bio-waste compost (97 % removal of 96 $gCH_4 \cdot m^{-2} \cdot d^{-1}$ influent flux). They attributed the lower removal rates in compost to the formation of EPS, and increased microbial competition (respiration increased from 0.33 to 24.11 $mgO_2 \cdot g^{-1}$, dry basis). It is possible in this case that the EPS may have become a substrate for other aerobic microorganisms.

The physical characteristics of a potential biofilter medium are important in minimizing settlement and therefore maintaining the pore structure. Screening materials to one size specification is one way to achieve better physical characteristics. Another is to use a particle size distribution (PSD) standard, however, none have been recommended in the literature. One standard that can be used was developed by the United States Golf Association (USGA). The USGA has developed a PSD specification for root zone mixtures, used for putting greens (USGA 2004). The standard is used to optimize air

penetration, water retention and drainage, and minimize compaction to enhance turfgrass growth. To achieve this, the standard calls for a minimum sand content of 0.60 $g \cdot g^{-1}$ (dry basis). Organic soils, such as peat and compost, are normally added to fertilize the turfgrass mixture. The USGA PSD was thought to be suitable in developing a biofilter medium, since similar characteristics are desired.

1.1 Current Research

The scope of the current investigation was to develop a biofilter medium for a field-scale application. In the current research a sand-compost-perlite (SCP) and 100% compost mediums were compared. From the literature there have been mixed results when direct comparison between sand and compost has been made. The SCP mixture was mostly composed of sand (0.80, 0.18 and 0.018 $g \cdot g^{-1}$, dry basis, sand, compost, and perlite), and was based on the USGA standard since similar material characteristics are desired. On the one hand, the main advantage of using sand is that it was expected to settle and compact less than compost. This implies that physical characteristics, such as porosity, would be better maintained. On the other hand, compost has been well established as a potential biofilter medium, as shown in Table 2.1. Compost is composed of organic matter and nutrients that enhance microbiological growth.

Compost was used in the SCP mixture to provide a methanotrophic seed, as well as to improve the nutrient and water holding characteristics. Perlite, an inorganic amendment, was added to further improve the physical characteristics of the mixture. Perlite is a uniform, porous material with good water retention characteristics and insulating properties (Williams and Taylor 1998).

Both mediums were filled into respective columns and were fed simulated LFG in an upflow manner. The mediums were applied a methane load of 134 $gCH_4 \cdot m^{-2} \cdot d^{-1}$, that was expected in a field trial, for 218 days. There were three objectives for this experiment. First, was to determine whether the SCP mixture, developed based on the USGA standard, was as effective as compost at removing the influent CH_4 flux. Second, was to determine which medium compacted more and whether this affected the results. Settlement in the columns was measured and material properties, such as bulk density (BD) and total air space (TAS), were analyzed before and after the experiment. Third, was to determine whether EPS production, measured after the column operation, had an effect on the methane removal rates. Furthermore, several other properties (pH, EC, total carbon and nitrogen) were analyzed before and after the experiment to gain insight into any changes that occurred in the mediums as a result of the column operation.

2.0 Materials and Methods

2.1 Medium Selection and Characterization

Compost was used in one column as the filter medium. The compost was taken from an open windrow operation at the Leduc and District Regional Waste Management Authority's landfill site. The source of the compost was from a local separation program and was composed mostly of yard-waste. The compost was turned twice per month for six months and then was left to cure for one year. The compost was then passed through a 1.27 cm screen.

The second column was filled with the SCP mixture. The sand portion was composed of three different sands (Tee Bar Sod Farms Ltd., Edmonton, AB): washed sand (WS), un-

washed sand (UWS), and garden sand (GS). The PSD of the WS met the USGA specifications, however the UWS and the GS were added to increase the finer soil fraction (<0.15 mm). Finer silt and clay particles, which were more abundant in the UWS and GS, can provide more surface area for bacterial growth. As a result, the sand in the SCP mixture contained 0.67, 0.17, and 0.17 $g \cdot g^{-1}$ (dry basis) WS, UWS, and GS respectively. The Leduc yard-waste compost, previously described, was used in the SCP mixture. The perlite (Tee Bar Sod Farms Ltd., Edmonton, AB) used was of medium grade (2-3.4 mm). The final SCP mixture was prepared using ratios of 0.80, 0.18, and 0.02 $g \cdot g^{-1}$ (dry basis) sand-mix, compost, and perlite respectively.

Each medium was mixed manually in a respective pile. The pile was then split into four quadrants. Two quadrants were selected to fill the columns, while 30 L of that remaining was used for characterization and placed in a sealed container in cold storage (4°C). Moisture was added to the compost and the sand mixture, since both were thought to be in the lower range for supporting biogenic activity. The MC of the compost was adjusted to 0.31 $g \cdot g^{-1}$ (wet basis) by adding water and mixing manually. Similarly, the MC of the sand mixture was adjusted to 0.10 $g \cdot g^{-1}$ (wet basis).

Several material property testing procedures used are outlined in Table 2.2, while the remaining are described herein. For each test method, the material placed in the cold storage container was thoroughly mixed, and the appropriate sample quantity was taken. The PSD for SCP was conducted using sieves with pore openings of 4.76, 2, 0.85, 0.425, 0.25, 0.15, and 0.075 mm. The PSD for compost was conducted using sieves with pore openings of 6.3, 4, 2, 0.85, 0.425, and 0.25 mm. The BD of SCP was determined by dividing the weight added to the column by the volume filled. The TAS and porosity

were calculated as described by Ball and Smith (2001). The total carbon and nitrogen (CN) analysis was conducted with a Leco® TrueSpec CN Carbon/Nitrogen Determinator (Leco Co., St. Joseph, MI). Before the analysis, samples (10 g) were air dried for 24 h at 36°C, and were then passed through a 1 mm screen. Two compost samples, and one SCP sample were analyzed for CN. Norwest Labs (Edmonton, Alberta) conducted the compost maturity analysis. The method is based on the Test Method for the Evaluation of Composting and Compost (TMECC) 05.08-B Carbon Dioxide Evolution Rate (2002). However, Norwest Labs conducted the test over one day rather than four, citing that the extended duration does not significantly affect the results. Two compost samples were analyzed for maturity.

Table 2.2. Material Testing Procedures

Property	Compost	SCP	# of Samples
PSD	02.02-B Sample Sieving For Aggregate Size Classification (TMECC 2002)	47.4 Sieve Analysis (Mechanical Method) (Sheldrick and Wang 1993)	2
MC	03.09-A Total Solids and Moisture (TMECC 2002)	51.2 Gravimetric Method With Oven Drying (Topp 1993)	3
BD	03.01-A Quick Test for Bulk Density, Porosity/Pore Space, Free Airspace and Water Holding Capacity of Compost (TMECC 2002)	-	3
PD	Specific Gravity of Soil Solids (Das 2002)		3
OM	05.07-A Loss on Ignition Method (TMECC 2002)		3
pH	04.11-A 1.5: Slurry pH (TMECC 2002)	16.3 Soil pH in 0.01 $CaCl_2$ (Hendershot et al. 1993)	3
EC	04.10-A 1.5: Slurry Method, Mass Basis (TMECC 2002)	18.2.4 Fixed-Ratio Extract (Janzen 1993)	3

2.2 *Column Setup and Operation*

The columns (55 cm ID, 182 cm depth) used, shown in Figs. 2.1 and 2.2, were constructed out of steel, and allowed for viewing through a plexiglass window. A gas mixture, composed of 0.60 and 0.40 $L \cdot L^{-1}$ CH_4 and CO_2 respectively, was used to simulate the methanogenic phase of LFG generation and was fed from a cylinder (Praxair Inc., Edmonton, AB). The gas was moistened by feeding it through of a 10 L Nalgene® carboy, filled with 3 L of water. From the carboy, the simulated LFG was supplied to the bottom of each column. The simulated LFG was fed at a rate of 0.06 $L \cdot min^{-1}$, which corresponded to a methane application rate of 134 $gCH_4 \cdot m^{-2} \cdot d^{-1}$ (see Appendix A for calculation). This was similar to the expected influent flux in a field-scale biofilter trial (Zeiss 2002). The first stage of the column (bottom) was composed of 0.32 m drainage stones (Red River Soils Ltd., Winnipeg, MB), used to distribute the LFG over the entire area of the filter. Any leachate that was generated during the column operation was not removed, and therefore remained in the gas distribution layer. The next stage consisted of the loosely filled biofilter medium (1.25 m). The filter depth was selected to be as close as possible to that used in a field-scale biofilter trial (1.5 m). The compost and SCP columns were filled with 1.37 and 1.27 m of material respectively, to account for settlement. A geotextile was used between the gravel and filter material to prevent mixing. The final stage of the column (top) was used as headspace (0.25 m) to simulate atmospheric air. Air was fed into the headspace at a rate of 0.4 $L \cdot min^{-1}$, which was in the range used by other researchers who setup similar columns (Kightley et al. 1995; Felske and Widmann 2004). Effluent gas was collected at the top of the columns, in Plenum® tubing, passed through a rotameter to measure flow, and then released into an exhaust vent.

Fig. 2.1. Column Design (Not to Scale)

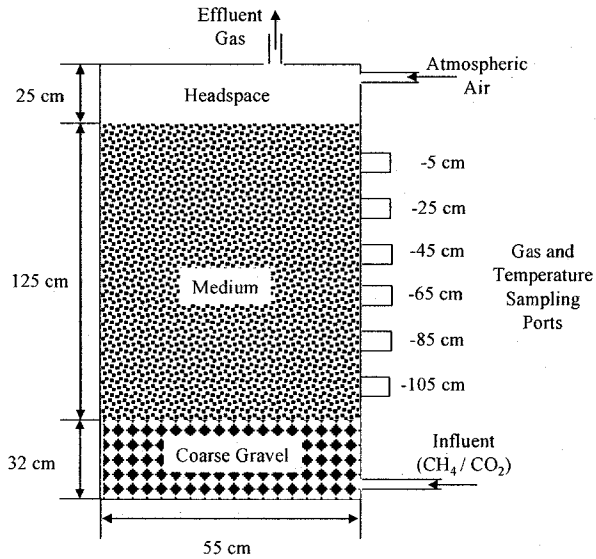

Fig. 2.2. Picture of Column Setup

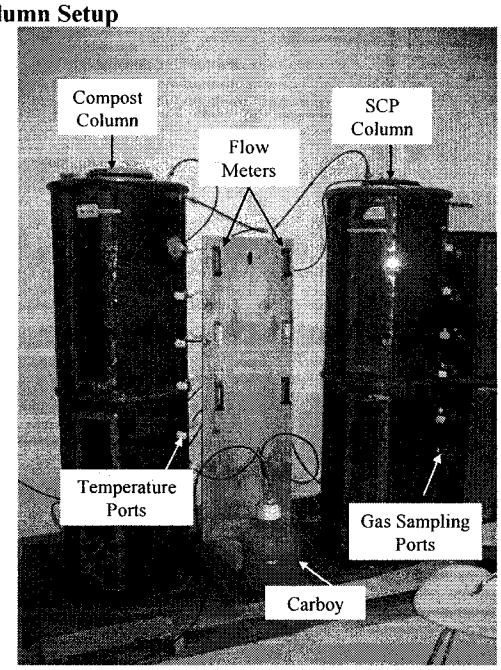

To monitor gas composition and temperature, sampling ports were constructed 20 cm apart, and were located at the -5, -25, -45, -65, -85, and -105 cm depths from the surface of the filter bed (Figs. 2.1 and 2.2). Temperature ports were constructed out of PVC end

caps, which could be opened to allow for the insertion of the temperature probe. Temperature was also monitored in the headspace of each column (through the atmospheric air influent connector). Gas sampling ports consisted of steel tubing (ID: 0.156 cm) that was placed through the center of a PVC end cap (separate from the temperature port). The interior portion of the steel tubing extended to center of the column. Low density polyethylene (LDPE) tubing was connected to the exterior end of the steel tubing. Gas samples could be collected through the LDPE tubing, which could be opened and closed with a thumb screw clamp. Additional gas samples were collected from the inflow (after the carboy) and outflow of each reactor. The inflow tubing (Plenum®) had a T connection, with one section going to the column, and the other going to a needle valve. The outflow sample could be collected from the effluent tubing.

Gilmont® rotameters (Barnant Co., Barrington, IL), equipped with needle valves, were used to control atmospheric air (range: 0.1 to 1 $L \cdot min^{-1}$) and LFG (range: 0.05 to 0.1 $L \cdot min^{-1}$) influents. The effluents from each column were measured using Cole Palmer® (Anjou, QC) rotameters (range: 0.04 to 0.5 $L \cdot min^{-1}$). Column temperatures (range: -250 to 287°C) were analyzed using a 60 cm, type T, thermocouple probe (Digi-Sense®, Vernon Hills, IL), and a HH21 microprocessor thermometer (OMEGA Engineering Inc., Stamford, CT). All gas samples were collected using 2L Tedlar bags (Fisher Scientific Co., Ottawa, ONT), and analyzed with a CP-2003P (Varian Inc., Pao Alto, CA) micro gas chromatography (GC) instrument, equipped with a thermal conductivity detector. A CP_Molsieve 5A column (110°C, 152 kPa, 110 s run time) was used to analyze O_2 (range: 0 to 0.30 $L \cdot L^{-1}$), N_2 (range: 0 to 0.80 $L \cdot L^{-1}$), and CH_4 (range: 0 to 0.80 $L \cdot L^{-1}$), while a HayeSep A (50°C, 152 kPa, 110 s run time) column was used to analyze CO_2 (range: 0 to 40 $L \cdot L^{-1}$). A previous calibration was verified by using standard samples.

Each standard was made directly from a cylinder of a known volumetric concentration or by mixing gases at the same temperature and pressure. Standard gas samples, such as atmospheric air, the simulated LFG, and a mixture of CH_4, CO_2, and N_2 (1, 1, and 98 % respectively), were used to verify the calibration curve each time the instrument was used. High purity Helium (0.99999 $L \cdot L^{-1}$ He) was used as the carrier gas. Varian Star (version 5.50) software was used to operate the GC instrument and view the results.

The columns were operated for 218 days, from June 2nd, 2005 until January 25th, 2006. The columns were operated at room temperature (20°C). From September 6th (day 97) until September 19th (day 110), the columns were only fed atmospheric air while waiting for parts for repair. Sampling events were conducted 69 times over the length of the experiment (approximately twice per week). The sampling procedures used in the experiment are outlined in Table 2.3. Usually a full (influent, effluent, and 6 ports) and a partial (influent and effluent only) gas analyses were conducted once per week respectively.

Table 2.3. Column Sampling Procedure

Step	Description
1	The effluent flow was recorded.
2	The effluent gas sample was collected. The sample bag was placed on the effluent tubing connector. The sampling bag was opened after allowing the effluent flow to purge the air in the headspace for a few seconds. The sample was collected for two minutes.
3	Gas samples were collected from the six ports, starting at the -5cm depth, and then proceeding to the next one. The port clamp was opened and a syringe was used to flush the port by drawing column air. The sample bag was placed on the port connector and the gas sample was collected as described in step #2.
4	The influent gas sample was collected. The sample bag was placed on the connector and the needle valve was opened. The gas sample was collected as described in step #2.
5	Temperature measurements were collected starting with the headspace and then to the downward sampling ports. The tip of the thermocouple probe was inserted into the center of the column. Temperature was recorded once the thermometer reading had stabilized.
6	Gas samples were analyzed with the GC instrument. This was always done on the same day as the sampling event. Standard samples were run to ensure the calibration curve was valid. Gas was pushed out of the sample bags to purge air from the headspace, prior to connecting to the GC. Samples were normally analyzed in triplicate.

The methane influent and effluent flows could be calculated as:

[1] $$J_{CH4} = \frac{\rho \times Q \times C_{CH4}}{A}$$

where J_{CH4} ($gCH_4 \cdot m^{-2} \cdot d^{-1}$) is the influent or effluent flux, ρ ($g \cdot m^{-3}$) is the density of CH_4 as calculated with the ideal gas law, Q ($m^3 \cdot d^{-1}$) is the influent or effluent flow, C_{CH4} ($m^{-3} \cdot m^{-3}$) is the influent or effluent concentration of methane, and A is the surface area of the medium (0.24 m^2). From Eq.1 a mass balance could be used to determine the percentage of CH_4 removed:

[2] $$CH_4 \text{ Removed } (\%) = \frac{Jin_{CH4} - Jout_{CH4}}{Jin_{CH4}} \times 100$$

where the subscripts in and out denote the influent and effluent CH_4 flux respectively. Sample calculations are included in Appendix A.

2.3 Post-Experiment Analysis

After completion of the experiment, the columns were dismantled to conduct a post-experiment analysis. Each medium was removed in six 20 cm depth segments respectively (5-25, 25-45, 45-65, 65-85, 85-105, and 105-125 cm), as well as the top 5 cm was removed as one segment. A quartering method was used to make three sub-samples from each depth segment. The material removed from each respective segment was placed in a pile on a tarp, as shown in Fig. 2.3. The material was mixed manually and then divided into four quadrants (Fig. 2.3a). Two quadrants were selected randomly (Fig. 2.3b), based on random numbers generated in Microsoft® Excel, and were re-mixed into a new pile (Fig. 2.3c). The mixing, dividing into four quadrants, and randomly selecting two quadrants steps were repeated until the desired sub-sample size (1 L) was remaining (Fig. 2.3d). Similarly, the same quartering method was used to obtain each aliquot-sample, used for analysis, from the respective sub-sample. Both sub-samples and aliquot-samples were placed in cold storage (4°C).

Fig. 2.3. Quartering Method for Sub-Sample Selection

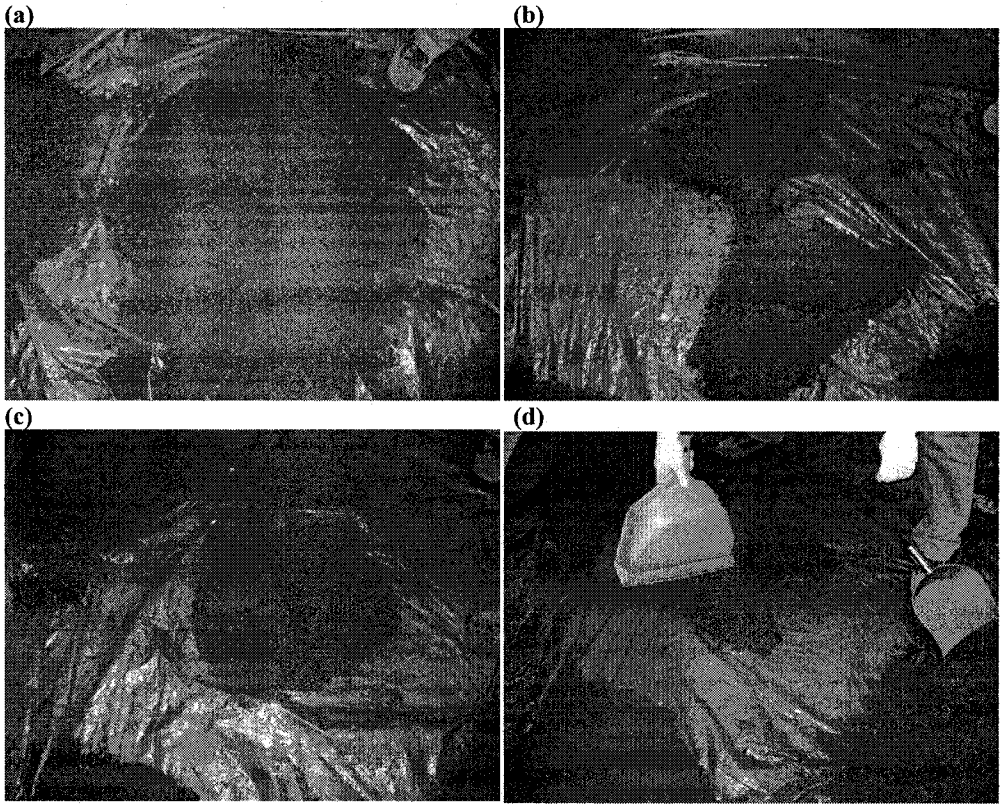

Each segment was analyzed for BD, MC, PD, pH, EC, and CN. Table 2.4 shows the number of sub-samples analyzed, for each respective depth segment, for each material property. The BD was determined by dividing the weight of the segment removed by the volume occupied. The MC, PD, pH, conductivity, and CN were determined as described in Table 2.2. In addition, the labile polysaccharides and methane oxidation potential were determined. The labile polysaccharides was determined as described by Lowe (1993), and was used as an estimate of the quantity of EPS in the mediums. In this method, a hydrolysis procedure was used to convert the soil sample labile polysaccharides to saccharide monomers. The dextrose glucose (D-Glucose) content of the sample, used to estimate the labile polysaccharides content, was then measured by a colorimetric method using a phenol-sulfuric acid reagent. The methane oxidation

potential (MOP) was measured at the University of Calgary. Samples (10-12 g) from both columns were analyzed in duplicate from the 5-25, 25-45, and 45-65 cm depth segments. MC was not adjusted, and ranged from 0.287-0.325 and 0.128-0.153 $g \cdot g^{-1}$ (wet basis) for compost and SCP respectively, during the test. The samples were placed in 260 ml airtight dark glass bottles, which were sealed with Teflon-Silicon septa caps. Methane (15 ml) was injected at initial headspace concentrations of 0.06-0.09 $L \cdot L^{-1}$, and the bottles were then incubated at 22°C until the headspace CH_4 concentration was less than 0.01 $L \cdot L^{-1}$, or approximately 24 hrs had surpassed. Gas samples (2 ml) were drawn from the bottles and analyzed for CH_4, CO_2, and O_2 using GC, generally every 2-4 hrs. Depending on the results, the data were fitted either to zero (linear) or first (exponential) order kinetic models. The zero order model show's that the substrate (CH_4) is not limiting, while the first order model show's that the sample is substrate (CH_4) limiting.

Table 2.4. Post-Experiment Sampling Quantities

Property	Depth Segments	Sub-Samples per Depth Segment Analyzed[a]
MC	All	3
PD	All	1
pH	All	2
EC	All	2
CN	All	2
Labile Polysaccharides	All	2
MOP	5-25, 25-45 and 45-65 cm	1

[a]Sub-samples analyzed in duplicate aliquot-samples respectively

3.0 Results

The PSDs of SCP and compost are shown Fig. 2.4. The USGA PSD specification for the root zone mixture for golf course putting greens is also shown in Fig. 2.4. The SCP mixture met the USGA criteria, with the exception that there are some coarser particles (3 % greater than 3.4 mm) that are not specified in the standard. The compost was coarser in texture, however, the sieve analysis was conducted on a wet basis (and then dried for reporting on a dry weight basis), as per TMECC 02.02-B. Conducting the sieve analysis on a wet basis likely resulted in larger particle agglomerates, and therefore made the PSD coarser in texture.

Fig. 2.4. PSD of Mediums Compared to the USGA Specification

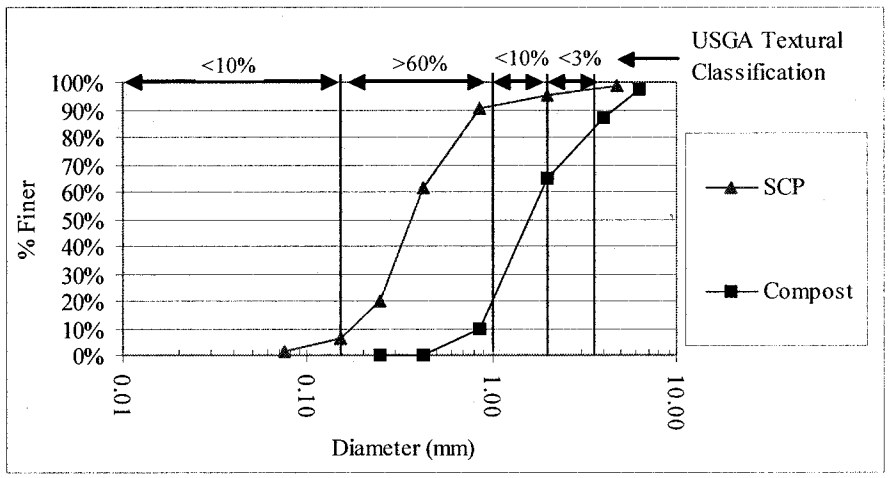

The properties of the two mediums, including the standard error (SE), are summarized in Table 2.5. Both the compost and SCP mediums were porous with large TAS values. Both mediums contained nutrients in organic and nitrogen forms. Both had near neutral pHs and low EC. The compost, which is from the same origin in both mediums, was mature as compared to the Canadian Council of Ministers of the Environment compost

standard (< 4 mgC-$CO_2 \cdot g^{-1}OM \cdot d^{-1}$) (CCME 2005). The initial MC was larger for compost than SCP. The compost was more porous and therefore it was assumed that it had a larger water holding capacity.

Table 2.5. Compost and SCP Properties

Property	Compost	SE	SCP	SE
MC ($g \cdot g^{-1}$, wet basis)	0.31	0.0035	0.15	0.006
BD ($g \cdot L^{-1}$, wet basis)	772.48	6.56	1273.12	-
Porosity ($L \cdot L^{-1}$)	0.69	-	0.49	-
TAS ($L \cdot L^{-1}$)	0.45	-	0.31	-
OM ($g \cdot g^{-1}$, dry basis)	0.20	0.0011	0.05	0.00015
Total Carbon ($mg \cdot g^{-1}$, dry basis)	88.80	1.36	17.63	-
Total Nitrogen ($mg \cdot g^{-1}$, dry basis)	8.35	0.05	1.44	
CN	10.64	-	12.24	-
pH	7.14	0.011	7.22	0.008
EC at 20°C ($dS \cdot m^{-1}$)	2.18	0.014	0.82	0.011
Maturity ($mgC\text{-}CO_2 \cdot g^{-1}OM \cdot d^{-1}$)	2.00	0.28	-	-

Methane removal rates are shown in Fig. 2.5 for both mediums, with 100% removal equating to the treatment of 134 $gCH_4 \cdot m^{-2} \cdot d^{-1}$. Both mediums showed a rapid biogenic acclimation phase, as 100 % methane removal was achieved on day 5. For the first 96 days monitored, the compost showed near constant 100% removal, while the SCP fluctuated. From day 111 onward, both mediums showed near 100% removal rates.

Fig. 2.5. Methane Removal Rate

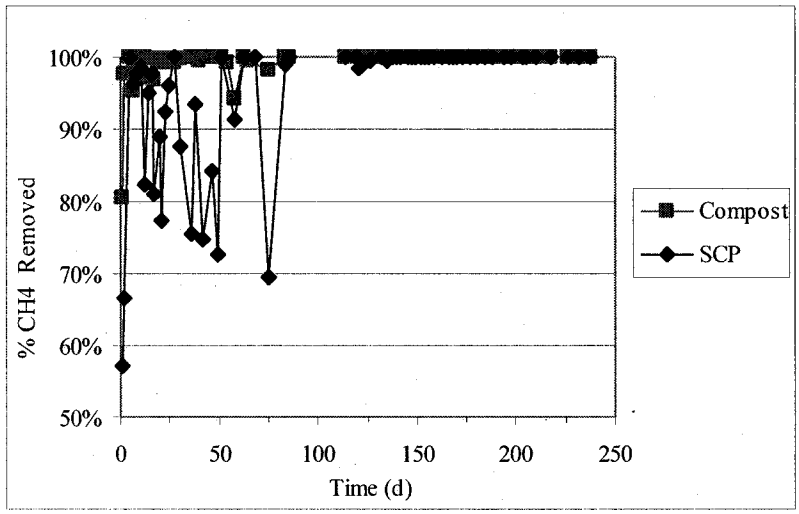

Figure 2.6 shows the gas profiles for SCP and compost for days 1, 166, and 238. On day 1 (Figs. 2.6a and 2.6b) both columns showed atmospheric oxygen penetration beyond the -25 cm depths. The gas composition analyses for the lower depths of compost, on day 1, were not determined due to a malfunction with the GC instrument. Both mediums, on days 166 (Figs 2.6c and 2.6d) and 233 (Figs. 2.6e and 6f), showed near anaerobic conditions below the -25 cm depth. Since oxygen was consumed, this indicated that the majority of methane oxidation was occurring in the top 25 cm of both mediums. The concentrations of CH_4 and CO_2 are being reduced in the lower depths (below -25 cm depth) as a result of dilution, mixing with the penetrating nitrogen gas.

Fig. 2.6. SCP and Compost Gas Profiles

(a) SCP day 1 **(b) Compost day 1**

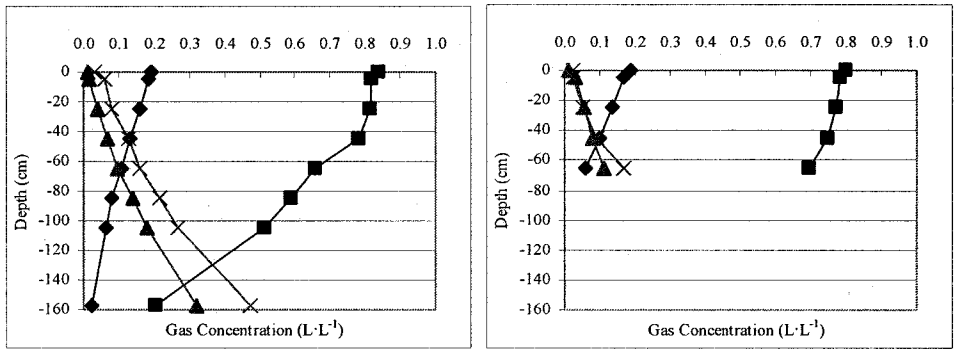

(c) SCP day 166 **(d) Compost day 166**

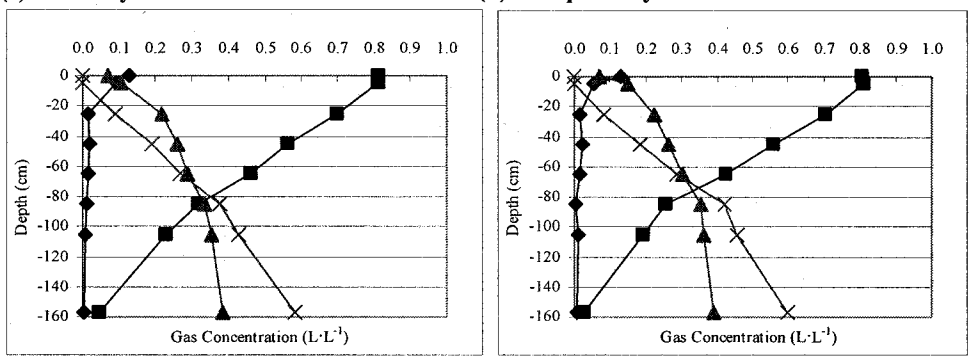

(e) SCP day 238 **(f) Compost day 238**

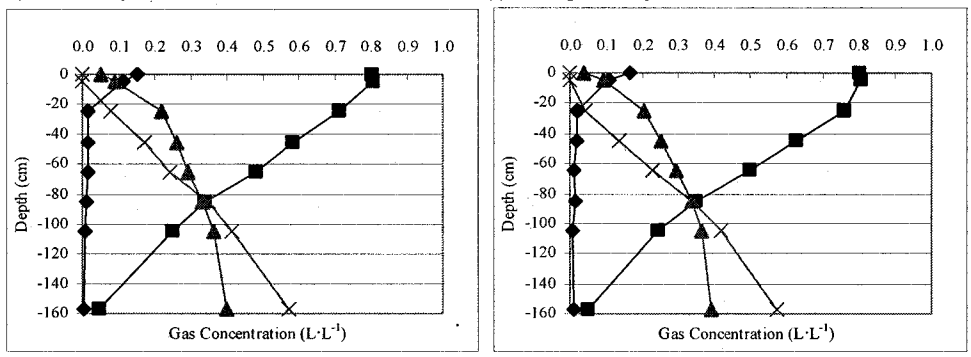

The average temperature results are shown in Fig. 2.7. Both columns showed maximum temperature at the -25 cm depth. Biogenic methane oxidation is an exothermic process, and therefore the temperature profile indicated that the majority of the activity was occurring around the -25 cm depth.

Fig. 2.7. Average Temperature Profiles of SCP and Compost

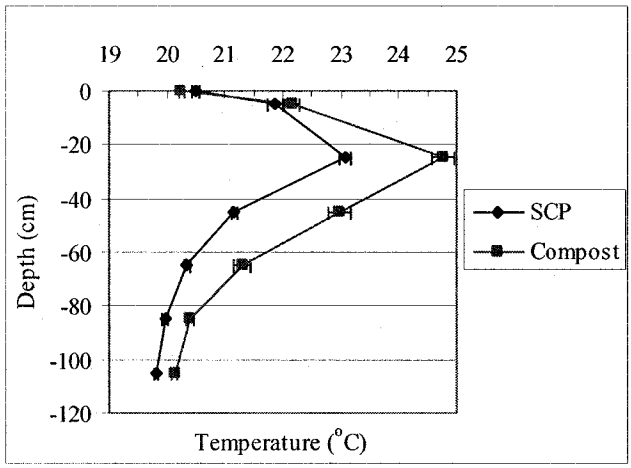

Note: SE bars are shown; some SE may be too small to be visible.

Figure 2.8 shows the post-experiment results for BD, TAS, and MC, including the initial values prior to the start of the column operation. The BD (Fig. 2.8a) for SCP remained relatively constant with depth, with an increase in the bottom layer measured (-95 cm). This was in contrast with compost, which showed increasing BD with depth, with the exception at the -95 cm depth. The observed settlement was 3 cm for SCP, and 6.5 cm for compost. The observed settlement occurred prior to the start of the influent LFG feed, and occurred over 2-3 days. No further settlement was observed. The MC profiles (Fig. 2.8b), at the -15 cm depth, show a maximum value for compost, and an increase for SCP over the starting value. The TAS profiles (Fig. 2.8c) show generally a reduction for both mediums from the initial value, with that in compost being larger. TAS will decrease as a result of increases in MC and BD. The latter changed more dramatically in the compost medium, and was therefore the main cause for the decrease in TAS. A value of zero TAS was assigned for compost at the -75 cm depth, as the calculated value was negative. This was most likely caused by inaccuracies in measuring the bulk density. A

source of error may have been not using a level instrument when removing each respective depth segment.

Fig. 2.8. Post-Experiment BD, TAS, and MC Profiles of SCP and Compost

(a) BD

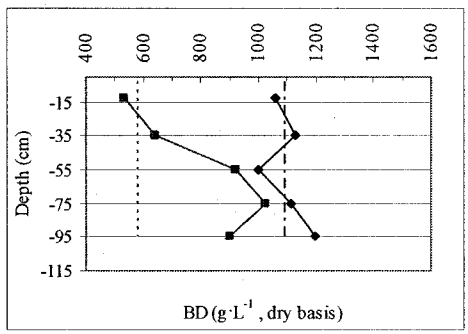

(b) MC

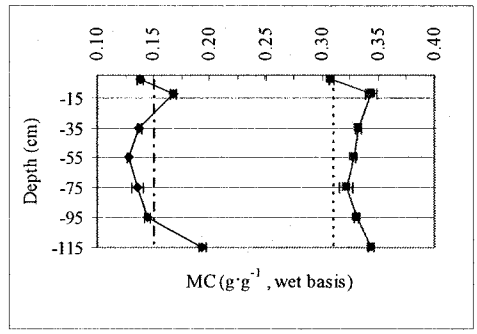

(c) TAS

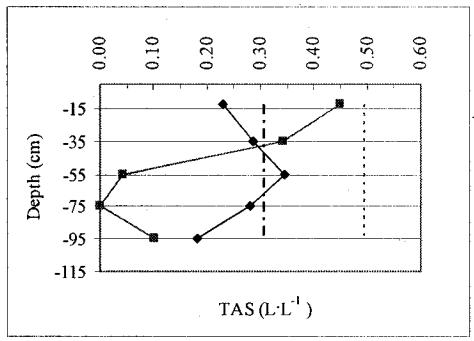

Note: Fig. 2.8b shows SE bars; some SE may be too small to be visible.

SCP — Starting Value for SCP — Compost ····· Starting Value for Compost

Figure 2.9 shows the post experiment profiles for pH, EC, total carbon, and total nitrogen, including the initial values. The pH profiles (Fig. 2.9a) show a rising trend with increasing depth for both SCP and compost, with the latter being more pronounced. The pH values at the -2.5 cm depth, for both mediums, were lower than the initial values. The EC profiles (Fig. 2.9b) show a decrease in the initial values for both mediums. The compost, from the -35 cm depth to the bottom, showed a larger drop in EC from the initial values than SCP. The total carbon and nitrogen profiles (Figs. 2.9c and 2.9d), for

both mediums, shows maximum values at the -15 cm depth. In particular, the total nitrogen of compost at the –15 cm depth increased 25 % from the starting value. The total nitrogen content of the SCP had decreased from the starting value at all depths.

Fig. 2.9. Post-Experiment pH, Conductivity, Total Carbon, and Total Nitrogen Profiles of SCP and Compost

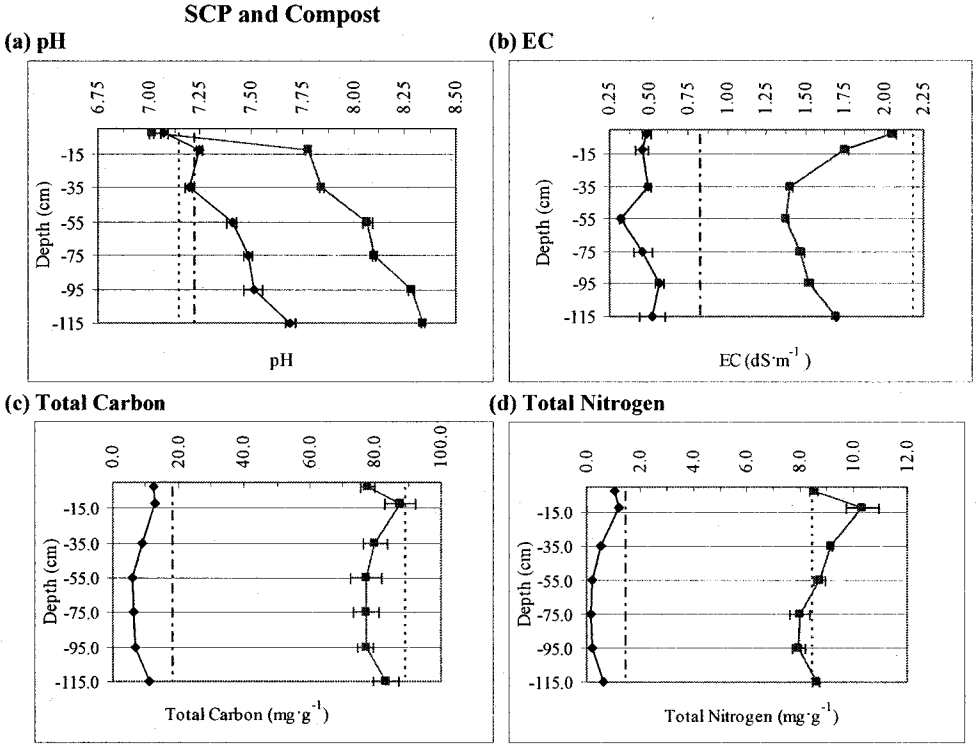

Note: SE bars are shown; some SE may be too small to be visible.

Table 2.6 shows the first order kinetic MOP results, which indicated that the initial headspace concentration (0.06-0.09 $LCH_4 \cdot L^{-1}$) used in the test resulted in substrate (CH_4) limitation for the bacteria. The results are shown as per gram of OM per day. Both mediums showed the highest oxidation rates at the -12.5 cm depth, with that measured in SCP being larger than compost. Furthermore, they show decreasing oxidation rates with increasing depth. The -55 cm depth for SCP showed zero order kinetic MOP results,

which indicated that the substrate (CH_4) was not limiting at the initial headspace concentration of methane used (0.06-0.09 $LCH_4 \cdot L^{-1}$). The oxidation rate for the -55 cm depth was 910.4 (SE = 47.2) $\mu molCH_4 \cdot gOM^{-1} \cdot d^{-1}$.

Table 2.6. Methane Oxidation Potential Results

Depth (cm)	CH_4 Oxidation Rate ($gOM^{-1} \cdot d^{-1}$)			
	SCP		Compost	
	CH_4 Oxidation Rate	SE	CH_4 Oxidation Rate	SE
-12.5	8.06	0.69	6.34	0.05
-35	3.22	0.37	3.99	0.40
-55	-	-	2.17	0.94

The labile polysaccharides profiles, used to estimate the EPS content, of both mediums are shown in Fig. 2.10. The labile polysaccharides content was approximated by the D-Glucose content of the sample. Both compost and SCP showed maximum labile polysaccharides at the -15 cm depth. The initial labile polysaccharide content of each medium was not analyzed.

Fig. 2.10. Post-Experiment Labile Polysaccharides Profiles of SCP and Compost

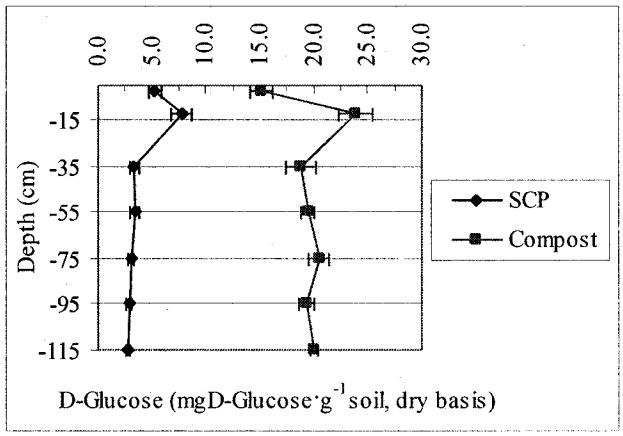

Note: SE bars are shown; some SE may be too small to be visible.

4.0 Discussion

Both compost and SCP showed a quick acclimation to the simulated LFG influent, achieving a removal rate of 134 $gCH_4 \cdot m^{-2} \cdot d^{-1}$ in five days. This was longer than the 2 days observed by Park et al. (2002) for a fertilized loamy sand (61 % removal of the 525 $gCH_4 \cdot m^{-2} \cdot d^{-1}$ influent flux), but less than the 15 days observed by Humer and Lechner (1999a) for a MSW compost (100% removal of 166 $gCH_4 \cdot m^{-2} \cdot d^{-1}$ influent flux). After the period of no simulated LFG feed, days 97 to 110, both mediums showed near 100% CH_4 removal for the remaining of the experiment (Fig. 2.5). This demonstrated that both compost and SCP are capable of removing methane fluxes expected in a field-scale biofilter. This was in contrast to previous experiments that compared mineral and organic based mediums, that found differing removal capabilities (Humer and Lechner 1999a; Felske and Widmann 2004). Those studies, however, did use slightly larger influent fluxes (144 and 166 $gCH_4 \cdot m^{-2} \cdot d^{-1}$) than the current study (134 $gCH_4 \cdot m^{-2} \cdot d^{-1}$).

After the initial acclimation phase, for the first 96 days, the methane removal rates for SCP varied between 69.6-100% (Fig. 2.5). It was unclear what caused the fluctuation; however, EPS production and microbiological competition were thought to be possible causes. As mentioned in the introduction, other authors have reported peak methane removal rates, followed by lower steady state values which have been attributed to EPS production (Hilger et al. 2000; Streese and Stegmann 2003; Wilshusen et al. 2004a). This was not the case in the current experiment, where long-term methane removal rates remained at 100%. The maximum labile polysaccharides contents observed (23.9 and 7.8 $mgD\text{-}Glucose \cdot g^{-1}$, dry basis, for compost and SCP respectively) were much lower than that reported by Wilshusen et al. (2004a), who found a maximum D-Glucose content of

150 $mg \cdot g^{-1}$ (dry basis) at the -10 cm depth in a leaf and manure compost after 220 days. However, in that study a higher influent flux rate (520 $gCH_4 \cdot m^{-2} \cdot d^{-1}$) was used, which resulted in larger removal rates (110 to 400 $gCH_4 \cdot m^{-2} \cdot d^{-1}$) and therefore possibly more EPS production. Felske and Widmann (2004) attributed competition by other non-methanotrophic aerobic bacteria as one of the reasons for a decline in the methane oxidation performance of a bio-waste compost. This was indicated by an increase in the respiration activity from 0.33 $mgO_2 \cdot g^{-1}$ (dry basis) at the beginning of the experiment, to 24.11 $mgO_2 \cdot g^{-1}$ (dry basis) at the end. In the current study the maturity of the mediums were not measured in the post-experiment analysis. However, another indication of maturity is temperature change. Both compost and SCP showed a consistent temperature profile, as shown in Fig. 2.7, throughout the experiment. An indication of competition by other non-methanotrophic microorganisms would have been changing temperature profiles, including increased temperature as a result of increased biogenic activity, which was not observed in the current study.

The steady environmental conditions of the columns allowed for the development of a methane oxidation horizon; an area where the majority of the biogenic activity was occurring. For both mediums the methane oxidation horizon was in the top 25 cm. This was indicated by the gas profiles (Figs. 2.6c-2.6f) for both mediums, which showed that oxygen was consumed in the top 25 cm. Furthermore, the methane oxidation horizon was indicated by the maximum temperatures at the -25 cm depth, and the largest MC, total carbon and nitrogen, MOP, and labile polysaccharides values at the -15 cm depth. Similarly, others have found methane oxidation horizons in the top 10 to 30 cm in column experiments (Kightley et al. 1995; Hilger et al. 2000; Wilshusen et al. 2004a).

The MOP test yielded zero and first order results at the initial headspace concentrations used (0.06-0.09 $LCH_4 \cdot L^{-1}$). Since the zero order kinetics indicated that CH_4 was not limited, the results showed that there was a smaller active population of methane oxidizing bacteria in SCP at the -55 cm depth, than all other samples analyzed. The first order results (Table 2.6) show that there was a more active population of methane oxidizing bacteria at the -12.5 cm depth in both mediums. The oxidation rate for SCP (8.06 $gOM^{-1} \cdot d^{-1}$) was higher than compost (6.34 $gOM^{-1} \cdot d^{-1}$) at that depth, which indicated a more active population in SCP. The expression of the oxidation rate per gram of OM allows for the normalization to a comparable unit, since compost (0.20 $g \cdot g^{-1}$, dry basis) contained more OM than SCP (0.05 $g \cdot g^{-1}$, dry basis). The larger oxidation rate in SCP may have been caused by more optimal environmental conditions, such as the initial headspace CH_4 concentration (0.086 and 0.065 $L \cdot L^{-1}$ for SCP and compost respectively) and MC (0.14 and 0.29 $mg \cdot g^{-1}$ (wet basis) for SCP and compost respectively). Comparing oxidation rates at the optimal MC and using the same initial CH_4 headspace concentration would have allowed for a better comparison of which medium achieved a better MOP result.

The compost medium became compacted with depth, as showed by the BD profile (Fig. 2.8a). The compaction and increased MC (Fig. 2.8b) resulted in a decrease in the TAS (Fig. 2.8c). The SCP profile, by contrast, showed less BD and TAS changes. This demonstrated that the usage of a sand based medium, following the USGA PSD specification, resulted in less compaction than that observed in compost. However, this did not affect the methane removal rates of either medium. In a field-scale trial though, traffic on the biofilter's surface (maintenance and measurements) may result in more

compaction than observed in the lab-scale experiment. This could cause a larger decrease in TAS than observed in the current experiment, and cause lower removal rates.

The temperature profiles (Fig. 2.7) showed maximum values for both mediums at the -25 cm depth, as a result of the microbial activity. At the -25 cm depth, compost (24.8°C) retained warmer temperatures than SCP (23.1°C). There are several possibilities for the differences in temperatures observed, including quantities of heat released from biogenic origins (including methane oxidation and compost self-heating), and the thermal properties of the mediums. In particular, the thermal values of the mediums are of importance since in a field application they will be exposed to ambient temperatures. In Alberta, this means exposure to cold winter temperatures that can drop below freezing for prolonged periods. Determining the heat capacity and heat conductivity would allow for a better evaluation of which medium is a better insulator, and therefore more suitable for a colder climate.

The total carbon and nitrogen contents were largest at the -15 cm depth (Figs. 2.9c and 2.9d), for compost and SCP. Kightley et al. (1995) found the highest total carbon (20 $mg \cdot g^{-1}$, dry basis) and nitrogen (2 $mg \cdot g^{-1}$, dry basis) values at the -20 cm depth, in sand amended with sewage sludge. This was expected since 19-69% of methane oxidized has been found to be assimilated into biomass (Whalen et al. 1990). Atmospheric nitrogen fixation was the likely reason for the 25% increase in total nitrogen at the -15 cm depth in compost. Type II methanotrophs have been shown to be capable of fixing atmospheric nitrogen (Wilshusen et al. 2004b). Nitrogen fixation is an energy demanding process, and would indicate nitrogen limitation. The reason for the drop in the total nitrogen content in the SCP was unclear. Ammonium, nitrite, and nitrate forms of nitrogen could

be lost in leachate (Sawyer et al. 2003), which was generated in both columns but not measured. Both de-nitrification (Turner and Hummel 1992) and nitrification (Boeckx and Van Cleemput 1996) were reported to produce nitrous oxide, which could account for another loss of nitrogen due to volatilization. More insight could have been gained by analyzing the concentration of important nitrogen nutrients, such as organic nitrogen, ammonium, and nitrate, before and after the experiment. This would allow for an assessment of whether these important nutrients were becoming limiting and whether nitrogen fertilization would be required.

The pH profiles (Fig. 2.9a), for both mediums, showed a decrease in pH at the -2.5 cm depth. The two major cell biosynthesis pathways for methanotrophs, the RuMp and serine pathways, produce 0.118 and 0.102 moles of H^+ ions per mol of CH_4 oxidized respectively (Hilger and Humer 2003). Therefore, a decrease in pH in the methane oxidation horizon was expected, and was similar to that observed by Hilger et al. (2000), who found pH decreased from 6.4 to 5.7 in the top 2.4 cm of a sandy loam soil. At the -15 and -35 cm depths, the pH in the SCP remained similar to that at the beginning, while the pH in the compost increased. The increase in pH in the compost may be related to the atmospheric nitrogen fixation observed. Hilger et al. (2000) reported that dinitrogen fixation leads to the consumption of four protons for the production of one mol of NH_4^+, used for cell synthesis. The increased pH in the lower depths of both mediums can be attributed to a reducing environment, as a result of the absence of oxygen. This was also observed in flooded rice field soils, where increasing pH has been related to a lowering in the soil solution redox potential (Sahrawat 2005).

The EC profile of both mediums (Fig. 2.9b) showed a decrease in salinity from the starting values. Both columns generated leachate (not measured), and at the -105 cm depth showed increased MCs (Fig. 2.8b). This indicated the downward flow of moisture, which was assumed to have contained soluble salts, most likely explaining the reduction in conductivity. Gebert at al. (2003) measured the conductivity of the leachate generated from a biofilter consisting of expanded clay. The leachate reached conductivities as high as 15 $dS \cdot m^{-1}$, since the expanded clay contained a large initial salt content, before reducing to 2 $dS \cdot m^{-1}$ after 1.5 years of operation.

5.0 Conclusion

Both compost and SCP demonstrated that they can be potentially used as biofilter mediums. The long-term results showed that they were both capable of removing an influent flux of 134 $gCH_4 \cdot m^{-2} \cdot d^{-1}$. The SCP compacted less than compost, as indicated by a smaller increase in BD, though this did not affect the removal rates of either medium. However, in a field installation traffic on the biofilter medium's surface could cause further settlement and compaction in compost and cause a lowering of the removal rates. The use of the USGA PSD specification was found to be suitable when developing a sand based biofilter medium. Maximum labile polysaccharides values (used to estimate the EPS content) of 23.9 and 7.8 mgD-Glucose$\cdot g^{-1}$ (dry basis) for compost and SCP respectively were found at the -12.5 cm depth, and did not affect the performance of either medium. Measurement of several other material properties is recommended in order to further evaluate the mediums. The thermal conductivity and heat capacity values would give insight into the insulating characteristics, which is of importance in a cold northern climate. As well, an analysis of the organic nitrogen, ammonium, and nitrate

concentrations, would allow for an assessment of whether these important nutrients have become limiting.

6.0 References

Ball, B. C., and Smith, K. A. 2001. Gas movement and air-filled porosity. *In* Soil and environmental analysis. *Edited by* K. A. Smith and C. E. Mullins. Marcel Dekker Inc., New York, NY. pp. 499-538.

Bender, M., and Conrad, R. 1995. Effect of CH4 concentrations and soil conditions on the induction of CH4 oxidation activity. Soil Biology and Biochemistry **27:** 1517-1527.

Boeckx, P., and Van Cleemput, O. 1996. Methane oxidation in a neutral landfill cover soil: influence of moisture content, temperature, and nitrogen-turnover. J. Environ. Qual. **25:** 178-183.

CCME. 2005. Guidelines for compost quality. PN 1340, Canadian Council of Ministers of the Environment, Ottawa, Ont.

Chiemchaisri, W., Wu, J. S., and Visvanathan, C. 2001. Methanotrophic production of extracellular polysaccharide in landfill cover soils. Water Sci. Technol. **43:** 151-158.

Christophersen, M., Linderod, L., Jensen, P. E., and Kjeldsen, P. 2000. Methane oxidation at low temperatures in soil exposed to landfill gas. J. Environ. Qual. **29:** 1989-1997.

Das, B. M. 2002. Soil mechanics laboratory manual. Oxford University Press, New York, NY.

Edmonds, R. D. 2000. Turfgrss science and management. Delmar, Albany, NY.

Felske, C., and Widmann, R. 2004. Engineering strategies for efficient methane oxidation in landfill cover liners. Proceedings of the 19th International Conference on Solid Waste Technology and Management, Philadelphia, PA.

Gebert, J., and Grongroft, A. 2006. Performance of a passively vented field-scale biofilter for the microbial oxidation of landfill methane. Waste Manage. **26:** 399-407.

Gebert, J., Groengroeft, A., and Miehlich, G. 2003. Kinetics of microbial landfill methane oxidation in biofilters. Waste Manage. **23:** 609-619.

Hanson, R. S., and Hanson, T. E. 1996. Methanotrophic bacteria. Microbiological Reviews **60:** 439-471.

Hendershot, W. H., Lalande, H., and Duquette, M. 1993. Soil Reaction and Exchange Acidity. *In* Soil sampling and methods of analysis. *Edited by* M. R. Carter. Lewis Publishers, Boca Raton, F.L. pp. 141-146.

Hilger, H., and Humer, M. 2003. Biotic landfill cover treatments for mitigating methane emissions. Environmental Monitoring and Assesment **84:** 71-84.

Hilger, H. A., Wollum, A. G., and Barlaz, M. A. 2000. Landfill methane oxidation response to vegetation, fertilization, and liming. J. Environ. Qual. **29:** 324-334.

Humer, M., and Lechner, P. 1999a. Alternative approach to the elimination of greenhouse gases from old landfills. Waste Manage. Res. **17:** 443-452.

Humer, M., and Lechner, P. 1999b. Methane oxidation in compost cover layers on landfills. Proceedings Sardinia 1999, 7th International Waste Management and Landfill Symposium, Caliari, Italy.

Janzen, H. H. 1993. Soluble salts. *In* Soil sampling and methods of analysis. *Edited by* M. R. Carter. Lewis Publishers, Boca Raton, F.L. pp. 161-166.

Kightley, D., Nedwell, D. B., and Cooper, M. 1995. Capacity for methane oxidation in landfill cover soils measured in laboratory-scale soil microcosms. Appl. Environ. Microbiol. **61:** 592-601.

Lowe, L. E. 1993. Total and labile polysaccharide analysis of soils. *In* Soil sampling and methods of analysis. *Edited by* M. R. Carter. Lewis Publishers, Boca Raton, FL. pp. 373-376.

Mor, S., De Visscher, A., Ravindra, K., Dahiya, R. P., Chandra, A., and Van Cleemput, O. 2006. Induction of enhanced methane oxidation in compost: Temperature and moisture response. Waste Manage. **26:** 381-388.

Park, S., Brown, K. W., and Thomas, J. C. 2002. The effect of various environmental and design parameters on methane oxidation in a model biofilter. Waste Manage. Res. **20:** 434-444.

Sahrawat, K. L. 2005. Fertility and organic matter in submerged rice soils. Current Science **88:** 735-739.

Sawyer, C. N., McCarty, P. L., and Parkin, G. F. 2003. Chemistry for environmental engineering and science. McGraw Hill, New York, NY.

Sheldrick, B. H., and Wang, C. 1993. Particle Size Distribution. *In* Soil Sampling and Methods of Analysis. *Edited by* M. R. Carter. Lewis Publishers, Boca Raton, F.L. pp. 499-512.

Streese, J., and Stegmann, R. 2003. Microbial oxidation of methane from old landfills in biofilters. Waste Manage. **23:** 573-580.

TMECC. 2002. Test methods for examination of composting and compost. U.S Composting Council, Holbrook, N.Y.

Topp, G. C. 1993. Soil water content. *In* Soil sampling and methods of analysis. *Edited by* M. R. Carter. Lewis Publishers, Boca Raton, FL. pp. 541-558.

Turner, T. R., and Hummel, N. W. 1992. Nutritional requirements and fertilization. *In* Turfgrass. *Edited by* D. V. Waddington, R. N. Carrow, and R.C.Shearman. American Society of Agronomy Inc., Crop Science Society of America Inc., and Soil Science of America Inc., Madison, WI.

USGA. 2004. USGA Recommendations for a method of putting green construction [online]. Available from http://www.usga.org/turf/course_construction/green_articles/putting_green_guidelines.html [cited 27-Apr-06].

Whalen, S. C. 2005. Biogeochemistry of methane exchange between natural wetlands and the atmosphere. Environ. Eng. Sci. **22:** 73-87.

Whalen, S. C., Reeburgh, W. S., and Sandbeck, K. A. 1990. Rapid methane oxidation in a landfill cover soil. Appl. Environ. Microbiol. **56:** 3405-3411.

Williams, C. F., and Taylor, D. H. 1998. Soil conditioners for sports turf area. *In* Handbook of soil conditioner. *Edited by* A. Wallace and T. E. Richard. Marcel Dekker, New York, NY.

Wilshusen, J. H., Hettiaratchi, J. P. A., and Stein, V. B. 2004a. Long-term behavior of passively vented aerated compost methanotrophic biofilter columns. Waste Manage. **24:** 643-653.

Wilshusen, J. H., Hettiaratchi, J. P. A., De Visscher, A., and Saint-Fort, R. 2004b. Methane oxidation and formation of EPS in compost: Effect of oxygen concentration. Environ. Pollut. **129:** 305-314.

Wuebbles, D. J., and Hayhoe, K. 2002. Atmospheric methane and global change. Earth-Science Reviews **57:** 177-210.

Zeiss, C. 2002. Methane oxidation as an engineered greenhouse gas reduction method for solid waste landfills. GMEF 1130, The Federation of Canadian Municipalities, Ottawa, Ont.

3 Field-Scale Treatment of Landfill Gas with a Methane Oxidizing Biofilter

1.0 Introduction

Methane (CH_4) is 21 times more effective than carbon dioxide (CO_2) at trapping heat that is reflected from the earth's surface, and therefore plays an important role in global climate change accounting for 20 % of total greenhouses gases (Whalen 2005). Worldwide anthropogenic sources account for 68% of emissions, with natural gas production, rice fields, and landfills being major contributors. The latter has been reported to account for 10 (Whalen 2005) to 17 % (Wuebbles and Hayhoe 2002) of worldwide anthropogenic methane emissions.

Municipal solid waste (MSW) landfills produce gas, with the majority of the mixture containing equal volumes of CH_4 and CO_2 in the methanogenic phase, as a result of the anaerobic biodegradation of the organic fraction of the waste. There are four practices for an operator to deal with landfill gas (LFG): flaring, energy conversion, gas well venting, and simply covering the waste with soil. The latter two are the most economic and technically feasible solutions for smaller community landfills. With any approach some methane, which migrates through the landfill cover soil, is naturally removed by methanotrophic bacteria. These bacteria, ubiquitous in aerobic soils as a result of global methane concentrations of 1.75 ppmV (Whalen 2005), oxidize methane as described by:

[1] $CH_4 + 2O_2 \longrightarrow CO_2 + 2H_2O + \text{biomass} + \text{heat}$

Biogenic CH_4 oxidation has been found to remove 10-100% of landfill methane surface emissions (Hilger and Humer 2003). Landfill cover soils (i.e. daily cover, permanent low permeable clay covers) are typically compacted with the aim to seal the landfill body, and are not optimized to support bacteria. To support a high level of biogenic activity, a medium is required that is porous (to allow the movement of gases and air) and contains nutrients. Therefore, another cost-effective approach to treat methane is to apply such a medium (i.e. methane oxidation layer) in the landfill cover system. Two approaches, a biocover and biofilter, have been used in field-scale trials. In the biocover approach, the methane oxidation layer was applied to replace the intermediate and final landfill covers. In the biofilter approach, the LFG was either trapped by a liner or accumulated in a collection system, and then passed (passively or actively) through the biofilter medium.

Rajbhandari et al. (2006) used a thin biocover (0.3 to 0.4 m) as the temporary cover for 5 m waste lifts. A mixture of compost and tree mulch (9:1, wet weight) was used for the second waste lift, and was found to emit low methane fluxes ($< 7.9\ gCH_4 \cdot m^{-2} \cdot d^{-1}$) over one month of monitoring. Humer and Lechner (2001) used several biocover designs for a permanent cover placed over 10-15 m of MSW, at a landfill that experienced reasonably high surface emissions ($66.5\text{-}266\ gCH_4 \cdot m^{-2} \cdot d^{-1}$) despite a LFG collection system. They found that applying a 0.4 m layer of sewage sludge compost, over one year of monitoring, led to high methane surface concentrations at times (101-1000 ppmV of hydrocarbons). Another approach consisted of applying a 0.9 m layer of MSW and sewage sludge compost respectively, over 0.3 m of coarse gravel used as a gas distribution layer. This approach resulted in no methane surface concentrations

measured. Barlaz et al. (2004) used a similar biocover approach, and found low surface emissions (<15 $gCH_4 \cdot m^{-2} \cdot d^{-1}$) after more than one year of monitoring. The biocover consisted of a 0.15 m clay layer over the waste, followed by 0.15m of tire shreds, used as a gas distribution layer, and then 1m of yard waste compost.

Gebert and Grongroft (2006) passively fed LFG from a gas collection system, connected to two wells, to a biofilter for treatment. The biofilter was composed of two chambers (6 and 9 m^3), each filled with 67 cm of porous expanded clay, covered with 1.5 cm of sand, and then with 10 cm of humic topsoil covered with grass. They found the biofilter to be capable of removing 62 % of the annual methane load, with a maximum observed removal of 1920 $gCH_4 \cdot m^{-2} \cdot d^{-1}$ (in that case 100 % removal of the influent flux). The limiting factors were colder winter temperatures (the temperatures at the -5 cm depth dropped as low as -5.7^{0}C), and high fluxes which prevented atmospheric oxygen supply into the biofilter. The latter was affected by high advective LFG flows as a result of changing atmospheric pressure (Gebert and Groengroeft 2006). Flux reversals were observed on average every 20 hrs, and were attributed to the inverse relationship between the rate of change of atmospheric and LFG pressure (measured in the biofilter supply pipe).

The approach used in the current investigation was based on that used by Zeiss (2002), which was to integrate a biofilter into the landfill cover. In the current approach, shown in Fig. 3.1, the first layer consists of the MSW, followed by a gas distribution layer, and then a geomembrane, which is used as a gas barrier. An option to increase the influent landfill flux is to use a gas well, such as a PVC pipe surrounded by gravel that extends the length of the waste and that is perforated in the bottom 3-5 m. A wooden frame

contains the biofilter medium. The inner walls of the frame are also lined with a geomembrane, which is plastic welded to the other piece covering the tire shreds. The surrounding area around the frame is backfilled with cover soil. By covering the area with a geomembrane, the influent LFG is expected to flow though the biofilter medium where biogenic methane oxidation will occur.

Fig. 3.1. Biofilter Integrated Into the Landfill Cover

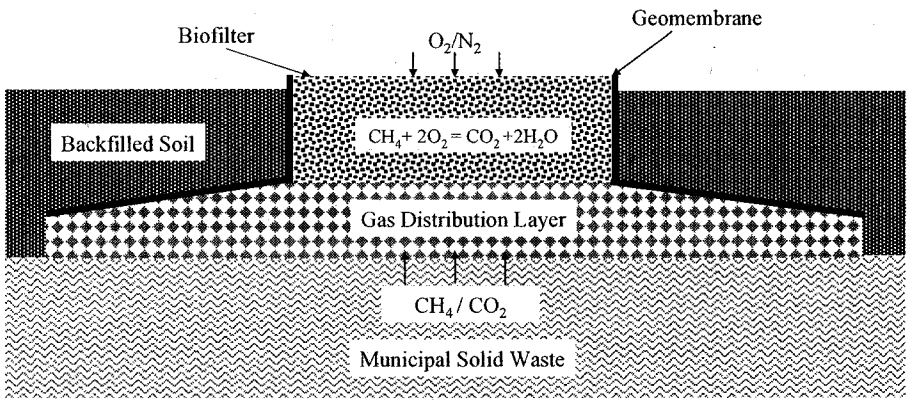

Several important design criteria in using the integrated biofilter approach include the area of waste covered, the biofilter medium and its dimensions. The biofilter surface area ratio (SAR) is described as:

[2] $$\text{Biofilter SAR} = \frac{\text{Surface Area of Waste Covered } (m^2)}{\text{Surface Area of Medium } (m^2)}$$

The ratio describes the surface area of waste covered to that of the biofilter. This ratio assists in determining the surface area of the biofilter, based on the methane flux emitted from the corresponding waste. The depth of the biofilter can then be selected to maximize the contact time between LFG, penetrating atmospheric oxygen, and the methanotrophic bacteria. The biofilter medium needs to provide the methanotrophic

seed, be biologically mature to prevent competing microbiological processes, contain nutrients, and be porous for microbial growth and gas movement.

Zeiss (2002) used a similar approach to that shown in Fig. 3.1 (no gas well) and used a biofilter SAR of 10.8. Using yard-waste compost as the biofilter medium, they found low surface emissions (< 15 $gCH_4 \cdot m^{-2} \cdot d^{-1}$) on four monitoring events. The remaining three monitoring events resulted in higher emissions, with an effluent flux of 28 $gCH_4 \cdot m^{-2} \cdot d^{-1}$ being the largest observed. The higher CH_4 surface emissions were attributed to colder biofilter medium temperatures and degradation, as well as dropping atmospheric pressure. The overall methane removal rate was estimated to be 72 %.

Temperature and moisture levels are critical biofilter operational aspects. With every subsequent 10°C increase in temperature, methane oxidation is know to increase by 2-3 fold until an optimal range is achieved (Stepniewski and Pawlowska 1996). Insufficient moisture results in slower microorganism growth as a result of limited water film (for microorganism growth) and substrate availability (since CH_4 and O_2 must dissolve in water to become bioavailable). Too much moisture will limit the distribution of LFG and atmospheric air by reducing the air space in the medium.

The scope of the current investigation was to develop an effective biofilter design. Several design factors such as the SAR and the use of a gas well were examined. Three pilot biofilters were integrated into the landfill cover at the Leduc and District Regional Landfill (AB). Two biofilters were constructed with a SAR of 10.8, with one containing a gas well, while a third site was built with a biofilter SAR of 4.8. It was anticipated that the use of the gas well would result in larger LFG influent fluxes, and therefore the effect

of this on the biofilter's performance could be examined. The biofilter surface area was increased to lower the SAR from 10.8 to 4.8, which allowed for an assessment of lowering the anticipated influent LFG fluxes on the biofilter's performance. The performance objectives were 80 % removal of the influent methane flux, and maintaining temperature and moisture levels above 20°C and 0.25 $L \cdot L^{-1}$ respectively. Surface emissions and gas composition, moisture content (MC), and temperature profiles were measured over a 10 month period.

2.0 Materials and Methods

2.1 Site Selection

The Leduc and District Regional Landfill is located 1.6 km east of the city of Leduc (AB). The landfill has been in operation since 1986, and accepts non-hazardous municipal and commercial wastes. Approximately 35,000 tones of waste are deposited yearly. The northeast section of the landfill has been filled to capacity, and has a temporary cover consisting of approximately 0.6 m of clay soil.

Site 1 was an existing biofilter constructed for the study conducted by Zeiss (2002). The site was located on a slope that contained MSW that was last active in 1995. Site 2 was located on the top of the landfill (20 m). This site was selected since it contained a gas well, consisting of a PVC pipe (0.20 m ID). It was actively being filled with MSW until the commencement of the pilot biofilter construction (July 2005). The gas well was perforated in the bottom five meters, and was surrounded with a layer of gravel. Site 3 was selected to be on top of the landfill (20 m), as this allowed for a comparison with sites 1 (slope) and 2 (top of the landfill but with a gas well). Site 3 was placed over waste

that was last deposited in 2000. Sites 1 and 3 were located in the non-active section of the landfill and were integrated into the temporary clay landfill cover soil. Site 2 was located at an intersecting point between the active and non-active part of the landfill, and was backfilled with 0.5- 1 m of soil.

2.2 Pilot Biofilter Design

Table 3.1 shows the design properties for each pilot biofilter. Site 1, the existing site, had a SAR of 10.8. The use of the gas well at site 2 was expected to increase the influent CH_4 flux. The same SAR (10.8) was used for sites 1 and 2, which allowed for a comparison of the effect of the gas well at site 2. At site 3, a SAR of 4.8 was used by increasing the surface area of the biofilter (20.9 m^2). This allowed for an assessment of reducing the influent CH_4 flux loading rate on the biofilter's performance. The location of the sites also allowed for a comparison of the effect of being on top or on the slope of the landfill body, since LFG tends to migrate laterally more readily than vertically. A biofilter medium depth of 1.5 m was selected for all sites, to provide a maximum contact area for methane treatment. In addition, this depth allowed for the insulation of the lower layers in the medium.

Table 3.1. Pilot Biofilter Design Properties

Properties	Site 1	Site 2 (Gas Well)	Site 3 (Large Biofilter)
Location on the Landfill Body	Slope	Top	Top
SAR	10.8	10.8	4.8
Surface Area of MSW Covered (m^2)	100	100	100
Biofilter Surface Area (m^2)	9.3	9.3	20.9
Biofilter Depth (m)	1.5	1.5	1.5
Gas Well (Yes/No)	No	Yes	No

Figures 3.2a-3.2b shows several construction pictures for site 2. A 0.8 m layer of tire shreds (Fig. 3.2a) was used as the gas distribution layer. This layer was used to distribute the LFG and prevent high point sources into the medium. The tire shreds were placed to be slightly sloped downwards from the center. The tire shreds, composed of passenger and light-truck vehicle tires, were processed by Rubber Tech. (Legal, AB), and were provided by the Tire Recycling Authority of Alberta (Edmonton, AB). An Enviro Liner® 6040 geomembrane (Layfield Geosynthetics & Industrial Fabrics Ltd., Edmonton, AB) was placed over the tire shreds (Fig. 3.2b). The geomembrane was composed of two separate pieces that were welded together by a plastic seam. The first piece covered the tire shreds, while the second lined the inner walls of a wooden frame (Fig. 3.2c) that contained the biofilter. Compost was selected as the biofilter medium, and was placed in the wooden frame (Fig. 3.2d). The compost, of yard-waste origin, was taken from an open windrow operation at the Leduc Landfill. The compost was turned twice per month for six months and then was left to cure for one year. The compost was passed through a 1.27 cm screen.

Fig. 3.2. Construction of Pilot Biofilters

(a) Tire Shreds **(b) Geomebrane**

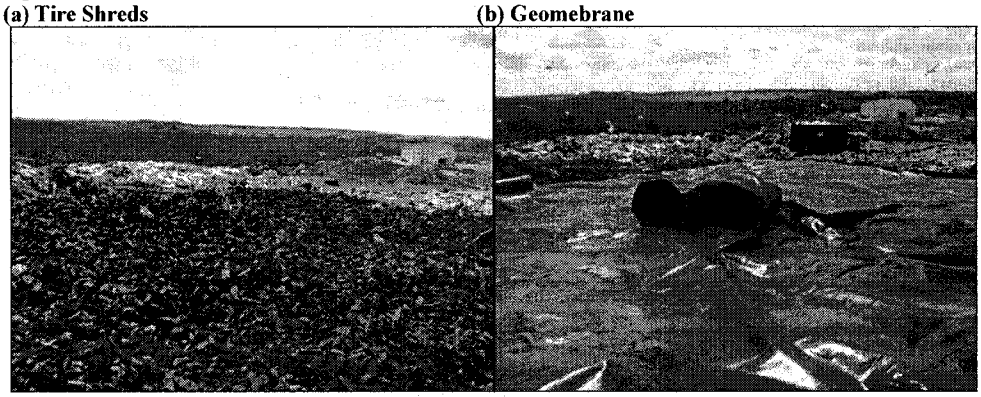

(c) Wooden Frame **(d) Partially backfilled site**

2.3 Analytical Methods

The yard-waste compost was analyzed following the methods outlined by the Test Methods for the Evaluation of Compost and Composting (TMECC). The bulk density (BD), moisture content (MC), organic matter (OM), pH, electrical conductivity (EC), and maturity were tested using TMECC methods 03.01-A, 03.09-A, 05.07-A, 04.11-A, 04.10-A, and 05.08-B respectively (TMECC 2002). The total air space (TAS) and porosity were calculated as described by Ball and Smith (2001). The total carbon and nitrogen (CN) analysis was conducted with a Leco® TrueSpec CN Carbon/Nitrogen Determinator (Leco Co., St. Joseph, MI). Before the analysis, samples (10 g) were air dried for 24 h at

36°C, and were then passed through a 1 mm screen. Sample calculations for determining the material properties are included in Appendix B.

The pilot biofilters were each equipped with monitoring instruments at different depths (-20, -55, -90, -125, and -160 cm), and quadrants (A-D). Fig. 3.3 shows the placement of the polyethylene gas collection tubing, thermocouple sensors (type K), and time domain reflectometry (TDR) probes. The gas collection tubing (0.64 cm ID) was connected to a perforated PVC end cap (1.27 cm ID and 10 cm length). The end cap was placed in the biofilter and was used as a filter to prevent the tubing from getting clogged with soil particles when gas samples were collected. A Landtec GEM® 2000 (Colton, CA) gas analyzer was used to measure the CH_4, CO_2, and O_2 concentrations at the different depths and quadrants shown in Fig. 3.3. The balance of the sum of those gases was considered to be the nitrogen concentration. Additional thermocouple sensors were placed in the shade at each site to measure ambient temperature, as well at the surface (-5 cm depth) of each biofilter. All sites contained temperature data loggers for continuous measurements.

Fig. 3.3. Instrumentation Placement (Not to scale)

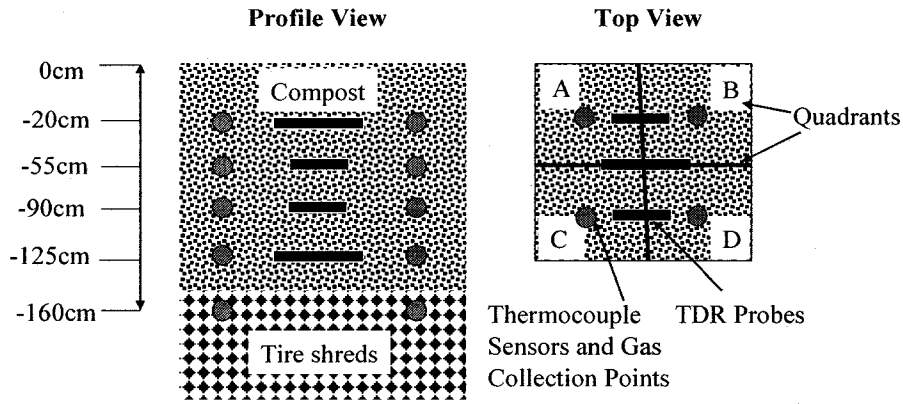

Moisture Point® (ESI Environmental Sensors Inc., Victoria, BC) TDR probes were used to measure volumetric MC. Site 2 was equipped with a data logger for continuous moisture measurements, while manual measurements were required at sites 1 and 3. The placement of the TDR probes, shown in Fig. 3.3, was for sites 1 and 2 only. Each TDR probe is composed of several segments, in which volumetric MC is measured over the respective segment length. Longer TDR probes (5 segments, 120 cm total sensor length) were placed in the center of the filter bed at the –20 and –125 cm depths. Shorter TDR probes (4 segments, 60 cm total sensor length) were placed between the quadrants AB and CD at the –55 and –90 cm depths. For site 3, shorter TDR probes were placed vertically in-between each quadrant (AB, BC, CD and AD), such that measurements were recorded in 15 cm increments to a depth of 60 cm. The TDR system was calibrated for determining the actual volumetric MC of the compost (see Appendix C). This was conducted by filling a column with compost at different moisture levels (0.09 - 0.36 $g \cdot g^{-1}$, wet basis). At each respective moisture level the volumetric MC was determined with a TDR probe. The BD and gravimetric MC of the compost were then determined. Therefore, a calculated volumetric MC, based on the gravimetric MC and BD, could be compared to the TDR measurement. After repeating the test at different moisture levels and bulk densities, the following linear relationship was observed to predict the volumetric MC of compost based on the TDR measurement:

[3] $$MC_v = 1.13 \cdot MC_{TDR} + 0.078 \qquad R^2 = 0.95$$

where MC_v ($L \cdot L^{-1}$) is the predicted volumetric MC, and MC_{TDR} ($L \cdot L^{-1}$) is the averaged result from the TDR probe.

Surface emissions (CH_4 and CO_2) were measured by using static flux chambers. Frames (0.38 m^2) were buried at least 5 cm into the surface of the four quadrants of each biofilter medium. The chambers could then be placed on to top of the frames and were sealed with water or an anti-freeze mixture during colder periods. The combined volume of the frame (not buried) and chamber is 0.13 m^3. Each chamber contained a fan to mix the accumulating gas in order that a representative gas sample could be collected. A valve on the chamber exterior was equipped with a needle to collect gas samples. Most chambers also contained a thermocouple sensor to measure temperature. Gas samples were collected in 7 ml Vacutainers® serum tubes (Becton Dickinson, Franklin Lakes, NJ), equipped with rubber septum lids, every 10 minutes in duplicate for 60 minutes. The CH_4 (and similarly the CO_2) flux could then be determined:

[3] $$J_{CH4} = \frac{\Delta C \cdot \rho \cdot V}{\Delta t \cdot A}$$

where J_{CH4} is the effluent flux ($gCH_4 \cdot m^{-2} \cdot d^{-1}$), $\Delta C/\Delta t$ is the slope of gas concentration versus time curve ($m^3CH_4 \cdot m^{-3}air \cdot d^{-1}$), ρ is the density of the gas determined from the ideal gas law ($g \cdot m^{-3}$), V is the combined volume (m^3) of the chamber and frame, and A is the surface area (m^2) of the filter covered by the frame. The slope was determined using linear regression, and analyzed for significance (usually a p-value < 5 %) using analysis of variance (ANOVA). The flux was equal to zero when no significant relationship was observed. The atmospheric pressure values were taken from an Environment Canada's weather station (Environment Canada 2006), located at the Edmonton International Airport, which is approximately 30 km northwest from the landfill site. Sample calculations are included in Appendix A.

Monitoring events were conducted once per month to manually measure gas composition, moisture profiles (sites 1 and 2), and surface emissions. Gas samples collected from the flux chambers were transported to the Alberta Research Council (Edmonton, AB) and were analyzed, usually within 24 hrs, with a Varian CP-4900® (Palo Alto, CA) micro gas chromatography (GC) instrument, equipped with a thermal conductivity detector. A Molsieve 5A column (90°C, 200 kPa, 60 s run time) was used to analyze oxygen, nitrogen, and methane concentrations, while a Pora PLOT Q column (65°C, 200 kPa, 60 s run time) was used to measure carbon dioxide concentrations. The GC was calibrated by purchasing standard gas mixtures from Praxair Inc. (Edmonton, AB). High purity helium (0.99999 $L \cdot L^{-1}$ He) was used as the carrier gas. CP- Maitre Elite software was used to operate the GC.

During the operation of the biofilters, the influent LFG flux rate was unknown. To determine a methane removal rate, the influent LFG flux was assumed to equal the effluent LFG flux, since theoretically every unit of volume of CH_4 that is oxidized produces an equal volume of CO_2. The following equation was used to calculate the CH_4 influent flux (Zeiss 2002):

[4] $$Jin_{CH4} = Cin_{CH4} \times [Jout_{CH4} + Jout_{CO2}]$$

where Jin_{CH4} is the influent methane flux ($LCH_4 \cdot m^{-2} \cdot d^{-1}$), $Jout_{CH4}$ and $Jout_{CO2}$ are the respective effluent methane and carbon dioxide fluxes ($LCH_4 \cdot m^{-2} \cdot d^{-1}$), and Cin_{CH4} is the concentration of methane ($L \cdot L^{-1}$) in the tire shreds (160 cm depth). Since in practice the stochiometric coefficients for CO_2 production have been found to be in the range of 0.2-

0.9 (Stepniewski and Pawlowska 1996), Eq. 4 will underestimate the methane influent flux. The methane removal rate was determined by the following equation:

$$[5] \qquad CH_4 \text{ Removed} = \frac{Jin_{CH4}\text{-}Jout_{CH4}}{Jin_{CH4}} \times 100$$

where CH_4 removed (%) is the percentage of methane removed in the biofilter. The use of Eq. 5 sometimes yielded negative results, since the influent flux calculated with Eq. 4 resulted in lower values than the observed effluent methane flux. In these instances, the methane removal rate was assigned a value of zero. Sample calculations using Eqs. 4 and 5 are included in Appendix A.

3.0 Results

Several physical, chemical, and biological properties are shown in Table 3.2, including the standard error (SE), for the yard-waste compost. The large TAS (0.46 $L \cdot L^{-1}$) and porosity (0.69 $L \cdot L^{-1}$) were beneficial for gas distribution and microbial growth. The low EC (2.75 $dS \cdot m^{-1}$) and neutral pH (7.49) were suitable for the growth of the methanotrophic bacteria. The OM (0.18 $g \cdot g^{-1}$) provided nutrients for the bacteria. The compost was biologically mature (1.02 $mgC\text{-}CO_2 \cdot g^{-1}OM \cdot d^{-1}$), which was required, since it was undesirable to have competing microbiological processes.

Table 3.2. Yard-Waste Compost Properties

Property	Compost	SE
MC ($g \cdot g^{-1}$, wet basis)	0.31	0.001
BD ($g \cdot L^{-1}$, wet basis)	772.48	6.56
Porosity ($L \cdot L^{-1}$)	0.69	-
TAS ($L \cdot L^{-1}$)	0.49	-
OM ($g \cdot g^{-1}$, dry basis)	0.18	0.003
Total Carbon ($mg \cdot g^{-1}$, dry basis)	81.01	0.90
Total Nitrogen ($mg \cdot g^{-1}$, dry basis)	8.50	0.14
CN	9.53	-
pH	7.49	0.02
Conductivity at 25°C ($dS \cdot m^{-1}$)	2.75	0.03
Maturity ($mgC\text{-}CO_2 \cdot g^{-1}OM \cdot d^{-1}$)	1.02	0.04

Figures 3.4a and 3.4b show the average CH_4 and CO_2 surface emissions, measured from 8 monitoring events conducted from the fall of 2005 to the spring of 2006. Sites 1 and 2 were operational in August (2005), while site 3 was operational in November (2005). Generally low CH_4 surface emissions (< 15 $gCH_4 \cdot m^{-2} \cdot d^{-1}$) were measured from all sites. The CO_2 surface emissions were higher, as expected, since LFG gas is typically composed of equal volumes of CH_4 and CO_2 and the former was being oxidized in the biofilter. Since larger CO_2 fluxes were observed at site 2 for 6 of 8 monitoring events, there was most likely a larger overall average influent flux of LFG at that site. Site 3 showed lower CO_2 surface emissions than the other sites, which indicated lower influent LFG flows. The first monitoring event (October 25th) showed large CH_4 and CO_2 emissions for sites 1 and 2 (site 3 was not operational yet). Another high CH_4 emission (>15 $gCH_4 \cdot m^{-2} \cdot d^{-1}$) event was observed for site 1 on March 21st.

Fig. 3.4. CH_4 and CO_2 Surface Emissions
(a) CH_4 Emissions ($g \cdot CH_4 \cdot m^{-2} \cdot d^{-1}$)

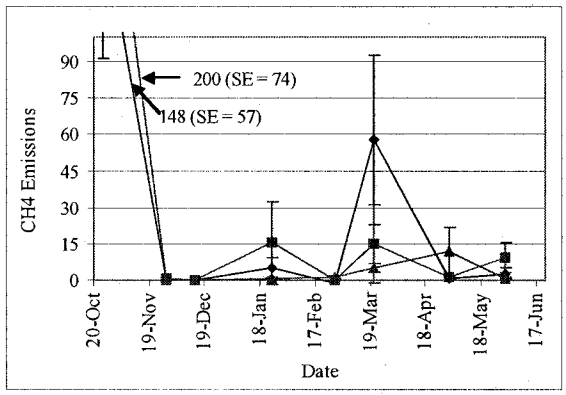

(b) CO_2 Emissions ($g \cdot CO_2 \cdot m^{-2} \cdot d^{-1}$)

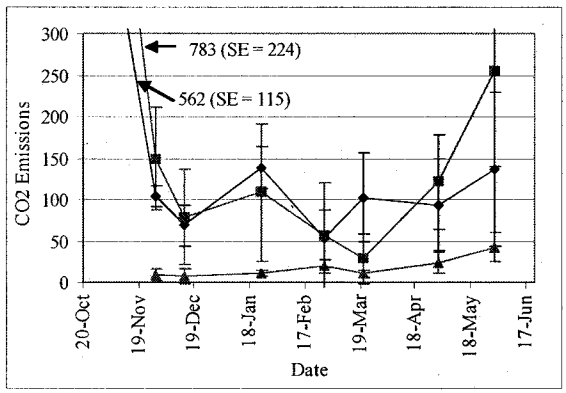

Site 1 Site 2 (Gas Well) Site 3 (Large Biofilter)

Note: SE bars are shown; some SE may be too small to be visible.

Figure 3.5 shows the calculated methane removal rates, as described by Eq. 5, for all sites. As mentioned, a calculated negative removal rate was assigned a value of zero, such as on March 21st. The average removal for sites 1, 2, and 3 were 76, 68, and 35 % respectively, not meeting the 80% removal objective. Using Eq. 4 the average influent methane fluxes were calculated (converting to a gravimetric basis using the ideal gas law) to be 37.4, 53.5, and 1.2 $gCH_4 \cdot m^{-2} \cdot d^{-1}$ for sites 1, 2, and 3 respectively. Two instances in Fig. 3.5 show higher than 100% removal. This was as a result of measuring a negative methane effluent flux, possibly indicating soil uptake of atmospheric methane.

Fig. 3.5. Methane Removal Rates

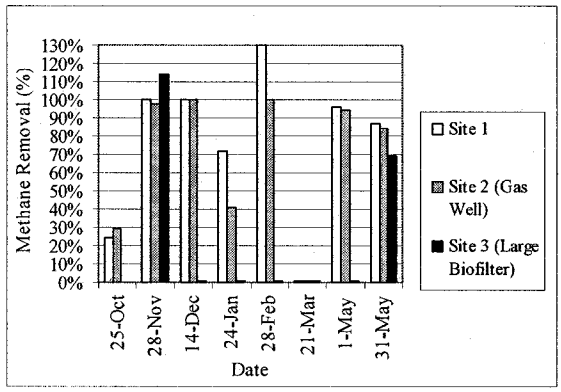

The higher emissions observed on the first monitoring event most likely occurred as a result of advective LFG flows. Figures 3.6a and 3.6b show the relationship between rate of atmospheric pressure change, during the flux chamber measurements, and CH_4 and CO_2 emissions. The emissions from all the sites have been grouped together for Figs. 3.6a and 3.6b. The two highest emissions points on both figures are from the first monitoring event. Though the fitted curves in both figures have a low coefficient of determination ($R^2 \leq 0.40$), they do show the inverse relationship between the rate of atmospheric pressure change and surface emissions.

Fig. 3.6. Relationship Between Changing Atmospheric Pressure and Surface Emissions
(a) CH_4 Emissions ($g \cdot CH_4 \cdot m^{-2} \cdot d^{-1}$) **(b) CO_2 Emissions ($g \cdot CO_2 \cdot m^{-2} \cdot d^{-1}$)**

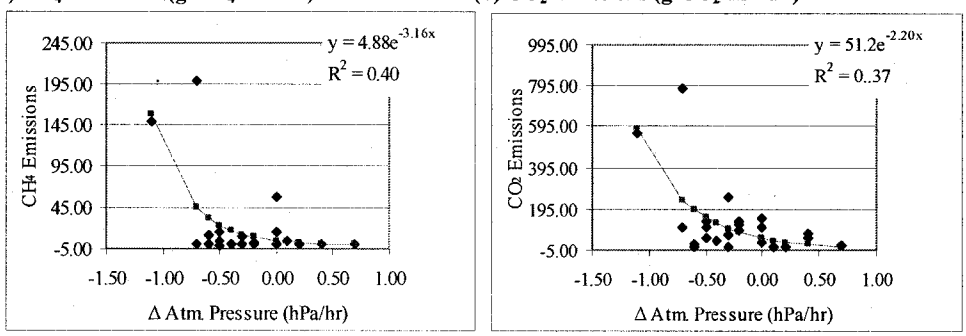

Figures 3.7a-3.7f show the average gas composition profiles for several selected days, for sites 1 and 2. On October 25th, Figs. 3.7a and 3.7b, high CH_4 concentrations were measured throughout both biofilters. Low oxygen concentrations (< 0.01 $L \cdot L^{-1}$) were measured at -20 cm depth at both sites. The calculated N_2 concentrations showed some atmospheric air penetration. By contrast, both sites on November 28th, Figs. 3.7c and 3.7d, showed larger quantities of N_2 penetrating the biofilters. This had the effect of diluting the CH_4 gas in the anaerobic zone of the filter (-55 to -160 cm depth). Oxygen was found to be penetrating both biofilters to a maximum of 55 cm on that day. The further reduction of CH_4 concentration in the aerobic part of the filter was caused by methane oxidation and dilution with nitrogen gas. The May 1st monitoring event, Figs. 3.7e and 3.7f, showed results in-between the former two shown. Higher concentrations of CH_4 were observed, through out the biofilter depth, than on November 28th, but less than that observed on October 25th. A low oxygen concentrations (0.015 $L \cdot L^{-1}$) was measured at the -20 cm depth at site 1, while none was measured at site 2. The average oxygen concentration measured at the -20 cm depth for sites 1 and 2, for all 8 monitoring events, were 0.046 and 0.038 $L \cdot L^{-1}$ respectively. Also, the average CH_4 concentrations measured at the -160 cm depth for sites 1 and 2, for all 8 monitoring events, were 0.32 and 0.44 $L \cdot L^{-1}$ respectively.

Fig. 3.7. Gas Composition Profiles

(a) Site 1 25-Oct

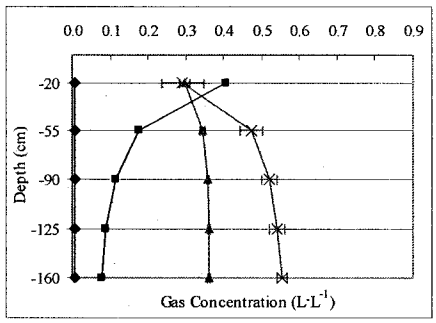

(b) Site 2 (Gas Well) 25-Oct

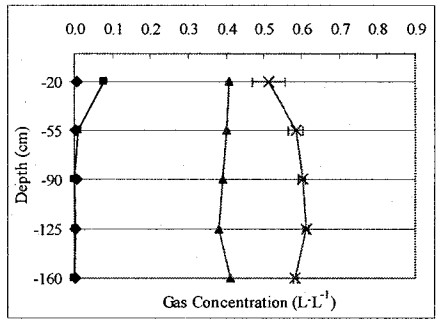

(c) Site 1 28-Nov

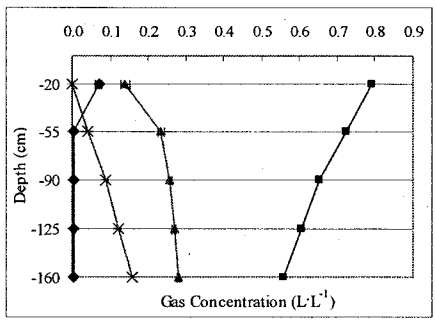

(d) Site 2 (Gas Well) 28-Nov

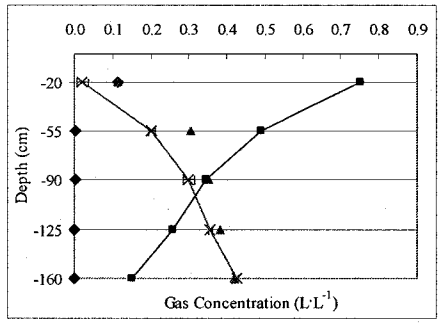

(e) Site 1 1-May

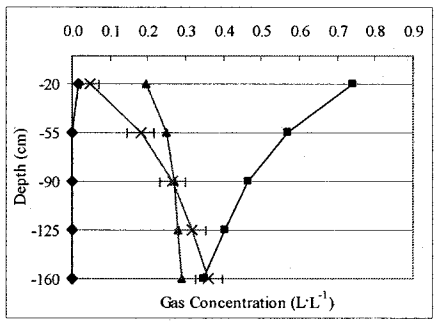

(f) Site 2 (Gas Well) 1-May

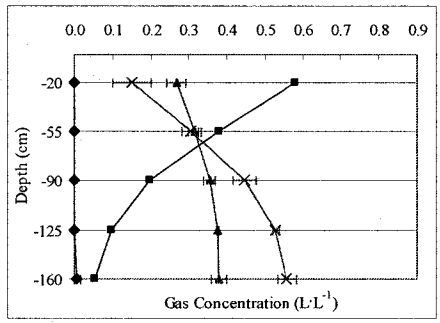

(g) Site 3 (Large Biofilter) 28-Nov

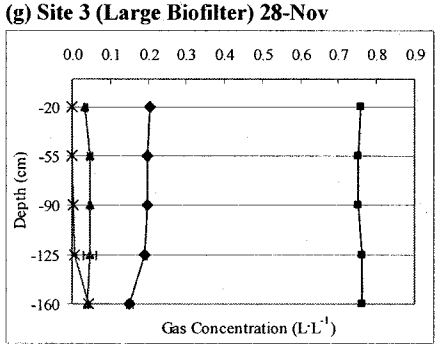

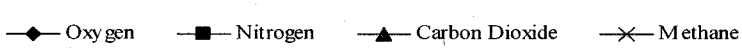

Note: SE bars are shown; some SE may be too small to be visible.

By contrast to the gas profiles observed for sites 1 and 2, site 3 showed generally much smaller concentrations of LFG, as shown in Fig. 3.7g. During the November monitoring event, the CH_4 and CO_2 concentrations were less than 0.10 $L \cdot L^{-1}$ though out the biofilter. The atmospheric air concentrations remained high even at the -160 cm depth. The average CH_4 and O_2 concentrations at the -160 cm depth, measured for all 7 monitoring events, were 0.076 and 0.14 $L \cdot L^{-1}$ respectively.

The averaged daily temperature statistics for sites 1 and 2 are shown in Table 3.3. Site 1 showed warmer temperatures towards the surface of the biofilter medium, with a maximum average value observed at the -20 cm depth. By contrast, site 2 showed warmer temperatures in the deeper layers of the biofilter medium, with a maximum value observed at the -125 cm depth. As mentioned in the introduction, one objective was to maintain temperatures above 20°C. Table 3.3 also shows the percentage of days in which the average temperature was above 20°C, for sites 1 and 2. Site 2 was clearly achieving the objective more frequently than site 1. The minimum, maximum, and amplitude values describe the temperature variations observed, and are also shown in Table 3.3. For both sites, the amplitude decreases with increasing depth. Figures 3.8a and 3.8b show examples of the temperature profiles for sites 1 and 2, for all depths, during the last three weeks of May. The temperature trend at the -20 cm, for both sites, appears to be dependent on ambient temperature.

Table 3.3. Sites 1 and 2 Average Daily Temperature Statistics

Depth	Site 1 (°C)					Site 2 (°C)				
	Min	Max	Avg	Amp	% Days >20°C	Min	Max	Avg	Amp	% Days >20°C
Ambient	-24.3	25.2	0.8	49.5	4.0%	-24.5	22.7	2.4	47.2	1.4%
-20 cm	9.4	46.6	27.6	37.2	75.3%	11.1	43.1	26.5	32.0	78.7%
-55 cm	11.7	35.7	25.6	24.0	82.8%	16.0	39.2	27.6	23.2	87.2%
-90 cm	11.1	31.8	23.1	20.8	62.0%	20.9	38.2	29.8	17.3	100 %
-125 cm	11.7	30.6	22.4	18.9	61.6%	23.5	38.6	31.3	15.1	100 %
-160 cm (Tire Shreds)	10.4	29.0	20.6	18.6	53.8%	29.0	39.5	34.5	10.5	100 %

Fig. 3.8. Daily Temperature Change

(a) Site 1

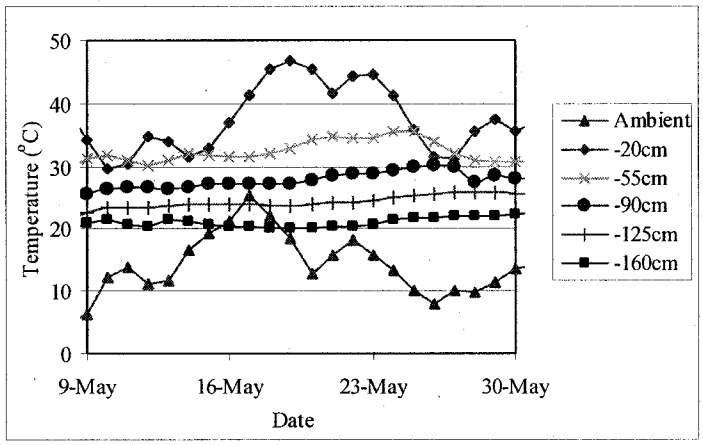

(b) Site 2

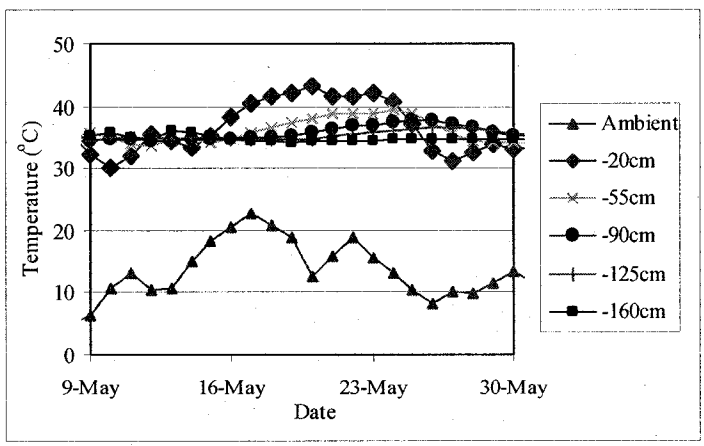

Table 3.4 shows the averaged daily temperature statistics for sites 3. The site showed colder temperatures than sites 1 and 2, and was never above 20°C. However, similar to sites 1 and 2, the amplitude declined with increasing depth.

Table 3.4. Site 3 Average Daily Temperature Statistics

	Site 3 (°C)				
Depth	Min	Max	Avg	Amp	% Days >20°C
Ambient	-12.9	21.4	1.6	34.3	1.8%
-20 cm	-5.7	19.8	1.3	25.5	0.0%
-55 cm	-1.3	19.4	2.0	20.7	0.0%
-90 cm	0.2	17.8	4.0	17.7	0.0%
-125 cm	-2.2	17.0	5.2	19.2	0.0%
-160 cm	3.5	16.4	8.2	12.9	0.0%

Figures 3.9a-3.9c show the calculated volumetric MC profiles (Eq. 3), based on the TDR measurements, for all three sites on several selected days. Sites 1 and 2 (Figs. 3.9a and 3.9b) were generally meeting the 0.25 $L \cdot L^{-1}$ objective. In particular, site 2 showed a higher MC at all depths. The moisture objective was met on November 25th at site 3 (Fig. 3.9c), however, the most recent data (March 21st) showed drier conditions.

Fig. 3.9. Moisture Profiles

(a) Site 1

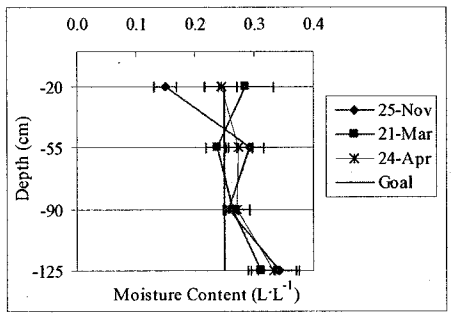

(b) Site 2 (Gas Well)

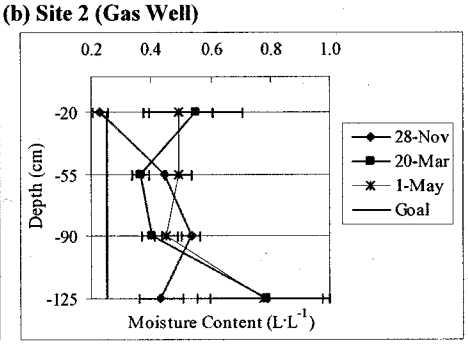

(c) Site 3 (Large Biofilter)

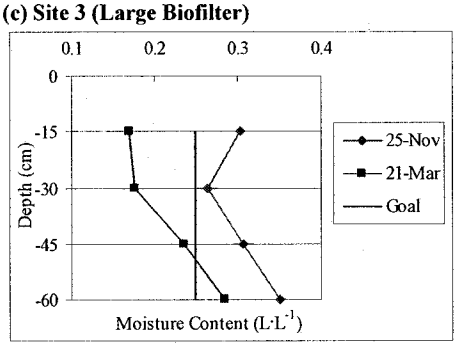

Note: SE bars are shown; some SE may be too small to be visible.

4.0 Discussion

Sites 1 and 2 generally showed low (< 15 $gCH_4 \cdot m^{-2} \cdot d^{-1}$) methane surface emissions (Fig. 3.4). Barlaz et al. (2004) and Rajbhandari et al. (2006) found low surface emissions (< 15 $gCH_4 \cdot m^{-2} \cdot d^{-1}$) when applying a yard-waste compost and compost-mulch mixture (respectively) as biocover mediums. Two monitoring events showed negative methane fluxes resulting in removal rates greater than 100% (Fig. 3.5). This was observed for sites 1 and 3 on February 28th and November 28th respectively. Barlaz et al. (2004) observed negative fluxes in a biocover, using a yard-waste compost as the medium, for 59 of 107 flux chamber measurements. They attributed this to the biocover uptake of atmospheric methane, which was most likely the reason for the negative fluxes observed in the current study.

The average methane removal rates were 76 and 68 % for sites 1 and 2 respectively, not meeting the 80 % removal rate objective. The site 1 result was similar to that found by Zeiss (2002), who found an average methane removal rate of 72 % (at site 1 using Eqs. 4 and 5) using yard-waste compost as the biofilter medium. The average influent methane fluxes (37.4 and 53.5 $gCH_4 \cdot m^{-2} \cdot d^{-1}$ for sites 1 and 2 respectively) calculated based on Eq. 4, were lower than what was used in a lab-scale experiment (134 $gCH_4 \cdot m^{-2} \cdot d^{-1}$). In the lab-scale experiment, the same compost that was used in the pilot biofilters removed long-term (218 days) 100 % of the influent methane flux (see Chapter 2). Therefore, a higher removal rate for sites 1 and 2 was expected. It's important to highlight that Eqs. 4 and 5 are the best estimates of the methane influent flux and removal rates. Despite not meeting the 80 % removal objective, the biofilter approach used was still thought to be successful at reducing methane surface emissions. This was as a result of the low surface emissions (< 15 $gCH_4 \cdot m^{-2} \cdot d^{-1}$) that were generally observed. The use of a SAR of 10.8 appears to be appropriate, as the calculated influent fluxes were lower than what the compost medium was found to be capable of removing.

To analyze further what caused high surface emissions (>15 $gCH_4 \cdot m^{-2} \cdot d^{-1}$) at sites 1 and 2, Table 3.5 shows a summary of the results for October 25th and March 21st. The methane surface emission (14.7 $gCH_4 \cdot m^{-2} \cdot d^{-1}$) for site 2 on March 21st was also considered high given the low methane removal rate (0 %) observed. To analyze these results, Table 3.5 also shows a comparison to the May 1st monitoring event, when methane emissions were low. Since oxygen was found on average (0.046 and 0.038 $L \cdot L^{-1}$ for sites 1 and 2 respectively) at low levels at the -20 cm depth, the majority of the methane oxidation was suspected to be taking place in the top 55 cm. Therefore, Table 3.5 shows the average temperature and MC values from the -20 cm depth on the

respective days. The October 25th event shows that despite warm temperatures and sufficient moisture levels at site 2, the surface emissions were high as a result most likely of advective influent methane flows, caused by a large negative rate of atmospheric pressure change. On March 21st, sufficient moisture levels and steady atmospheric pressure were observed. The high methane emissions were attributed to the low temperatures observed at the -20 cm depth. Both biofilter mediums showed a decreasing temperature trend at the -20 cm depth from the preceding monitoring event as result most likely of colder winter temperatures during that period (daily averaged ambient temperatures reached as low as -15°C during that period). The May 1st event shows that despite dropping atmospheric pressure, low methane surface emissions were observed. Both sites showed warm temperatures and sufficient moisture levels on that day. Therefore, dropping atmospheric pressure and low temperatures at the -20 cm depth were identified as the respective contributing factors for the high methane surface emissions observed on the October 25th and March 21st monitoring events.

Table 3.5. Comparison of Results for Site 1 and 2, for Several Selected Days

Result	25-Oct		21-Mar		1-May	
	Site 1	Site 2	Site 1	Site 2	Site 1	Site 2
CH_4 Emissions ($gCH_4 \cdot m^{-2} \cdot d^{-1}$)	148.2	199.6	57.7	14.7	1.4	11.6
CO_2 Emissions ($gCO_2 \cdot m^{-2} \cdot d^{-1}$)	562.3	782.5	102.4	28.4	93.6	121.4
Methane Removal (%)	24%	29%	0%	0%	96%	94%
Δ Atm. Pres. ($hPa \cdot hr^{-1}$)	-1.1	-0.7	0	0	-0.2	-0.2
Temp. (°C) at -20 cm	36.4	31.7	12.3	12.5	36.6	35.1
Moisture (L·L) at the -20 cm	N/A	0.37	0.29	0.55[a]	0.24[b]	0.49

[a]Observed on 20-Mar
[b]Observed on 24-Apr

Figures 3.6a ansd 3.6b shows the relationship between rate of atmospheric pressure change and surface emissions. As mentioned, the large drop in atmospheric pressure was suspected of causing the high surface emissions on October 25th. Others have also observed this relationship. Poulsen at al. (2003) showed that the rate of atmospheric pressure change was the controlling factor in short-term (24 hr) surface emissions. Long-term (1 year) surface emissions were showed to be most dependent on the rate of atmospheric pressure change, and soil moisture content and gas permeability. Gebert and Goengroeft (2006) showed a similar relationship, which was as the rate of atmospheric pressure decreased, the rate of LFG pressure increased, as measured in the biofilter supply pipe (which was connected to a collection system). They suggested that the rate of advective LFG flow trough a collection system will be dependent on the degree the landfill cover seals the body. The more permeable a landfill cover soil is, the more paths there are for LFG to migrate out of the landfill body. The lower the permeability of the landfill cover soil, the less paths there are for LFG to migrate out of the landfill body, and the more likely it will move to a gas collection system, or through a porous biofilter integrated into the landfill cover as in this case. This may explain why on November 28th, the atmospheric pressure dropped 0.7 $hPa \cdot hr^{-1}$, which was the same drop observed at site 2 during the October 25th monitoring event, but no methane surface emissions were observed.

Generally, oxygen was only found at the -20 cm depth for sites 1 and 2, and on average was less than 0.05 $L \cdot L^{-1}$. This indicated that the methane oxidation horizon, the area where the methanotrophic bacteria are most active, was in the top 20-55 cm as indicated by the consumption of oxygen. Humer and Lechner (2001) found O_2 penetrating to 50-90 cm depths, in a MSW compost used as a biocover medium. During the first

monitoring event O_2 diffusion may have been limited by the advective LFG flow. Gebert and Grongroft (2006) found this to be a limiting factor in their biofilter's removal capabilities. Changes in TAS will also impact O_2 penetration. This may explain why on November 28th the largest O_2 concentration (0.12 $L \cdot L^{-1}$) was observed at site 2 (Fig. 3.7d), as the MC (0.23 $L \cdot L^{-1}$) was lower (Fig. 3.9a) than observed on other monitoring events.

The biofilter temperature depends on several factors, the major ones being ambient temperature, heat released from methane oxidation, the quantity of influent LFG, and the thermal characteristics of the medium. The objective to maintain average temperatures above 20°C was achieved at sites 1 and 2 at all depths. However, site 2 met the objective more frequently (Table 3.3). Site 2 showed larger LFG influent flows (since larger CO_2 effluent fluxes were observed on 6 of 8 monitoring events) and concentrations at the -160 cm depth (tire shreds), most likely explaining the warmer conditions observed there. The use of the gas well at site 2 may explain the larger LFG influent flows and concentrations observed there. However, it's also possible the site was generating more LFG (i.e. hot spot) from the waste below it than site 1. The temperatures at the -20 cm depth were impacted by the daily changes in ambient temperatures (Figs. 3.8a and 3.8b), which was also observed by Gebert and Grongroft (2006). For the May data shown, the temperatures at all depths for both sites were generally warmer than ambient temperatures, highlighting the impact of biofilter warming due to LFG and microbial activity.

The MC profiles (Figs 3.9a and 3.9b) show that sites 1 and 2 were generally meeting the moisture objective of 0.25 $L \cdot L^{-1}$. However, site 2 showed larger moisture levels through

out the biofilter medium. Site 2 had a berm built around it, consisting of stockpiled cover soil (not by design), which may have prevented some wind desiccation. The higher LFG influent flows and concentrations in the tire shreds observed at site 2 may have resulted in more condensation (as LFG is typically saturated with moisture). In addition, the higher average methane influent fluxes at site 2 could have resulted in more oxidation and water production. The MC at sites 1 and 2 will be continued to be monitored over the summer months, to determine if drying due to warmer temperatures occurs.

Site 3, which was designed with a smaller biofilter SAR (4.79), showed smaller LFG concentrations (Fig. 3.7f) and CH_4 and CO_2 surface emissions (Figs. 3.4a and 3.4b) than site 1 and 2. However, the CO_2 surface emissions have shown an increasing trend, with an effluent flux of 42.6 $gCO_2 \cdot m^{-2} \cdot d^{-1}$ observed on May 31st. Temperatures were never observed to rise over 20°C (Table 3.3), a further indication of lower LFG influent flows and methane oxidation. There were two causes identified that could possibly explain the inactivity in the biofilter medium. The first was that the location may not have been a hot spot for landfill gas generation. No surface emission measurements were conducted prior to the construction of the site. Any gas generated below the site may have moved laterally, as the site was built on top of the landfill (20 m) beside a slope. The use of a gas well, similar to site 2, may have resulted in larger LFG influent flows. The second was that, as a result of the large average concentrations of oxygen (0.14 $L \cdot L^{-1}$) observed in the tire shreds (-160 cm), there was the possibility that methane oxidation was occurring in the waste below the tire shreds. This is similar to what Humer and Lechner (2001) observed in the winter months during the operation of a biocover. They found that the majority of the methane had been oxidized before the interface between the distribution layer (coarse gravel) and sewage sludge medium. However, it is unclear if

they were suggesting that methane was being oxidized in the gas distribution layer or in the waste below (or both).

5.0 Conclusion

The approach to integrate a biofilter into the landfill cover showed promising results, despite sites 1 (76 %) and 2 (68 %) not meeting the 80 % removal objective. The selection of yard-waste compost as the biofilter medium and a SAR of 10.8 for sites 1 and 2 resulted generally in low surface emissions (< 15 $gCH_4 \cdot m^{-2} \cdot d^{-1}$). Site 2 showed larger LFG influent flows and concentrations, which most likely explains the warmer temperatures and wetter conditions observer there. It's possible that the use of the gas well at the site may have caused the larger LFG flows and concentrations. Low influent LFG fluxes at site 3 did not allow for a full assessment of using a SAR of 4.8. Since the site was located on top of the landfill, similar to site 2, lateral gas migration may have explained the low influent LFG fluxes. The use of a gas well at site 3 may have increased the influent LFG flows. The surface emissions on October 25th and March 21st were considered high for sites 1 (148.2 and 57.7 $gCH_4 \cdot m^{-2} \cdot d^{-1}$ respectively) and 2 (199.6 and 14.7 $gCH_4 \cdot m^{-2} \cdot d^{-1}$ respectively). This was attributed to decreasing atmospheric pressure observed on October 25th (1.1 and 0.7 $hPa \cdot hr^{-1}$ for sites 1 and 2 respectively), and lower temperatures at the -20 cm depth on March 21st (12.3 and 12.5°C for sites 1 and 2 respectively). Temperatures on average were higher than 20°C at sites 1 and 2, with warmer temperatures observed at site 2. The MC objective of 0.25 $L \cdot L^{-1}$ was generally met at sites 1 and 2, with wetter conditions observed at site 2. More future monitoring events will allow for an assessment of the biofilters performances over the warmer summer months.

6.0 References

Ball, B. C., and Smith, K. A. 2001. Gas movement and air-filled porosity. *In* Soil and environmental analysis. *Edited by* K. A. Smith and C. E. Mullins. Marcel Dekker Inc., New York, NY. pp. 499-538.

Barlaz, M. A., Green, R. B., Chanton, J. P., Goldsmith, C. D., and Hater, G. R. 2004. Evaluation of a biologically active cover for mitigation of landfill gas emissions. Environ. Sci. Technol. **38:** 4891-4899.

Environment Canada. 2006. Hourly data report for Edmonton International Airport [online]. Available from http://www.climate.weatheroffice.ec.gc.ca/ [cited 27-Jun-2006].

Gebert, J., and Groengroeft, A. 2006. Passive landfill gas emission - Influence of atmospheric pressure and implications for the operation of methane-oxidising biofilters. Waste Manage. **26:** 245-251.

Gebert, J., and Grongroft, A. 2006. Performance of a passively vented field-scale biofilter for the microbial oxidation of landfill methane. Waste Manage. **26:** 399-407.

Hilger, H., and Humer, M. 2003. Biotic landfill cover treatments for mitigating methane emissions. Environmental Monitoring and Assesment **84:** 71-84.

Humer, M., and Lechner, P. 2001. Design of a landfill cover layer to enhance methane oxidation - results of a two year field investigation. Proceedings Sardinia 2001 8th International Waste Management and Landfill Symposium, Margherita di Pula, Italy, pp. 541-550.

Poulsen, T. G., Christophersen, M., Moldrup, P., and Kjeldsen, P. 2003. Relating landfill gas emissions to atmospheric pressure using numerical modeling and state-space analysis. Waste Manage. Res. **21:** 356-366.

Rajbhandari, B. k., Hettiaratchi, J. P. A., and Hurtado, O. D. 2006. Thin biocovers: A novel approach in controlling methane emissions from landfill accepting biodegradable organic waste. Proceedings of the 21st International Conference on Solid Waste Technology and Management, Philadelphia, PA, 1, pp. 562-572.

Stepniewski, W., and Pawlowska, M. 1996. Chemistry for the protection of the environment 2. Plenum Press, New York, NY.

TMECC. 2002. Test methods for examination of composting and compost. U.S Composting Council, Holbrook, N.Y.

Whalen, S. C. 2005. Biogeochemistry of methane exchange between natural wetlands and the atmosphere. Environ. Eng. Sci. **22:** 73-87.

Wuebbles, D. J., and Hayhoe, K. 2002. Atmospheric methane and global change. Earth-Science Reviews **57:** 177-210.

Zeiss, C. 2002. Methane oxidation as an engineered greenhouse gas reduction method for solid waste landfills. GMEF 1130, The Federation of Canadian Municipalities, Ottawa, Ont.

4 Conclusion

The results from the lab and field experiments provided insight into the application of a methane oxidizing biofilter. The current section discusses the relationship between the experiments and the application to a full-scale system. The answers to the research questions, outlined in Chapter 1, are also presented.

1.0 Lab and Field Scale Relationship

Both compost and sand-compost-perlite (SCP) were shown to be suitable biofilter mediums. The results from the field experiment for compost further confirmed this. Two similarities were observed. First, both the lab and field usage of compost resulted in low methane surface emissions. In the lab experiment, from day 111 to 238, there were usually no surface emissions observed, while in the field experiment the effluent methane flux was generally measured to be less than 15 $gCH_4 \cdot m^{-2} \cdot d^{-1}$ for sites 1 and 2, respectively. However, the removal rates in the lab scale experiment were 100 % long-term, while in the field experiment they were 76 and 68 % for sites 1 and 2, respectively. The results from the field experiment were more dependent on climatic (temperature, moisture content, and atmospheric pressure) spatial and temporal variations. Second, oxygen was found to be depleted in the top 25 cm in the lab experiment, and in the top 20 to 55 cm at sites 1 and 2 in the field. This suggested, that in both experiments, the majority of the methane oxidation was occurring near the surface of the biofilter medium.

The use of SCP as a biofilter medium presents an alternative to compost, the principal advantage being that SCP was found to compact less than compost. In the field trial, as a result of monitoring surface emissions and maintenance, there was some traffic on the biofilter's surface. In a full-scale system, this would also likely be the case, as some measurements and maintenance (possibly mixing the biofilter's surface for aeration and removing any desiccation cracks, and removing snow cover) would be required. Therefore, the use of a less compactable medium would be beneficial. It's also important to highlight that medium replacement might eventually be necessary as a result of compaction. Eventually, it could be expected that paths of preferential flow will develop and overload certain parts of the biofilter medium resulting in high surface emissions. A potential advantage of SCP is that it would not need to be replaced as frequently as compost, possibly lowering the maintenance costs of operating a biofilter.

2.0 Pilot to Full Scale

From a greenhouse gas mitigation perspective, other methods that reduce the usage of landfills in general, such as waste reduction strategies, waste to energy, composting, and recycling are more effective long-term solutions for reducing greenhouse gas production. From a methane treatment perspective, the usage of a biofilter to treat methane gas presents a potential low cost alternative to the traditional flaring and energy conversion technologies. The biofilter alternative is more suitable for smaller landfills where the traditional treatment options can be both economically and technically non-feasible.

The results from the pilot biofilters (Chapter 3) indicate the approach is suitable for a full-scale application. However, more monitoring events are planned during 2006 and

should give further insight. One critical issue that needs to be addressed in the future is the frequency of advective LFG flow occurrences. This was observed on the October 25th monitoring event, at sites 1 and 2, to cause high methane surface emissions (>148 $gCH_4 \cdot m^{-2} \cdot d^{-1}$). The pilot biofilters were not designed to treat such large influent methane fluxes (> 200 $gCH_4 \cdot m^{-2} \cdot d^{-1}$). A reduction in the biofilter surface area ratio (SAR) could be used to treat larger influent methane fluxes. A reduction would be required since the biofilter medium surface area would be increased (such as at site 3, see Chapter 3).

There would be several considerations in applying the pilot biofilter approach to a full-scale system. In the case of full-scale system, the underlying assumption is it would be part of a post-closure plan for a landfill site (at least for the discussion herein). Therefore, according to Alberta Environment (2005), the final cover would consist of a 0.6 m barrier layer (maximum permeability of $1x10^{-7}$ $m \cdot s^{-1}$), followed by 0.35 m subsoil, and then 0.20 m topsoil. As a result of a low permeability landfill cover, the use of a biofilter geomembrane may not be required, and could be replaced with a lower cost geotextile that would be used to support the barrier layer and prevent mixing with the gas distribution layer. Also, a less permeable landfill cover could cause more landfill gas (LFG) to flow through the biofilter. Therefore, a scale-down factor in the biofilter surface area ratio (SAR) may be required. Determining the biofilter locations would depend on finding hot spots for LFG generation. Also, the results from the Chapter 3 showed that the use of a gas well can allow the passage of more influent LFG, and may be an important criterion when locating biofilters on top of the landfill body.

3.0 Answers to Research Questions

In developing the lab-scale experiment, the following research questions were asked:

1. Can a sand based medium, developed with a turfgrass standard, be as effective as compost at treating methane?

2. Will using a sand based medium reduce settlement when compared to compost? How will this affect the results?

3. Will the formation of exopolymeric substance (EPS), by the methanotrophic bacteria, have an effect on methane removal rates?

The SCP mixture, developed based on the United States Golf Association root zone mixture for turfgrass standard, was found to be as effective as compost at treating methane. Both mediums were found long-term (218 days) to be capable of removing 100 % of the influent flux (134 $gCH_4 \cdot m^{-2} \cdot d^{-1}$). The compost was found to have compacted more than SCP, as shown by bulk density (BD) profiles in Chapter 2. The compaction did not appear to affect the results, since both mediums achieved 100 % removal rates. However, as previously discussed, traffic on the biofilter's surface in a field installation could make using a less compactable medium more desirable. The labile polysaccharides, used to estimate the EPS quantity, were found at lower levels, 23.9 and 7.8 mgD-Glucose$\cdot g^{-1}$ (dry basis) for compost and SCP respectively at the -15 cm depth, than others have reported in the literature and were not found to affect the removal rates.

In developing the pilot biofilter experiment the research questions were:

1. Can 80 % of CH_4 emissions be removed by the pilot biofilters?

2. Can temperature (>20°) and moisture (>0.25 $L \cdot L^{-1}$) levels be adequate to support the methane oxidizing bacteria?

The removal rates for sites 1 (76 %) and 2 (68 %) were lower than the 80 % objective. However, the design employed, including using compost as the biofilter medium and a SAR of 10.8, was deemed successful at mitigating CH_4 emissions as low surface emissions (<15 $gCH_4 \cdot m^{-2} \cdot d^{-1}$) were generally observed. Temperature was on average warmer than 20°C for both sites 1 and 2. The moisture content objective of 0.25 $L \cdot L^{-1}$ was generally met at sites 1 and 2. Larger LFG influent flows and concentrations (at the -160 cm depth) at site 2 likely caused both the larger temperatures and moisture levels observed there. The larger LFG influent flows and concentrations were likely caused by the usage of a gas well at site 2. However, it's also possible that more LFG was generated from the waste than from site 1. Site 3, constructed with a SAR of 4.8, showed lower LFG concentrations and flows, compared to sites 1 and 2. It is possible that since the site was built on top of the landfill, similar to site 2, lateral gas migration might have explained the low influent LFG fluxes. The use of a gas well at site 3 might have increased the influent LFG flows.

4.0 References

Alberta Environment. 2005. Code of practice for landfills [online]. Available from http://environment.gov.ab.ca [cited 11-Jul-2006].

Appendix A - Flux and Methane Removal Rate Formulas and Sample Calculations

This section will present the formulas used and sample calculations for determining influent and effluent fluxes, and removal rates as described in Chapters 2 and 3.

A.1 Determining the Density of Methane or Carbon Dioxide

Equation 1, based on the ideal gas law, was used to determine the density of CH_4 or CO_2:

[1] $$\rho = \frac{P \times MW}{R \times T}$$

Where:

ρ = The density of CH_4 or CO_2 ($g \cdot m^{-3}$) using the ideal gas law
P = Atmospheric Pressure (Pa)
R = Ideal gas law constant (8.314 $J \cdot {}^{o}K^{-1} \cdot mol^{-1}$)
T = Temperature of the gas (^{o}K)
MW = Molecular weight of CH_4 or CO_2 (g)

For Chapter 2 , the lab-scale experiment, the atmospheric pressure used was 93,426 Pa, which was measured in the building the experiment was conducted in. The temperature used was 292 ^{o}K, as was measured in the laboratory. For Chapter 3, the field-scale experiment, the average daily atmospheric pressure was taken from the Environment Canada website (shown in the Chapter 3 reference list) for the Edmonton International Airport. The temperature in the flux chamber was measured during the field monitoring events.

For example, to determine the density (ρ) of CH_4 for the lab-scale experiment:

[1] $$\rho = \frac{93{,}426\ \text{Pa} \times 16\ \text{g}}{8.314\ \text{J}\cdot^{\circ}\text{K}^{-1}\cdot\text{mol}^{-1} \times 292^{\circ}\text{K}} = 615.7\ \text{g}\cdot\text{m}^{-3}$$

For example, to determine the density (ρ) of CH_4 for the field-scale experiment, on Oct 25th for site 1A (quadrant A):

[1] $$\rho = \frac{92{,}580\ \text{Pa} \times 16\ \text{g}}{8.314\ \text{J}\cdot^{\circ}\text{K}^{-1}\cdot\text{mol}^{-1} \times 295.5^{\circ}\text{K}} = 602.9\ \text{g}\cdot\text{m}^{-3}$$

A.2 Determining the Methane Influent and Effluent Fluxes and Removal Rates in the Lab-Scale Experiment

In Chapter 2, the lab-scale experiment, the simulated landfill gas was fed from a cylinder at a constant flow rate. Therefore, the CH_4 influent flux could be determined:

[2] $$Jin_{CH4} = \frac{\rho \times Q_{in} \times Cin_{CH4}}{A}$$

Where:
Jin_{CH4} = CH_4 influent flux ($gCH_4\cdot m^{-2}\cdot d^{-1}$)
Q_{in} = Influent flow (0.0864 $m^3\cdot d^{-1}$)
Cin_{CH4} = Concentration of CH_4 in the influent gas (0.6 $m^{-3}\cdot m^{-3}$)
A = Surface area of the column (0.24 m^2)

[2] $$Jin_{CH4} = \frac{615.7\ \text{g}\cdot\text{m}^{-3} \times 0.6\ \text{m}^3\cdot\text{m}^{-3} \times 0.0864\ \text{m}^3\cdot\text{d}^{-1}}{0.24\ \text{m}^2} = 133.0\ \text{gCH}_4\cdot\text{m}^{-2}\cdot\text{d}^{-1}$$

The effluent flow and CH_4 concentration were measured during each monitoring event. Therefore, the effluent flux could be determined:

[3] $$Jout_{CH4} = \frac{\rho \times Q_{out} \times Cout_{CH4}}{A}$$

Where:
$Jout_{CH4}$ = Effluent CH_4 flux ($gCH_4 \cdot m^{-2} \cdot d^{-1}$)
Q_{out} = Effluent flow ($m^3 \cdot d^{-1}$)
$Cout_{CH4}$ = Concentration of CH_4 in the effluent gas ($m^{-3} \cdot m^{-3}$)

For example, on day 7 the sand-compost-perlite column showed an effluent flow and CH_4 concentration of 0.576 $m^3 \cdot d^{-1}$ and 0.0026 $L \cdot L^{-1}$ respectively. Therefore, $Jout_{CH4}$ was:

[3] $$Jout_{CH4} = \frac{615.7\ g \cdot m^{-3} \times 0.576\ m^3 \cdot d^{-1} \times 0.0026\ L \cdot L^{-1}}{0.24\ m^2} = 3.8\ gCH_4 \cdot m^{-2} \cdot d^{-1}$$

To determine the CH_4 removal rate, a mass balance was used:

[4] $$CH_4\ \text{Removed}\ (\%) = \frac{Jin_{CH4} - Jout_{CH4}}{Jin_{CH4}}$$

In the example given, the CH_4 removal was:

[4] $$CH_4\ \text{Removed}\ (\%) = \frac{133 gCH_4 \cdot m^{-2} \cdot d^{-1} - 3.8\ gCH_4 \cdot m^{-2} \cdot d^{-1}}{133\ gCH_4 \cdot m^{-2} \cdot d^{-1}} = 97.1\ \%$$

A.3 Determining the Effluent Fluxes and Methane Removal Rates in the Field-Scale Experiment

During each monitoring event, as presented in Chapter 3, surface emissions (effluent flux) and concentration profiles were measured for each biofilter site. The surface emission measurements resulted in a concentration versus time plot, as shown in Fig A.1. This shows an example of the change in CH_4 concentration observed over time for site

1A on October 25th and November 28th. A linear regression line for each day is shown (solid black line).

Fig. A.1. CH_4 Concentration vs. Time Plot

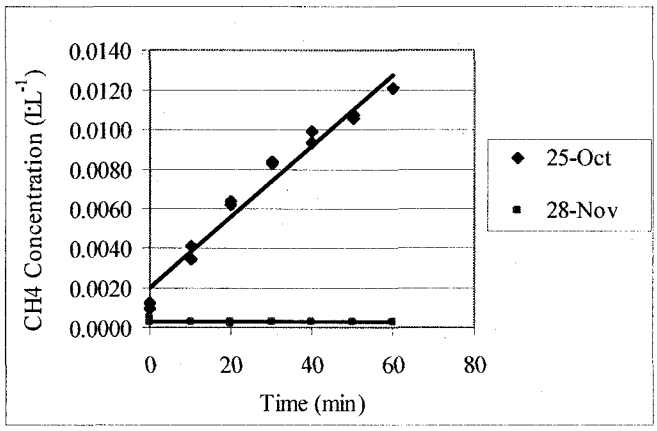

MS Excel® was used to determine the slope of the linear regression model and to conduct an analysis of variance (ANOVA). The ANOVA and linear regression results for October 25th are shown in Fig. A.2.

Fig. A.2. ANOVA and Linear Regression Results for October 25th for Site 1A

ANOVA

	df	*SS*	*MS*	*F*	*Significance F*
Regression	1	0.000180003	0.00018	338.866876	3.66445E-10
Residual	12	6.37429E-06	5.3119E-07		
Total	13	0.000186377			

	Coefficients	*Standard Error*	*t Stat*	*P-value*
Intercept	0.002035714	0.000351158	5.79714311	8.5112E-05
X Variable 1	0.000179286	9.73938E-06	18.4083371	3.6645E-10

The slope (X Variable) of the line was determined to be 0.0001793 $m^3 \cdot m^{-3} \cdot min^{-1}$. To conclude whether there was a significant relationship between the change in CH_4 concentration and time an ANOVA interpretation needed to be made:

Null Hypothesis: Ho: Slope = 0
Hi: Slope <>0

$\alpha = 5\ \%$

The null hypothesis was evaluated using the F statistic. The F computed (338.67) was greater than F critical (F critical = 4.74, $\alpha = 5\ \%$, 1 and 12 degrees of freedom). The null hypothesis was rejected. The variance in the model was due to the regression and not random error. There was a significant relationship between the change in CH_4 concentration and time.

For November 28th the linear regression and ANOVA results are shown in Fig. A.3.

Fig. A.3. ANOVA and Linear Regression Results for November 28th for Site 1A

ANOVA

	df	*SS*	*MS*	*F*	*Significance F*
Regression	1	1.94E-09	1.94E-09	4.53E-01	5.14E-01
Residual	12	5.15E-08	4.30E-09		
Total	13	5.35E-08			

	Coefficients	*Standard Error*	*t Stat*	*P-value*
Intercept	0.000328393	3.15787E-05	10.3991981	2.3424E-07
X Variable 1	-5.89286E-07	8.75835E-07	-0.6728275	0.51380552

The slope (X variable) was determined to be $-5.89\times10^{-7}\ m^3\cdot m^{-3}\cdot min^{-1}$. To conclude whether there was a significant relationship between the change in CH_4 concentration and time an ANOVA interpretation needed to be made:

Null Hypothesis: Ho: Slope = 0
Hi: Slope <>0
$\alpha = 5\ \%$

The null hypothesis was evaluated using the F statistic. The F computed (0.453) was less than F critical (4.74, $\alpha = 5\ \%$, 1 and 12 degrees of freedom). The null hypothesis was not rejected. The variance in the model was due to random error. There was not a significant

relationship between the change in CH_4 concentration and time. There was no observed surface emission.

To calculate the methane effluent flux, the following equations were used:

[5] $$Jout_{CH4} = \frac{\Delta C \times V}{\Delta t \times A}$$

[6] $$J_{CH4} = \frac{\Delta C \times \rho \times V}{\Delta t \times A}$$

Where:
$Jout_{CH4}$ = Volumetric Effluent CH_4 flux ($LCH_4 \cdot m^{-2} \cdot d^{-1}$)
J_{CH4} = Gravimetric Effluent CH_4 flux ($gCH_4 \cdot m^{-2} \cdot d^{-1}$)
$\Delta C/\Delta t$ = Slope of the CH_4 concentration versus time plot ($m^3 \cdot m^{-3} \cdot d^{-1}$)
V = Volume of the flux chamber (m^3)
A = Surface area cover by the flux chamber (m^2)

On October 25th, for site 1A, V and A were 0.0878 m^3 and 0.36 m^2 respectively. The ρ of CH_4, determined in Section A.1, was 602.9 $g \cdot m^{-3}$. The methane fluxes were calculated as:

[5] $$Jout_{CH4} = \frac{0.0001793\ m^3 \cdot m^{-3} \cdot min^{-1} \times (1440\ min \cdot d^{-1}) \times 0.0878\ m^3 \times (1000\ L \cdot m^{-3})}{0.36\ m^2}$$

[5] $$Jout_{CH4} = 62.9\ LCH_4 \cdot m^{-2} \cdot d^{-1}$$

and:

[6] $$J_{CH4} = \frac{0.0001793\ m^3 \cdot m^{-3} \cdot min^{-1} \times (1440\ min \cdot d^{-1}) \times 602.9\ g \cdot m^{-3} \times 0.0878\ m^3}{0.36\ m^2}$$

[6] $$J_{CH4} = 37.9\ gCH_4 \cdot m^{-2} \cdot d^{-1}$$

Similarly, the CO_2 flux was determined using equations 1 (MW of CO_2 is 44 g), 5, and 6, and using the ANOVA analysis. For October 25th, the CH_4 and CO_2 surface emissions

measured for site 1A-1D are shown in Table A-2. The average volumetric results for the CH_4 and CO_2 fluxes were 245 and 338 $L \cdot m^{-2} \cdot d^{-1}$ respectively. The average gravimetric results for the CH_4 and CO_2 fluxes were 148 and 562 $g \cdot m^{-2} \cdot d^{-1}$ respectively. As described in Ch. 3, the gas composition was measured at 5 depths, over four quadrants (A-D). On the October 25th monitoring event, the average CH_4 concentration at the -160 cm depth (tire shreds) was measured to be 0.55 $L \cdot L^{-1}$.

Table A.1. CH_4 and CO_2 Surface Emissions for Site 1 on October 25th

Quadrant	Volumetric (Eq. 5) Surface Emissions ($L \cdot m^{-2} \cdot d^{-1}$)		Gravimetric (Eq. 6) Surface Emissions ($g \cdot m^{-2} \cdot d^{-1}$)	
	CH_4	CO_2	CH_4	CO_2
A	62.9	190.9	37.9	316.4
B	199.8	332.1	121.0	552.9
C	260.8	346.1	157.9	576.2
D	457.6	484.2	276.2	803.7

To determine the methane removal rate, a mass balance was used. However, since the influent CH_4 flux was unknown, the effluent LFG flow assumed to equal the influent flow. Therefore, the influent CH_4 flux was determined by the following equation:

[6] $$Jin_{CH4} = Cin_{CH4} \times [Jout_{CH4} + Jout_{CO2}]$$

Where:
Jin_{CH4} = Volumetric Influent CH_4 flux ($LCH_4 \cdot m^{-2} \cdot d^{-1}$)
$Jout_{CH4}$ = Volumetric Effluent CH_4 flux ($LCH_4 \cdot m^{-2} \cdot d^{-1}$)
$Jout_{CO2}$ = Volumetric Effluent CO_2 flux ($LCO_2 \cdot m^{-2} \cdot d^{-1}$)

For the October 25th monitoring event, the influent CH_4 flux was therefore calculated as:

[6] $$Jin_{CH4} = 0.55\ L \cdot L^{-1} \times (245 + 338\ L \cdot m^{-2} \cdot d^{-1}) = 321\ LCH_4 \cdot m^{-2} \cdot d^{-1}$$

Therefore, the mass balance shown in Eq. 4 can be used to determine the CH_4 removal rate:

[4] $$CH_4 \text{ Removed } (\%) = \frac{(321\ LCH_4 \cdot m^{-2} \cdot d^{-1} - 245\ LCH_4 \cdot m^{-2} \cdot d^{-1})}{321\ LCH_4 \cdot m^{-2} \cdot d^{-1}} = 23.6\ \%$$

Appendix B – Material Characterization Sample Calculations

This section will present the formulas used and sample calculations for determining the material properties of compost and sand-compost-perlite (SCP) presented in Chapters 2 and 3 (compost only).

B.1 Particle Size Distribution (PSD)

The difference between methods in determining the PSD of compost and SCP is that the former is dried (70°C) after sieving, while the latter is dried (105°C) prior to sieving. Both are reported on a dry weight basis. Each sieve fraction was calculated as:

[1] $$Ri = (M_i \div M_B) \times 100$$

Where:

Ri = Relative contribution of sieve size fraction i to bulk mass of sample (%, dry basis)
M_i = Oven dry mass of individual sieve size fraction (dried at 70±5°C) (g)
i = Sieve fraction of interest
M_B = Oven dry mass of bulk sample (dried at 70±5°C) (g)

The results in Ch. 2 are presented as the percentage finer than the respective sieve fraction, which was calculated as:

[2] $$Fi = 100 - (Ri + \Sigma R_L)$$

Where:
Fi = Fraction of soil that is finer than sieve fraction i (%, dry basis)
ΣR_L = Sum of sieve fractions that are larger than sieve i (%, dry basis)

For example, after drying the fraction of compost that was retained in the 6.3 mm sieve, the mass of compost was 3.36 g. The summation of the oven dry weights from all the sieve fractions was 125.07 g. Therefore, Ri was determined as:

[1] $$R_{6.3mm} = 3.36\ g \div 125.07\ g \times 100 = 2.69\ \%$$

The percentage of soil that was finer than 6.3 mm (largest sieve) was determined as:

[2] $$F = 100\ \% - 2.69\ \% = 97.3\ \%$$

B.2 Moisture Content (MC) for Compost SCP

The difference between determine the MC for compost and SCP, is that the former is dried at 70°C, while the latter is dried at 105°C. The MC was determined with the following equation:

[3] $$MC = [M_w - M_d] \div M_w$$

Where:
MC = Moisture content of sample ($g \cdot g^{-1}$, wet basis)
M_d = Dry mass (g)
M_w = Wet mass, prior to drying (g)

For example a compost sample weighed 90.59 and 61.60 g prior to and after drying respectively. The MC was determined:

[3] $$MC = [90.59\ g - 61.60\ g] \div 90.59\ g = 0.3200\ g \cdot g^{-1}\ \text{(wet basis)}$$

B.3 Bulk Density (BD)

The BD was determined (wet or dry basis as dependent of whether the weight of the soil was reported on a dry or wet basis respectively) by the following equation:

[4] $$BD = M \div V$$

Where:
BD = Bulk density ($g \cdot L^{-1}$)
M = Mass of sample (g)
V = Volume of sample (L)

For example, for compost the wet weight was 1420.20 g, while the volume occupied was determined as 1.815 L, the BD was determined as:

[4] $$BD = 1420.20\ g \div 1.815\ L = 782.36\ g \cdot L^{-1}\ \text{(wet basis)}$$

B.4 Particle Density (PD)

The PD was determined by the following equation:

[5] $$PD = \rho \times M_s \div (M_s + M_w - M_{ws})$$

Where:
PD = Particle Density ($g \cdot L^{-1}$)
M_s = dry mass of soil (g)
M_w = Mass of water (g)
M_{ws} = Mass of water and soil (g)
ρ = density of water at 20°C (998.2 $g \cdot L^{-1}$)

The denominator ($M_s + M_w - M_{ws}$) represents the mass of water that occupies the soil volume. For example, a 500 ml beaker was filled with 659.20 g (M_w) of water. The same beaker was filled with compost (M_s = 78.55 g) and then filled with water to the 500

ml mark. The weight of the water and the soil was 695.00 g (M_{sw}). The PD was determined as:

[5] $PD = 998.20\ g \cdot L^{-1} \times 78.55\ g \div (78.55\ g + 659.20\ g - 695.00\ g) = 1834.12\ g \cdot L^{-1}$

B.5 Porosity and Total Air Space (TAS)

Porosity and TAS were determined by the following three equations:

[6] $$MC_v = MC \times BD_w \div \rho$$

Where:
MC_v = Volumetric water content ($L \cdot L^{-1}$)
BD_w = Bulk density ($g \cdot L^{-1}$, wet basis)
MC = Gravimetric MC ($g \cdot g^{-1}$, wet basis)
ρ = density of water at 20°C (998.20 $g \cdot L^{-1}$)

[7] $$\varepsilon = 1 - (BD_d \div PD)$$

Where:
ε = Porosity ($L \cdot L^{-1}$)
BD_d = Bulk Density ($g \cdot L^{-1}$, dry basis)
PD = Particle Density ($g \cdot L^{-1}$)

[8] $$TAS = \varepsilon - MC_v$$

Where:
TAS = Total Air Space ($L \cdot L^{-1}$)

For example, for compost it was determined that the average BD_d, BD_w, PD, and MC values were 772.58 $g \cdot L^{-1}$ (wet basis), 577.87 $g \cdot L^{-1}$ (dry basis), 1857.53 $g \cdot L^{-1}$, and 0.2519 $g \cdot g^{-1}$ (wet basis) respectively. Therefore, the volumetric MC, porosity, and TAS were determined as:

[6] $MC_v = 0.2519\ g \cdot g^{-1} \times 772.48\ g \cdot L^{-1} \div 998.20\ g \cdot L^{-1} = 0.20\ L \cdot L^{-1}$

[7] $\varepsilon = 1 - (577.87\ g \cdot L^{-1} \div 1857.53\ g \cdot L^{-1}) = 0.69\ L \cdot L^{-1}$

[8] $TAS = 0.69\ L \cdot L^{-1} - 0.19\ L \cdot L^{-1} = 0.49\ L \cdot L^{-1}$

B.6 Organic Matter (OM)

The organic matter was determined with the following equation:

[9] $$OM = (M_d - M_{550}) \div M_d$$

Where:
OM = Organic matter (loss on ignition at 550°C) ($g \cdot g^{-1}$, dry basis)
M_{550} = Mass of sample after ignition ay 550°C (g)
M_d = Mass of dried sample (g)

For example, a SCP sample had a dry mass of 11.0636 g, and after combustion at 550°C had a mass of 10.5342 g. The OM was determined as:

[9] $OM = (11.0636\ g - 10.5342\ g) \div 11.0636\ g = 0.04785\ g \cdot g^{-1}$ (dry basis)

B.7 Compost Maturity

The compost maturity was analyzed by placing a sample in a closed vessel. The vessel also contained a CO_2 trap, consisting of a beaker and 1M NaOH. The use of the trap allowed for the determination of the CO_2 production by the compost sample. After letting the vessel incubate for 24 hrs (34°C) the trap was removed and titrated with 0.67 M HCL, until the phenolphthalein end point (pH = 8.3). The titration was compared to that of another NaOH trap that was incubated with no sample (blank). The CO_2 evolution rate (ER) was then calculated as:

[10] $$CO_2\ ER = \frac{(HCL_s - HCL_b) \times (HCL_m \times 6\ g \cdot mol^{-1})}{M_s \times (1\text{-}MC) \times OM}$$

Where:
CO_2 ER = CO_2 production in compost ($mgC\text{-}CO_2 \cdot g^{-1}OM \cdot d^{-1}$)
HCL_s = Titration volume in compost sample (ml)
HCL_b = Titration volume in blank sample (ml)
HCL_m = Molarity of HCL (0.67 M)
6 = Conversion factor, i.e. 6 g of C-CO_2 trapped is equivalent to 1 mol of HCL titrated
M_s = Mass of sample (g)
MC = Moisture content of sample ($g \cdot g^{-1}$, wet basis)
OM = Organic matter ($g \cdot g^{-1}$, dry basis)

For example, for a compost sample, the following values were observed:

HCL_s =34.1 ml
HCL_b = 35.5 ml
M_s = 52.86 g
MC = 0.3575 $g \cdot g^{-1}$ (wet basis)
OM = 0.18 $g \cdot g^{-1}$ (dry basis)

Therefore, the CO_2 ER was calculated as:

$$[10]\ CO_2\ ER = \frac{(35.5\ ml - 34.1\ ml) \times (0.67\ M \times 6\ g \cdot mol^{-1})}{52.86\ g \times (1\text{-}0.3575\ g \cdot g^{-1}) \times 0.1789\ g \cdot g^{-1}} \times \frac{1000\ mg}{1\ g} \times \frac{1\ L}{1000\ ml}$$

[10] CO_2 ER = 0.93 $mgC\text{-}CO_2 \cdot g^{-1}OM \cdot d^{-1}$

Note the test was repeated for four days, with a new trap being placed in the vessel every day. The overall CO_2 ER was determined from the average result over the 4 days.

B.8 Labile Polysaccharides

The exopolymeric substance (EPS) content of a soil sample was approximated as labile polysaccharides. A standard curve was made by plotting known concentrations of D-glucose (dextrose) versus the absorbance readings at 490 nm in a spectrophotometer. The D-Glucose was prepared by mixing with concentrated H_2SO_4 and a phenol solution. Soil

samples were first passed through a hydrolysis procedure, and then prepared and measured as the standard samples. The standard curve is shown in Fig. B.1.

Fig. B.1. Standard Curve and Linear Regression Equation

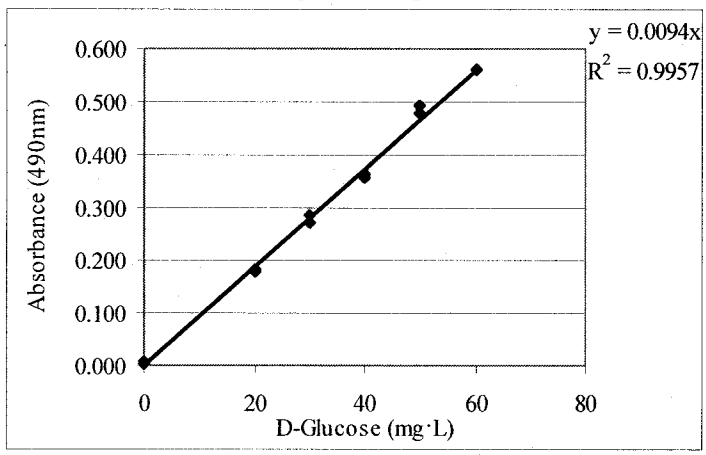

To determine the labile polysaccharides content of a sample the following equation was used:

[11] Labile Polysaccharides (D-glucose) = D-Glucose x V x D ÷ (M_s x (1-MC))

Where:

Labile Polysaccharides = Labile polysaccharides content (mgD-Glucose·g^{-1}, dry basis)
D-Glucose = D-Glucose concentration (mg·L)
V = Volume of sample solution (0.1 L)
D = Dilution Factor (for SCP 5-25 cm depth segment and all compost samples were diluted by a factor of 3)
M_s = Mass of sample (g)
MC = Moisture content of sample ($g \cdot g^{-1}$, wet basis)

For example, a SCP sample (0.97 g) from the 5-25 cm depth segment was analyzed with the spectrophotometer yielding a value 0.209 (490 nm). The concentration of glucose was determined from the standard curve (0.209/0.0094) and was 22.23 $mg \cdot L^{-1}$. The MC

of the sample was 0.17 $g \cdot g^{-1}$ (wet basis). The labile polysaccharides content of the soil was determine as:

[11] Labile Polysaccharides = 22.23 $mg \cdot L^{-1}$ x 0.1 L x 3 ÷ (0.97 x (1-0.17 $g \cdot g^{-1}$))
[11] Labile Polysaccharides = 8.3 mgD-Glucose$\cdot g^{-1}$ (dry basis)

B.9 Methane Oxidation Potential (MOP)

The results from each MOP test were plotted to determine if the removal of the headspace CH_4 was zero (linear) or first (exponential) order. Figure B.2 shows the MOP result for a SCP (replicate #1) sample from the 5-25 cm depth segment. The resulting plot shows an exponential shape, and therefore using MS Excel® trendline fitter, an exponential model was fitted to the data, yielding an exponential slope constant of -0.1321 hr^{-1}.

Fig. B.2. First Order MOP Results for SCP Sample (25-45 cm, Replicate #1)

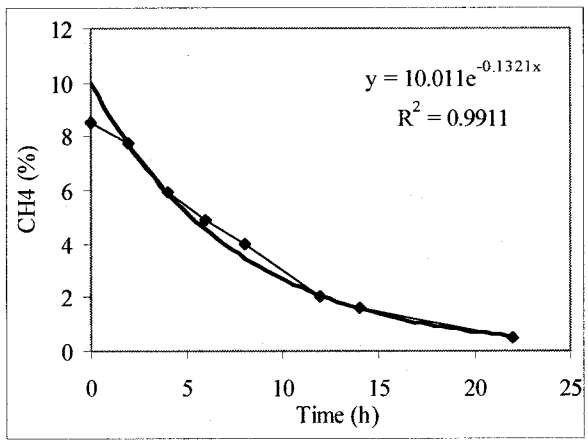

Similarly, Fig. B.3 shows an example of zero order result for a SCP (45-65 depth segment, replicate #1). The results are linear, and therefore the slope constant was -0.001977 $m \cdot m^{-3} \cdot h^{-1}$.

Fig. B.3. Zero Order MOP Results for SCP Sample (45-65 cm, Replicate #1)

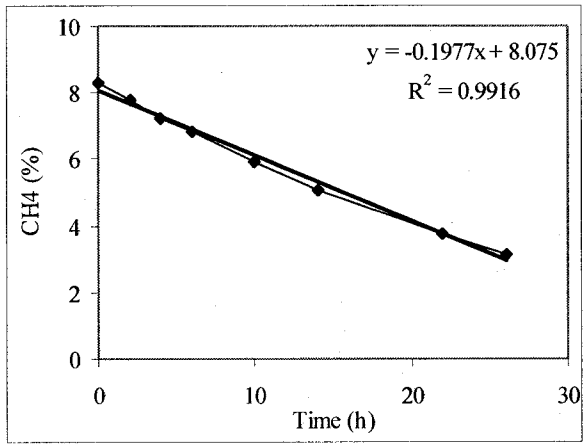

The first order results were expressed as $d^{-1} \cdot gOM^{-1}$. For the SCP sample shown in Fig. B.2, the dry weight was 8.69 g and the OM was 0.04813 $g \cdot g^{-1}$. The MOP was determined as:

MOP (First Order) = 0.1321 hr^{-1} x 24 $hr \cdot d^{-1}$ ÷ (8.69 g x 0.04813 $g \cdot g^{-1}$) = 7.6 $d^{-1} \cdot gOM^{-1}$

The zero order results were expressed as $\mu molCH_4 \cdot gOM^{-1} \cdot d^{-1}$. The first step was to convert the slope constant from a volumetric quantity to a gravimetric one. This was done using equation 1 from Appendix A (with the only difference using a temperature of 295°K), which yield a density of methane of 609.5 $g \cdot m^{-3}$. Also, the volume of the chamber used in the MOP test was 0.26 L. Therefore the MOP result for the SCP sample (10.34 g dry weight)shown Fig. B.3 was calculated as:

$$MOP = \frac{0.001977\ m \cdot m^{-3} \cdot h^{-1} \times 24\ h \cdot d^{-1} \times 609.5\ g \cdot m^{-3} \times 0.26\ L \times (1000 \times 1000\ \mu mol \cdot mol^{-1})}{10.34\ g \times 0.04813\ g \cdot g^{-1} \times 1000\ L \cdot m^{-3}\ 16\ gCH_4 \cdot mol^{-1}CH_4}$$

MOP (Zero Order) = 943.5 $\mu molCH_4 \cdot gOM^{-1} \cdot d^{-1}$

Appendix C - Time Domain Reflectometry Calibration

The Moisture Point® system works on the principles of time domain reflectometry (TDR). The system consists of a controller that is connected to a probe. The probe consists of several independent segments. Upon activating the controller, a radio-frequency signal is sent to each segment in the probe. The system measures the time delay for the signal to travel the length of the segment and back. As the moisture content (MC) of the soil increases, its dielectric capacity increases and the time delay increases. The system is factory calibrated to relate the time delay to volumetric MC. However, this was done for a sandy soil, and in order to get accurate readings for compost a calibration was required.

The calibration was done by comparing the TDR reading to the calculated volumetric MC of the compost sample. A column (Length 94.1 cm, ID = 3.8 cm) was filled with compost. The bulk density (BD) was determined by measuring the weight and volume of the compost. The TDR probe (type K, total length = 82.5 cm, 4 segments, 15 cm per segment) was inserted into the soil, and measurements were taken 5-7 times. The probe was then removed, the column was dropped several times to compact the compost. The BD was determined again. The probe was re-inserted, and the measurements were recorded. The process was repeated once more (i.e. the compost was compacted further). Afterwards a compost sample was dried (70^0C) for 24 h and the gravimetric MC was determined. The test was conducted at four gravimetric moisture contents (0.09- 0.36 $g \cdot g^{-1}$, wet basis). The volumetric MC was determined from the gravimetric MC and BD results by the following equation:

[1] $$MC_v = \frac{MC_g \times BD}{\rho}$$

where the MC_v ($L \cdot L^{-1}$) is the volumetric MC, MC_g ($g \cdot g^{-1}$, wet basis) is the gravimetric MC, BD ($g \cdot L^{-1}$, wet basis) is the bulk density, and ρ (0.9982 $g \cdot L^{-1}$) is the density of water at 20°C.

Table C.1 shows the results from the calibration. The TDR results show the overall average of the four segments over the 7 measurements. As expected, as the calculated volumetic MC increased the TDR readings increased.

Table C.1. Results from TDR Calibration

Calculated Volumetric MC			TDR Readings	
MC ($g \cdot g^{-1}$, wet basis)	BD ($g \cdot L^{-1}$, wet basis)	Volumetic MC ($L \cdot L^{-1}$)	TDR Results (Avg. from 4 segments)	SE
0.086	0.939	0.08	0.02	0.01
0.086	1.008	0.09	0.03	0.01
0.160	0.868	0.14	0.06	0.02
0.162	0.900	0.15	0.07	0.02
0.161	0.918	0.15	0.07	0.02
0.242	0.906	0.22	0.10	0.02
0.242	0.965	0.23	0.10	0.01
0.242	1.003	0.24	0.12	0.01
0.292	0.916	0.27	0.16	0.01
0.292	0.969	0.28	0.17	0.02
0.292	1.020	0.30	0.20	0.03
0.371	0.926	0.34	0.22	0.03
0.366	0.994	0.36	0.25	0.04
0.364	1.040	0.38	0.29	0.06
0.366	0.971	0.36	0.25	0.02
0.365	1.045	0.38	0.26	0.07
0.361	1.054	0.38	0.29	0.10

Figure C.1 shows the TDR readings versus the calculated volumetric MC. The linear regression line shows a good relationship between the two variables, and was used to calculate volumetric MC based on the TDR readings.

Fig. C.1. TDR Readings versus Calculated Vol. MC

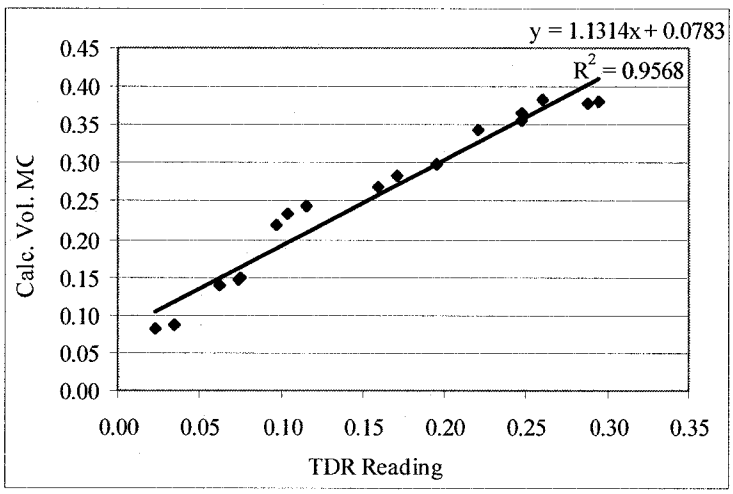

Appendix D – Material Characterization Results

D.1 Initial Material Characterization for Column Experiment

Table D.1. Compost Sieve Analysis (Replicate 1) Results

Sieve Number:	Opening [mm]	Dry Weight (g)	% Retained (Dry)	% Finer (Dry)
	6.3	3.36	2.69%	97.31%
5	4	12.43	9.94%	87.37%
10	2	26.31	21.04%	66.34%
20	0.85	67.14	53.68%	12.66%
40	0.425	15.83	12.66%	0.00%
60	0.25	0.00	0.00%	0.00%
end	0.001	0.0	0.00%	0.00%

Table D.2. Compost Sieve Analysis (Replicate 2) Results

Sieve Number:	Opening [mm]	Dry Weight (g)	% Retained (Dry)	% Finer (Dry)
	6.3	3.85	2.90%	97.10%
5	4	13.98	10.51%	86.59%
10	2	31.75	23.86%	62.73%
20	0.85	75.53	56.76%	5.98%
40	0.425	7.95	5.98%	0.00%
60	0.25		0.00%	0.00%
end	0.001		0.00%	0.00%

Table D.3. Sand Compost Perlite Sieve Analysis (Replicate 1) Results

Sieve Number:	Opening [mm]	Dry Weight (g)	% Retained (Dry)	% Finer (Dry)
4	4.76	6.3	0.19%	13.79%
10	2	18.5	0.56%	13.22%
20	0.85	24.9	0.76%	12.46%
40	0.425	146.7	4.48%	7.98%
60	0.25	177.4	5.42%	2.57%
100	0.15	55.4	1.69%	0.88%
200	0.075	24.2	0.74%	0.14%
end	0.0001	4.5	0.14%	0.00%

Table D.4. Sand Compost Perlite Sieve Analysis (Replicate 2) Results

Sieve Number:	Opening [mm]	Dry Weight (g)	% Retained (Dry)	% Finer (Dry)
4	4.76	6.1	1.22%	98.78%
10	2	18.3	3.67%	95.11%
20	0.85	14.6	2.93%	92.18%
40	0.425	130.7	26.22%	65.96%
60	0.25	220.1	44.15%	21.81%
100	0.15	78.9	15.83%	5.98%
200	0.075	24.2	4.85%	1.12%
end	< 0,075	5.6	1.12%	0.00%

Table D.5. Moisture Content Analysis Results

Sample	Net Sample Weight (g)	Net dry Weight (g)	Moisture Content ($g \cdot g^{-1}$, wet basis)
Sand Compost Perlite	101.24	86.68	0.144
Sand Compost Perlite	101.27	87.11	0.140
Sand Compost Perlite	78.79	66.57	0.155
Compost	90.59	61.60	0.320
Compost	90.5	62.35	0.311
Compost	90.9	62.57	0.312

Table D.6. Bulk Density Analysis Results

Sample	Net Sample Weight (g)	Moisture Content ($g \cdot g^{-1}$, wet basis)	Net dry Weight (g)	Volume of Sample (L)	Bulk Density ($g \cdot L^{-1}$, wet basis)	Bulk Density ($g \cdot L^{-1}$, dry basis)
Compost	1420.20	0.25	1062.41	1.82	782.45	585.33
Compost	1386.90	0.25	1037.50	1.82	764.10	571.61
Compost	1399.20	0.25	1046.70	1.82	770.88	576.67
Sand-Perlite-Compost	397850.00	0.15	339644.55	312.50	1273.12	1086.86

Table D.7. Particle Density Analysis Results

Sample	Dry Soil Weight (g)	Flask with Water & Sample (g)	Flask with Water (g)	Particle Density (20°C, $g \cdot L^{-1}$)
Compost	78.55	695.00	659.20	1834.17
Compost	77.05	712.70	679.30	1761.97
Compost	76.98	763.90	725.80	1976.46
Sand Column Mix	83.48	706.10	662.10	2110.61
Sand Column Mix	92.84	708.80	655.30	2355.65
Sand Column Mix	81.33	775.30	735.50	1954.84

Table D.8. Porosity and Total Air Space Results

Sample	Bulk Density ($g \cdot L^{-1}$, dry basis)	Particle Density (20°C, $g \cdot L^{-1}$)	Vol. Moisture Content ($L \cdot L^{-1}$)	Porosity ($L \cdot L^{-1}$)	Total Air Space($L \cdot L^{-1}$)
Compost	577.87	1857.53	0.24	0.69	0.45
Sand-Compost-Perlite	1086.86	2140.36	0.19	0.49	0.31

Table D.8. Organic Matter Analysis Results

Sample	Dry Sample Weight (g, 70°C)	Dry Sample Weight (g, 550°C)	Organic Matter ($g \cdot g^{-1}$, dry basis)
Compost	11.6518	9.1727	0.2128
Compost	10.2165	8.13	0.2042
Compost	10.8877	8.7383	0.1974
Sand-Compost-Perlite	11.0636	10.5342	0.0479
Sand-Compost-Perlite	10.6059	10.106	0.0471
Sand-Compost-Perlite	10.8483	10.3122	0.0494

Table D.9. Total Carbon and Nitrogen Analysis Results

Total Carbon or Nitrogen	Compost Sample	
	1	2
Total Carbon ($mg \cdot g^{-1}$, dry basis)	89.76	87.83
Total Nitrogen ($mg \cdot g^{-1}$, dry basis)	8.38	8.31

Table D.10. pH Analysis Results

Replicate	Sand-Compost-Perlite (pH)	Compost (pH)
1	7.23	7.16
2	7.21	7.13
3	7.21	7.14

Table D.11. Electrical Conductivity Analysis Results

Replicate	Sand-Compost-Perlite ($dS \cdot m^{-1}$)	Compost ($dS \cdot m^{-1}$)
1	0.83	2.18
2	0.80	2.16
3	0.82	2.20

D.2 Initial Material Characterization for Field-Scale Experiment

Table D.12. Moisture Content Analysis Results

Sample	Net Sample Weight (g)	Net dry Weight (g)	Moisture Content ($g \cdot g^{-1}$, wet basis)
Compost	48.53	33.67	0.31
Compost	48.43	33.41	0.31
Compost	47.64	32.8	0.31

Table D.13. Organic Matter Analysis Results

Sample	Dry Sample Weight (g, 70°C)	Dry Sample Weight (g, 550°C)	Organic Matter ($g \cdot g^{-1}$, dry basis)
Compost	8.3914	6.9712	0.1692
Compost	10.3013	8.3750	0.1870
Compost	12.4497	10.2049	0.1803

Table D.14. Total Carbon and Nitrogen Analysis Results

Total Carbon or Nitrogen	Sample		
	1	2	3
Total Carbon ($mg \cdot g^{-1}$, dry basis)	79.92	82.40	80.70
Total Nitrogen ($mg \cdot g^{-1}$, dry basis)	8.49	8.70	8.30

Table D.15. pH Analysis Results

Sample	Sample #1 (pH)		Sample #2 (pH)	
Replicate	1	2	1	2
Compost	7.49	7.45	7.49	7.52

Table D.16. Electrical Conductivity Analysis Results

Sample	Sample #1 ($dS \cdot m^{-1}$)		Sample #2 ($dS \cdot m^{-1}$)	
Replicate	1	2	1	2
Compost	2.71	2.76	2.70	2.84

Table D.17. Compost Maturity Analysis Results

Sample	Net Sample Mass (g)	Total Solids ($g \cdot g^{-1}$, wet basis)	Titration Volume (ml)				mg $C\text{-}CO_2\text{-}gOM^{-1}d^{-1}$			
			Day 1	Day 2	Day 3	Day 4	Day 1	Day 2	Day 3	Day 4
Blank			35.5	37.8	36.75	38.55	-	-	-	-
Compost	52.86	0.64	34.1	36.34	35.25	36.75	0.932	0.972	0.999	1.199
Compost	54.29	0.64	34.1	35.67	35.55	36.80	0.908	1.381	0.778	1.135
Compost	50.51	0.64	34.3	36.32	35.7	36.60	0.836	1.032	0.732	1.359

D.3 Post Column Experiment Analysis

Table D.18. Post-Experiment Moisture Content Analysis Results (Sand-Compost-Perlite)

Depth (cm)	Moisture Content ($g \cdot g^{-1}$, wet basis)					
	1-1	1-2	2-1	2-2	3-1	3-2
0-5	0.134	0.148	0.142	0.141	0.136	0.129
5-25	0.167	0.162	0.166	0.166	0.168	0.177
25-45	0.139	0.140	0.129	0.139	0.142	0.135
45-65	0.128	0.127	0.129	0.123	0.130	0.131
65-85	0.131	0.158	0.129	0.139	0.125	0.131
85-105	0.142	0.139	0.146	0.155	0.147	0.139
105-125	0.183	0.199	0.190	0.188	0.199	0.201

Table D.19. Post-Experiment Moisture Content Analysis Results (Compost)

Depth (cm)	Moisture Content ($g \cdot g^{-1}$, wet basis)					
	1-1	1-2	2-1	2-2	3-1	3-2
0-5	0.316	0.309	0.306	0.308	0.308	0.303
5-25	0.342	0.345	0.367	0.338	0.337	0.335
25-45	0.338	0.337	0.326	0.334	0.327	0.332
45-65	0.330	0.328	0.327	0.328	0.325	0.333
65-85	0.332	0.325	0.322	0.297	0.329	0.326
85-105	0.330	0.324	0.336	0.332	0.333	0.327
105-125	0.352	0.342	0.343	0.347	0.342	0.336

Table D.20. Post-Experiment Bulk Density Analysis Results (Sand-Compost-Perlite)

Depth (cm)	Depth Removed (m)	Sample Weight (kg)	Bulk Density ($g \cdot L^{-1}$, wet basis)	Bulk Density ($g \cdot L^{-1}$, dry basis)
0-5	-	-	-	-
5-25	0.20	66.90	1274.98	1061.24
25-45	0.20	68.40	1304.91	1125.76
45-65	0.20	60.40	1145.29	998.67
65-85	0.20	67.50	1286.95	1112.49
85-105	0.20	73.00	1396.69	1194.81
105-125	-	-	-	-

Table D.21. Post-Experiment Bulk Density Analysis Results (Compost)

Depth (cm)	Depth Removed (m)	Sample Weight (kg)	Bulk Density ($g \cdot L^{-1}$, wet basis)	Bulk Density ($g \cdot L^{-1}$, dry basis)
0-5	-	-	-	-
5-25	0.25	53.65	808.49	530.41
25-45	0.17	42.62	958.22	639.97
45-65	0.20	71.70	1370.76	920.59
65-85	0.20	78.80	1512.42	1025.90
85-105	0.20	70.40	1344.82	900.39
105-125	-	-	-	-

Table D.22. Post-Experiment Particle Density Analysis Results (Sand-Compost-Perlite)

Depth (cm)	Particle Density ($20^{\circ}C$, $g \cdot L^{-1}$)	
	1-1	1-2
0-5	2111.1	1978.3
5-25	1849.0	1971.1
25-45	2156.4	2050.6
45-65	1987.6	1946.8
65-85	2082.6	1997.6
85-105	1961.7	1917.5
105-125	1845.8	1979.6

Table D.23. Post-Experiment Particle Density Analysis Results (Compost)

Depth (cm)	Particle Density ($20^{\circ}C$, $g \cdot L^{-1}$)	
	1-1	1-2
0-5	2091.7	1987.8
5-25	1945.5	1949.0
25-45	1811.1	1959.6
45-65	1750.9	1883.4
65-85	1875.2	1909.6
85-105	2059.6	1906.6
105-125	1722.7	1880.4

Table D.24. Post-Experiment Porosity and TAS Analysis Results (Sand-Compost-Perlite)

Depth (cm)	Bulk Density ($g \cdot L^{-1}$, dry basis)	Particle Density (20°C, $g \cdot L^{-1}$)	Vol. Moisture Content ($L \cdot L^{-1}$)	Porosity ($L \cdot L^{-1}$)	Total Air Space($L \cdot L^{-1}$)
0-5	-	2044.7	-		
5-25	1061.2	1910.0	0.21	0.44	0.23
25-45	1125.8	2103.5	0.18	0.46	0.29
45-65	998.7	1967.2	0.15	0.49	0.35
65-85	1112.5	2040.1	0.17	0.45	0.28
85-105	1194.8	1939.6	0.20	0.38	0.18
105-125	-	1912.7	-	-	-

Table D.25. Post-Experiment Porosity and TAS Analysis Results (Compost)

Depth (cm)	Bulk Density ($g \cdot L^{-1}$, dry basis)	Particle Density (20°C, $g \cdot L^{-1}$)	Vol. Moisture Content ($L \cdot L^{-1}$)	Porosity ($L \cdot L^{-1}$)	Total Air Space($L \cdot L^{-1}$)
0-5	-	2039.7	-	-	-
5-25	530.4	1947.2	0.28	0.73	0.45
25-45	640.0	1885.4	0.32	0.66	0.34
45-65	920.6	1817.1	0.45	0.49	0.04
65-85	1025.9	1892.4	0.49	0.46	*0.00*
85-105	900.4	1983.1	0.45	0.55	0.10
105-125	-	1801.5	-	-	-

Table D.26. Post-Experiment pH Analysis Results (Sand-Compost-Perlite)

Depth (cm)	Sample #1 (pH)		Sample #2 (pH)	
	1-1	1-2	2-1	2-2
0-5	7.03	7.1	7.08	7.08
5-25	7.21	7.27	7.24	7.27
25-45	7.24	7.19	7.16	7.19
45-65	7.34	7.41	7.45	7.42
65-85	7.51	7.43	7.52	7.48
85-105	7.59	7.57	7.46	7.43
105-125	7.65	7.68	7.75	7.68

Table D.27. Post-Experiment pH Analysis Results (Compost)

Depth (cm)	Sample #1 (pH)		Sample #2 (pH)	
	1-1	1-2	2-1	2-2
0-5	7.02	7.03	7.00	7.00
5-25	7.75	7.79	7.77	7.80
25-45	7.85	7.82	7.84	7.87
45-65	8.12	8.07	8.02	8.06
65-85	8.09	8.09	8.12	8.10
85-105	8.29	8.30	-	8.26
105-125	8.34	8.33	8.35	8.33

Table D.28. Post-Experiment Electrical Conductivity Analysis Results (Sand-Compost-Perlite)

Depth (cm)	Sample #1 ($dS \cdot m^{-1}$)		Sample #2 ($dS \cdot m^{-1}$)	
	1-1	1-2	2-1	2-2
0-5	0.56	0.49	0.47	0.43
5-25	0.39	0.57	0.43	0.45
25-45	0.47	0.50	0.55	0.47
45-65	0.31	0.33	0.30	0.35
65-85	0.51	0.31	0.48	0.55
85-105	0.55	0.63	0.54	0.56
105-125	0.30	0.57	0.64	0.59

Table D.29. Post-Experiment Electrical Conductivity Analysis Results (Compost)

Depth (cm)	Sample #1 ($dS \cdot m^{-1}$)		Sample #2 ($dS \cdot m^{-1}$)	
	1-1	1-2	2-1	2-2
0-5	1.98	2.06	2.03	2.12
5-25	1.72	1.69	1.78	1.81
25-45	1.45	1.42	1.38	1.37
45-65	1.34	1.37	1.42	1.36
65-85	1.46	1.41	1.47	1.53
85-105	1.56	1.52	0.00	1.49
105-125	1.69	1.70	1.70	1.69

Table D.30. Post-Experiment Total Carbon Analysis Results (Sand-Compost-Perlite)

Depth (cm)	Total Carbon ($mg \cdot g^{-1}$, dry basis)			
	1-1	1-2	2-1	2-2
0-5	10.67	12.16	12.96	13.83
5-25	12.45	11.39	12.88	14.69
25-45	11.71	7.21	10.01	7.13
45-65	7.69	6.14	4.99	5.72
65-85	6.12	6.03	6.81	6.18
85-105	6.01	7.20	4.13	10.14
105-125	9.73	13.41	9.88	11.65

Table D.31. Post-Experiment Total Nitrogen Analysis Results (Sand-Compost-Perlite)

Depth (cm)	Total Nitrogen ($mg \cdot g^{-1}$, dry basis)			
	1-1	1-2	2-1	2-2
0-5	1.15	0.85	1.30	0.95
5-25	1.29	0.92	1.37	1.32
25-45	0.91	0.30	0.75	0.24
45-65	0.52	0.00	0.20	0.06
65-85	0.26	0.00	0.37	0.00
85-105	0.25	0.17	0.10	0.35
105-125	0.65	0.73	0.70	0.51

Table D.32. Post-Experiment Total Carbon Analysis Results (Compost)

Depth (cm)	Total Carbon ($mg \cdot g^{-1}$, dry basis)			
	1-1	1-2	2-1	2-2
0-5	82.76	74.34	76.10	78.19
5-25	78.20	86.28	87.51	98.59
25-45	73.17	80.90	77.53	88.00
45-65	70.98	86.74	69.67	81.56
65-85	68.18	80.86	83.85	76.43
85-105	75.93	79.32	72.28	80.67
105-125	76.67	91.26	78.77	85.63

Table D.33. Post-Experiment Total Nitrogen Analysis Results (Compost)

Depth (cm)	Total Nitrogen ($mg \cdot g^{-1}$, dry basis)			
	1-1	1-2	2-1	2-2
0-5	8.75	8.14	8.61	8.59
5-25	9.42	9.77	10.42	11.73
25-45	9.07	9.27	9.23	9.10
45-65	8.31	9.17	8.69	8.80
65-85	7.62	8.27	8.78	7.38
85-105	8.52	7.63	7.97	7.73
105-125	8.73	8.78	8.26	8.67

Table D.34. Post-Experiment Labile Polysaccharides Results (Sand-Compost-Perlite)

Depth (cm)	Exopolymeric Substance (mgD-Glucose$\cdot g^{-1}$, dry basis)			
	1-1	1-2	2-1	2-2
0-5	4.99	5.60	3.95	6.52
5-25	8.26	6.23	8.87	0.00
25-45	3.21	2.56	4.44	3.32
45-65	4.19	3.39	3.89	2.31
65-85	3.88	2.97	2.87	2.58
85-105	2.54	3.48	3.22	2.46
105-125	2.28	2.85	2.73	2.99

Table D.35. Post-Experiment Labile Polysaccharides Results (Compost)

Depth (cm)	Exopolymeric Substance (mgD-Glucose$\cdot g^{-1}$, dry basis)			
	1-1	1-2	2-1	2-2
0-5	17.24	12.74	15.89	14.94
5-25	23.63	21.74	22.38	27.67
25-45	19.80	19.99	20.47	15.17
45-65	18.52	20.11	18.75	20.55
65-85	22.31	20.39	21.00	18.38
85-105	21.10	19.46	18.71	18.44
105-125	19.79	0.00	20.57	19.83

Table D.36. Post-Experiment First Order Methane Oxidation Potential Results

Sample	Depth (cm)	1st Order Slope (hr^{-1})		1st Order Slope ($d^{-1} \cdot g^{-1}$, dry basis)		1st Order Slope ($d^{-1} \cdot gOM^{-1}$, dry basis)	
		1-1	1-2	1-1	1-2	1-1	1-2
Sand-Compost-Perlite	5-25	0.132	0.149	0.365	0.411	7.58	8.55
Sand-Compost-Perlite	25-45	0.062	0.054	0.168	0.142	3.49	2.96
Compost	5-25	0.419	0.384	1.305	1.292	6.37	6.31
Compost	25-45	0.194	0.253	0.759	0.876	3.71	4.28
Compost	45-65	0.174	0.099	0.582	0.309	2.84	1.51

Table D.37. Post-Experiment Zero Order Methane Oxidation Potential Results

Sample	Depth (cm)	Zero Order Slope ($L \cdot L^{-1} \cdot h^{-1}$)		Zero Order Slope ($\mu mol \cdot g^{-1} \cdot d^{-1}$)		Zero Order Slope ($\mu mol \cdot gOM^{-1} \cdot d^{-1}$)	
		1-1	1-2	1-1	1-2	1-1	1-2
Sand-Compost - Perlite	45-65	0.00198	0.00158	45.4	42.2	943.8	877.0

Appendix E Column Operation Results

Table E.1. Sand-Compost-Perlite Column Oxygen Gas Profile Results

Day	Depth / Oxygen (%, vol. basis)							
	0	5	25	45	65	85	105	157
0	17.59%	21.17%	18.80%	15.82%	15.22%	14.49%	13.86%	21.03%
1	19.21%	18.56%	16.21%	13.20%	10.67%	8.10%	6.46%	2.32%
2	16.54%	16.03%	9.51%	3.56%	1.46%	1.23%	0.71%	0.75%
5	11.80%	7.08%	1.94%	1.10%	1.13%	1.53%	0.56%	0.26%
7	12.54%	8.98%	1.81%	2.00%	2.35%	2.44%	1.27%	1.12%
9	10.84%	5.84%	2.32%	2.69%	1.60%	0.56%	0.39%	0.71%
10	12.19%	7.57%	2.14%	1.44%	0.92%	1.49%	0.48%	1.76%
12	10.99%	7.60%	1.75%	1.88%	1.84%	1.25%	0.60%	1.56%
14	11.92%	8.67%	1.43%	1.40%	1.52%	0.71%	0.60%	0.30%
16	12.49%	8.32%	1.41%	1.60%	-	-	0.45%	0.45%
17	12.46%	9.68%	2.07%	1.63%	1.05%	0.67%	0.46%	1.07%
20	12.79%	8.66%	1.39%	1.05%	-	-	1.83%	2.44%
21	12.47%	8.56%	1.20%	1.79%	1.47%	0.96%	0.55%	0.40%
23	13.13%	9.68%	3.17%	1.00%	3.38%	3.48%	1.97%	0.48%
25	13.32%	10.02%	1.95%	1.51%	1.48%	0.79%	0.91%	0.62%
28	15.56%	11.78%	1.93%	2.09%	1.50%	2.35%	2.23%	0.77%
30	13.05%	8.76%	1.74%	2.12%	2.07%	1.04%	1.71%	0.96%
33	12.21%	8.25%	1.21%	1.05%	1.57%	0.78%	-	-
36	11.61%	7.65%	1.43%	0.94%	1.21%	0.89%	0.77%	1.01%
38	12.72%	11.35%	1.58%	1.93%	1.52%	1.36%	1.26%	2.53%
42	11.62%	8.43%	1.40%	1.12%	0.97%	1.70%	0.78%	2.49%
44	11.81%	8.99%	2.32%	3.15%	2.30%	-	1.06%	-
47	12.42%	9.53%	1.25%	0.87%	1.16%	0.60%	0.86%	1.90%
49	11.89%	8.45%	1.15%	1.74%	1.71%	1.58%	1.11%	2.37%
51	11.89%	8.71%	1.19%	1.51%	1.10%	0.70%	0.68%	1.50%
54	9.19%	7.31%	1.96%	1.22%	1.94%	2.68%	0.60%	8.69%
58	12.83%	-	-	-	2.69%	1.88%	-	0.95%
63	14.02%	-	-	-	-	-	-	10.98%
65	11.47%	8.32%	1.53%	1.34%	3.96%	-	1.29%	-
68	20.52%	19.51%	18.15%	18.04%	13.97%	11.71%	10.13%	2.02%
75	11.02%	-	-	-	-	-	-	1.47%
77	19.00%	17.91%	14.72%	13.32%	14.47%	11.74%	11.11%	-
84	20.90%	18.88%	18.82%	17.89%	16.50%	11.90%	10.77%	8.95%
86	18.83%	-	-	-	-	-	-	1.14%
114	15.35%	10.60%	1.86%	1.49%	1.57%	0.88%	1.06%	1.30%
119	14.14%	-	-	-	-	-	-	0.43%
121	13.04%	9.34%	1.74%	2.65%	2.30%	1.25%	1.39%	0.57%
124	10.73%	7.28%	1.47%	1.71%	2.45%	0.95%	1.05%	0.76%
126	12.53%	-	-	-	-	-	-	0.64%
128	15.73%	13.78%	3.31%	2.69%	2.48%	2.63%	-	-
132	13.41%	10.44%	2.17%	3.53%	4.66%	1.53%	0.78%	0.72%
135	11.21%	7.81%	1.55%	1.87%	1.71%	1.34%	1.13%	1.25%
138	13.70%	-	-	-	-	-	-	1.30%
140	15.72%	14.26%	2.39%	2.58%	2.07%	1.30%	0.85%	0.42%
142	16.66%	13.60%	2.00%	2.26%	1.83%	1.41%	0.82%	0.84%
145	16.53%	13.79%	2.45%	2.21%	1.49%	0.94%	0.70%	0.66%

147	15.51%	-	-	-	-	-	-	0.88%
149	15.97%	14.00%	2.14%	3.15%	2.28%	1.47%	0.55%	0.35%
152	16.56%	13.92%	1.83%	1.87%	1.63%	1.17%	0.76%	0.43%
154	14.25%	-	-	-	-	-	-	0.51%
156	14.02%	11.46%	1.48%	1.88%	1.57%	1.19%	0.65%	0.38%
159	15.10%	13.58%	2.13%	3.75%	2.70%	1.51%	1.16%	0.67%
163	14.57%	12.60%	1.85%	3.27%	2.10%	1.35%	0.88%	0.43%
166	12.71%	9.47%	1.53%	1.77%	1.46%	1.05%	0.69%	0.51%
168	15.47%	-	-	-	-	-	-	0.42%
170	13.99%	11.53%	1.45%	1.82%	1.18%	1.06%	0.61%	0.29%
173	13.21%	9.90%	1.72%	1.83%	1.02%	1.27%	0.86%	0.66%
177	14.95%	12.68%	1.67%	2.39%	1.60%	1.06%	0.82%	0.56%
181	13.62%	10.68%	1.74%	2.09%	1.98%	1.33%	1.38%	2.04%
184	14.35%	11.81%	1.80%	2.18%	1.57%	1.37%	0.79%	0.49%
188	15.11%	11.52%	1.33%	1.62%	1.51%	1.14%	1.16%	0.51%
194	13.82%	11.04%	1.35%	1.85%	1.52%	1.30%	0.77%	1.31%
198	14.43%	10.87%	2.07%	3.04%	1.82%	1.04%	0.82%	0.68%
203	12.96%	-	-	-	-	-	-	0.59%
205	13.92%	11.64%	1.87%	2.45%	1.91%	1.33%	0.73%	0.57%
210	13.08%	10.30%	1.59%	1.65%	1.36%	0.87%	0.74%	1.36%
218	17.01%	14.77%	2.14%	2.01%	1.79%	1.51%	1.31%	2.02%
226	12.81%	9.25%	1.75%	1.69%	1.32%	1.17%	2.12%	1.86%
232	14.97%	11.97%	1.70%	1.83%	1.56%	1.05%	1.39%	0.93%
238	15.42%	11.48%	1.66%	1.61%	1.43%	1.16%	0.69%	0.56%

Table E.2. Sand-Compost-Perlite Column Nitrogen Gas Profile Results

Day	Depth / Nitrogen (%, vol. basis)							
	0	5	25	45	65	85	105	157
0	80.26%	78.69%	79.79%	80.82%	81.48%	82.20%	82.84%	78.57%
1	83.83%	81.77%	81.65%	78.50%	65.94%	58.85%	51.29%	20.67%
2	76.48%	75.85%	71.81%	65.20%	59.01%	48.20%	37.60%	18.70%
5	79.99%	80.84%	70.79%	54.90%	45.95%	33.73%	24.84%	10.07%
7	79.48%	77.72%	72.75%	60.76%	54.04%	37.76%	38.73%	18.70%
9	81.19%	76.40%	66.72%	53.28%	43.34%	30.86%	23.63%	7.40%
10	79.79%	78.94%	71.06%	59.29%	44.67%	40.00%	29.74%	7.30%
12	78.36%	80.06%	70.49%	59.71%	52.92%	42.46%	31.43%	6.76%
14	79.99%	80.52%	71.69%	58.75%	50.41%	37.22%	29.49%	1.64%
16	79.88%	80.01%	70.17%	56.81%	-	-	27.21%	2.21%
17	77.85%	79.74%	71.83%	58.39%	48.98%	36.65%	28.61%	6.36%
20	79.32%	79.13%	70.99%	56.76%	-	-	29.15%	10.42%
21	77.91%	77.33%	62.43%	52.38%	43.31%	31.10%	22.80%	2.62%
23	79.26%	79.58%	83.73%	58.52%	54.70%	43.81%	33.56%	3.74%
25	79.57%	79.67%	73.06%	59.85%	51.34%	37.25%	29.02%	8.81%
28	79.52%	80.89%	79.12%	70.77%	59.62%	55.98%	49.50%	7.24%
30	79.00%	78.33%	68.87%	56.04%	49.37%	34.98%	29.56%	4.47%
33	77.88%	76.81%	63.43%	48.36%	40.73%	27.64%	-	-
36	78.44%	77.71%	64.19%	48.65%	40.51%	31.04%	23.11%	3.78%
38	80.20%	79.70%	71.03%	57.77%	48.22%	37.33%	32.39%	9.61%
42	77.76%	77.06%	63.68%	48.80%	39.75%	29.79%	20.68%	9.42%
44	78.42%	77.59%	65.36%	52.79%	45.89%	-	24.66%	-
47	79.00%	78.66%	67.00%	52.16%	42.70%	29.24%	22.50%	7.14%

49	78.34%	77.76%	63.39%	49.77%	42.36%	31.08%	22.81%	8.97%
51	79.88%	79.06%	69.26%	57.79%	48.81%	35.68%	27.55%	5.66%
54	76.35%	78.43%	61.40%	47.37%	43.32%	33.75%	21.42%	32.06%
58	79.49%	-	-	-	49.59%	37.46%	-	3.59%
63	77.62%	-	-	-	-	-	-	41.59%
65	78.57%	77.70%	64.40%	50.52%	46.34%	-	24.22%	-
68	78.59%	78.90%	79.01%	80.70%	84.06%	80.91%	71.41%	7.67%
75	76.93%	-	-	-	-	-	-	5.45%
77	79.20%	78.69%	77.76%	76.76%	75.64%	75.57%	73.94%	-
84	79.20%	78.25%	78.63%	78.89%	79.52%	80.01%	76.39%	33.56%
86	78.96%	-	-	-	-	-	-	4.24%
114	80.10%	80.86%	74.52%	60.40%	51.27%	36.70%	28.81%	5.49%
119	80.92%	-	-	-	-	-	-	6.59%
121	80.83%	81.34%	72.22%	59.79%	50.56%	35.57%	27.90%	5.92%
124	81.36%	81.61%	67.76%	52.95%	44.59%	28.52%	21.56%	4.90%
126	81.28%	-	-	-	-	-	-	5.19%
128	80.33%	80.49%	81.23%	72.95%	64.27%	50.69%	-	-
132	82.29%	81.25%	73.63%	62.89%	56.65%	40.21%	30.62%	10.53%
135	81.76%	81.65%	68.74%	53.75%	43.25%	28.94%	20.86%	6.15%
138	80.88%	-	-	-	-	-	-	8.32%
140	79.95%	80.98%	79.68%	69.04%	57.27%	40.97%	29.99%	6.50%
142	82.01%	81.08%	79.62%	67.93%	57.11%	40.99%	29.87%	6.29%
145	83.14%	83.05%	79.33%	64.43%	52.49%	35.37%	25.75%	5.54%
147	79.37%	-	-	-	-	-	-	8.26%
149	80.26%	80.75%	78.85%	65.75%	54.67%	37.68%	26.41%	3.89%
152	81.70%	80.84%	78.79%	65.91%	56.22%	41.39%	31.71%	7.19%
154	80.65%	-	-	-	-	-	-	5.57%
156	80.63%	80.80%	74.57%	62.19%	52.35%	37.73%	27.95%	5.59%
159	80.77%	80.50%	76.95%	66.53%	56.95%	41.15%	32.41%	8.05%
163	80.86%	82.28%	75.52%	64.46%	53.99%	38.83%	29.24%	5.97%
166	81.21%	81.35%	70.02%	56.38%	46.14%	31.72%	23.10%	4.82%
168	80.48%	-	-	-	-	-	-	5.94%
170	80.68%	80.84%	74.32%	62.05%	51.99%	37.95%	28.57%	5.53%
173	81.31%	81.53%	70.96%	55.78%	43.49%	29.06%	20.26%	3.80%
177	80.90%	81.27%	77.13%	65.65%	55.70%	40.52%	30.71%	6.68%
181	81.04%	81.30%	72.64%	58.77%	49.09%	34.57%	26.65%	10.55%
184	80.74%	81.06%	73.07%	59.84%	49.50%	35.16%	25.65%	5.14%
188	80.78%	80.99%	71.46%	61.92%	47.76%	37.16%	24.73%	5.69%
194	81.15%	81.42%	71.88%	59.18%	48.72%	34.68%	25.29%	7.75%
198	82.25%	81.04%	71.08%	59.25%	48.54%	34.05%	25.49%	6.10%
203	81.17%	-	-	-	-	-	-	4.80%
205	80.61%	80.70%	72.28%	60.40%	50.23%	35.65%	25.76%	5.64%
210	80.79%	80.72%	71.47%	57.99%	46.62%	31.63%	23.06%	5.81%
218	80.82%	80.49%	82.20%	72.35%	63.45%	48.63%	38.35%	13.41%
226	81.32%	81.34%	66.35%	52.24%	41.90%	28.94%	24.35%	8.59%
232	80.66%	80.76%	72.74%	60.73%	51.22%	36.93%	29.94%	7.89%
238	80.45%	80.96%	71.18%	58.44%	48.40%	34.29%	25.08%	4.81%

Table E.3. Sand-Compost-Perlite Column Carbon Dioxide Gas Profile Results

Day	Depth / Carbon Dioxide (%, vol. basis)							
	0	5	25	45	65	85	105	157
0	2.05%	0.15%	1.60%	3.62%	4.04%	4.22%	4.29%	0.12%
1	1.32%	1.79%	4.10%	7.03%	9.80%	14.22%	18.21%	32.00%
2	3.13%	4.23%	11.10%	18.58%	22.29%	26.25%	28.80%	34.66%
5	8.01%	12.73%	22.04%	27.54%	30.02%	33.07%	35.30%	38.78%
7	7.50%	11.93%	20.95%	24.79%	27.23%	31.48%	31.67%	35.44%
9	9.52%	14.77%	22.33%	26.13%	29.63%	33.58%	35.32%	37.72%
10	7.89%	12.57%	21.22%	25.75%	29.54%	30.93%	34.36%	36.79%
12	9.28%	12.49%	21.05%	24.39%	26.55%	29.98%	33.14%	37.14%
14	8.16%	11.43%	21.44%	25.68%	27.91%	32.11%	34.06%	39.31%
16	7.43%	11.85%	22.12%	26.38%	-	-	34.94%	39.16%
17	8.16%	10.73%	21.18%	25.97%	29.08%	32.62%	34.66%	37.77%
20	7.27%	11.81%	22.01%	26.96%	-	-	33.19%	35.24%
21	8.05%	12.48%	24.77%	27.14%	30.02%	33.35%	35.57%	39.17%
23	7.08%	10.86%	19.80%	26.00%	26.98%	30.35%	31.91%	38.96%
25	6.64%	10.16%	20.55%	25.14%	27.80%	32.05%	34.02%	37.64%
28	4.68%	8.39%	19.24%	21.85%	25.67%	26.39%	28.38%	37.76%
30	7.32%	11.72%	22.08%	25.46%	27.16%	31.92%	33.18%	37.84%
33	8.67%	12.99%	24.45%	28.83%	30.29%	34.05%	-	-
36	9.14%	13.49%	24.03%	28.85%	30.92%	33.46%	35.50%	38.02%
38	7.42%	9.12%	21.41%	25.68%	28.36%	31.59%	34.45%	35.59%
42	8.87%	12.56%	24.25%	28.62%	31.02%	32.82%	35.43%	35.34%
44	8.75%	12.07%	23.02%	25.72%	28.28%	-	34.81%	-
47	8.06%	11.25%	23.56%	28.10%	30.36%	34.00%	35.49%	36.68%
49	8.86%	12.99%	24.54%	27.80%	30.04%	32.76%	34.92%	35.68%
51	8.06%	11.58%	22.07%	26.08%	28.73%	32.49%	34.39%	37.11%
54	11.63%	15.22%	24.06%	28.71%	29.12%	31.29%	35.25%	26.29%
58	7.23%	-	-	-	26.46%	29.86%	-	38.49%
63	7.59%	-	-	-	-	-	-	22.16%
65	9.37%	12.92%	24.53%	28.82%	27.69%	-	35.16%	-
68	0.60%	1.45%	2.77%	3.01%	4.21%	6.40%	10.11%	36.77%
75	10.24%	-	-	-	-	-	-	37.73%
77	2.53%	3.81%	7.91%	10.03%	9.28%	12.86%	13.86%	
84	0.76%	1.85%	2.09%	2.78%	3.69%	6.78%	8.64%	24.46%
86	1.98%	-	-	-	-	-	-	38.24%
114	4.95%	9.27%	20.45%	25.04%	27.38%	31.63%	33.55%	38.82%
119	5.85%	-	-	-	-	-	-	38.40%
121	6.77%	10.33%	20.87%	24.33%	27.16%	31.96%	33.73%	38.34%
124	8.81%	12.59%	23.20%	26.96%	28.74%	33.94%	35.47%	38.46%
126	7.12%	-	-	-	-	-	-	38.34%
128	4.86%	6.77%	16.97%	20.74%	23.96%	28.47%	-	-
132	6.65%	9.76%	20.28%	23.05%	24.00%	31.09%	33.96%	37.76%
135	8.56%	12.02%	22.65%	26.76%	29.47%	33.61%	35.65%	38.30%
138	6.47%	-	-	-	-	-	-	37.88%
140	4.34%	6.56%	18.99%	22.97%	26.21%	31.41%	34.46%	39.05%
142	4.23%	6.76%	18.82%	22.35%	25.80%	30.68%	33.99%	38.82%
145	4.54%	7.04%	19.27%	23.55%	27.32%	32.48%	35.13%	38.81%
147	4.11%	-	-	-	-	-	-	37.66%
149	3.99%	5.06%	18.72%	22.12%	26.63%	32.09%	35.57%	39.96%
152	3.61%	5.73%	18.87%	23.29%	26.45%	31.29%	34.28%	39.41%

154	5.70%	-	-	-	-	-	-	39.55%
156	5.86%	8.63%	20.76%	24.56%	27.71%	32.21%	35.11%	39.59%
159	5.00%	6.67%	19.52%	21.71%	25.92%	31.31%	33.80%	39.12%
163	5.46%	7.96%	20.03%	22.81%	26.64%	31.64%	34.18%	39.01%
166	7.12%	10.32%	21.60%	25.97%	28.96%	33.27%	35.58%	38.68%
168	4.71%	-	-	-	-	-	-	38.97%
170	5.83%	8.55%	20.73%	24.35%	28.06%	32.19%	34.56%	39.09%
173	6.58%	9.85%	21.59%	26.14%	29.78%	33.69%	36.04%	38.93%
177	4.61%	7.06%	18.79%	21.96%	25.22%	29.80%	32.91%	38.60%
181	6.34%	9.52%	21.65%	25.09%	28.24%	32.71%	34.66%	37.00%
184	5.57%	8.41%	21.00%	24.89%	28.19%	32.27%	34.97%	39.18%
188	5.01%	8.58%	21.65%	24.95%	28.71%	32.43%	35.07%	38.93%
194	6.13%	9.13%	21.59%	25.50%	28.70%	32.59%	35.44%	38.52%
198	6.50%	9.34%	21.40%	25.04%	28.90%	33.52%	35.72%	39.45%
203	7.09%	-	-	-	-	-	-	39.95%
205	6.06%	8.60%	21.47%	25.21%	28.38%	32.92%	35.86%	39.65%
210	6.89%	10.02%	22.13%	26.64%	29.78%	34.13%	36.50%	38.96%
218	2.75%	4.42%	16.82%	18.46%	21.73%	26.45%	29.94%	36.77%
226	7.18%	10.94%	23.57%	27.84%	31.10%	34.56%	35.20%	38.36%
232	5.35%	8.43%	21.45%	25.32%	28.34%	32.88%	34.44%	38.79%
238	4.99%	9.02%	22.13%	26.21%	29.55%	33.53%	36.28%	39.87%

Table E.4. Sand-Compost-Perlite Column Methane Gas Profile Results

Day	Depth / Methane (%, vol. basis)							
	0	5	25	45	65	85	105	157
0	0.00%	0.00%	0.00%	0.00%	0.00%	0.00%	0.00%	0.00%
1	3.20%	5.97%	8.03%	12.73%	16.00%	21.69%	27.08%	47.33%
2	2.92%	3.80%	8.69%	15.81%	23.70%	36.97%	35.71%	49.30%
5	0.00%	0.04%	8.01%	19.53%	26.53%	36.60%	41.80%	53.07%
7	0.26%	1.89%	5.89%	14.78%	22.72%	35.54%	32.67%	47.96%
9	0.23%	3.84%	10.66%	20.75%	28.43%	37.77%	42.94%	55.71%
10	0.16%	1.51%	6.97%	15.96%	27.50%	30.06%	37.82%	55.26%
12	1.48%	0.32%	8.26%	16.39%	21.34%	29.32%	37.43%	55.93%
14	0.44%	0.12%	7.18%	16.77%	22.98%	32.74%	38.43%	59.86%
16	0.19%	0.50%	7.99%	17.87%	-	-	40.06%	59.46%
17	1.68%	0.30%	6.50%	16.75%	23.54%	32.74%	38.84%	56.55%
20	0.80%	1.16%	7.25%	17.81%	-	-	38.28%	54.17%
21	1.75%	2.33%	14.07%	21.16%	27.98%	37.20%	43.43%	59.20%
23	0.64%	0.40%	6.29%	17.24%	25.24%	35.21%	35.49%	58.80%
25	0.33%	0.48%	5.69%	15.85%	21.93%	32.39%	38.48%	54.71%
28	0.00%	0.00%	0.79%	6.79%	15.75%	17.62%	22.40%	56.12%
30	1.11%	1.47%	9.02%	18.56%	23.80%	37.28%	39.03%	58.16%
33	2.45%	3.09%	13.72%	26.01%	29.50%	40.20%	-	-
36	2.02%	2.60%	12.38%	25.94%	27.82%	37.36%	43.78%	59.15%
38	0.57%	0.57%	7.61%	17.81%	26.66%	32.76%	36.11%	54.83%
42	2.06%	2.69%	13.00%	24.00%	30.68%	38.45%	45.08%	54.27%
44	1.95%	2.53%	11.85%	20.66%	26.20%	-	42.27%	-
47	1.34%	2.40%	10.70%	21.52%	28.70%	38.55%	43.99%	56.06%
49	2.05%	2.86%	13.25%	23.30%	29.16%	37.72%	43.53%	54.82%
51	0.62%	1.25%	8.83%	17.70%	24.13%	33.70%	39.82%	57.19%
54	3.86%	4.94%	15.65%	26.38%	29.06%	35.57%	45.04%	35.55%

58	0.76%	-	-	-	24.80%	33.47%	-	57.96%
63	1.60%	-	-	-	-	-	-	30.08%
65	1.62%	3.04%	11.51%	21.65%	25.13%	-	41.93%	-
68	0.00%	0.00%	0.04%	0.67%	2.52%	5.53%	12.55%	58.21%
75	3.37%	-	-	-	-	-	-	57.26%
77	0.00%	0.00%	0.00%	0.00%	0.00%	0.00%	0.00%	
84	0.05%	0.00%	0.00%	0.00%	0.00%	1.46%	4.58%	36.34%
86	0.00%	-	-	-	-	-	-	57.74%
114	0.00%	0.00%	6.14%	16.58%	22.97%	27.84%	37.10%	56.42%
119	0.00%	-	-	-	-	-	-	56.82%
121	0.14%	0.07%	7.39%	16.34%	23.27%	34.43%	40.00%	57.07%
124	0.10%	0.45%	10.92%	21.56%	27.62%	39.70%	44.64%	57.28%
126	0.04%	-	-	-	-	-	-	57.94%
128	0.00%	0.00%	0.44%	6.03%	12.49%	23.15%	-	-
132	0.00%	0.08%	5.69%	13.24%	16.30%	30.78%	37.54%	53.19%
135	0.06%	0.39%	10.19%	21.08%	28.61%	39.40%	45.17%	56.36%
138	0.00%	-	-	-	-	-	-	54.50%
140	0.00%	0.00%	1.37%	9.76%	17.43%	29.35%	37.68%	56.07%
142	0.00%	0.00%	1.52%	10.23%	18.22%	30.00%	38.44%	56.76%
145	0.00%	0.00%	3.32%	13.16%	21.65%	34.12%	41.55%	57.02%
147	0.00%	-	-	-	-	-	-	54.11%
149	0.00%	0.00%	2.60%	11.79%	20.55%	32.71%	40.48%	58.19%
152	0.00%	0.00%	2.90%	11.84%	18.79%	29.43%	36.81%	55.60%
154	0.00%	-	-	-	-	-	-	56.90%
156	0.00%	0.00%	5.38%	14.28%	21.53%	31.73%	39.41%	56.91%
159	0.00%	0.00%	3.43%	10.66%	18.66%	30.13%	33.80%	55.42%
163	0.00%	0.00%	5.05%	13.34%	21.17%	32.67%	39.09%	57.48%
166	0.00%	0.00%	9.00%	18.96%	26.76%	37.60%	42.81%	58.29%
168	0.00%	-	-	-	-	-	-	57.19%
170	0.00%	0.01%	5.72%	14.66%	22.17%	32.27%	39.58%	57.86%
173	0.00%	0.05%	9.16%	20.52%	28.87%	39.36%	45.94%	58.75%
177	0.00%	0.00%	4.91%	13.51%	21.03%	32.06%	39.32%	57.00%
181	0.00%	0.00%	7.74%	17.00%	24.72%	36.53%	41.33%	53.42%
184	0.00%	0.00%	7.08%	16.44%	24.20%	34.66%	42.01%	58.23%
188	0.00%	0.00%	8.00%	14.88%	25.61%	33.24%	42.80%	57.56%
194	0.00%	0.00%	7.78%	17.15%	24.52%	34.82%	41.58%	54.91%
198	0.00%	0.00%	8.23%	16.89%	25.05%	35.23%	41.47%	56.49%
203	0.00%	-	-	-	-	-	-	57.66%
205	0.00%	0.01%	7.46%	16.33%	23.41%	34.44%	41.57%	57.07%
210	0.00%	0.03%	7.67%	18.31%	26.42%	36.90%	43.14%	56.63%
218	0.00%	0.00%	1.69%	9.57%	16.42%	26.95%	33.88%	51.38%
226	0.00%	0.06%	11.53%	21.72%	29.12%	38.42%	42.52%	54.09%
232	0.00%	0.00%	6.59%	15.25%	22.11%	32.75%	38.45%	54.95%
238	0.00%	0.03%	7.94%	17.10%	24.40%	34.81%	41.64%	57.44%

Table E.5. Compost Column Oxygen Gas Profile Results

Day	Depth / Oxygen (%, vol. basis)							
	0	5	25	45	65	85	105	157
0	14.41%	9.42%	8.94%	6.90%	6.39%	5.26%	5.07%	21.03%
1	18.92%	16.85%	13.53%	10.06%	6.00%	-	-	
2	16.21%	11.47%	3.72%	1.49%	-	3.34%	-	0.33%
5	14.24%	5.74%	1.49%	1.55%	-	0.57%	-	1.04%
7	15.55%	9.75%	1.66%	1.56%	2.22%	0.89%	1.18%	0.68%
9	15.26%	8.98%	1.55%	1.33%	1.43%	0.94%	0.77%	1.02%
10	15.26%	10.86%	3.08%	1.74%	2.22%	1.10%	0.71%	1.00%
12	15.03%	7.88%	2.55%	2.46%	1.48%	1.11%	0.63%	0.75%
14	14.57%	5.32%	2.70%	2.37%	1.62%	3.22%	1.14%	0.30%
16	15.51%	8.11%	2.21%	1.74%	1.15%	-	0.57%	0.47%
17	14.58%	7.22%	1.55%	1.24%	1.41%	0.85%	0.42%	0.21%
20	13.99%	7.00%	1.99%	1.51%	0.94%	-	-	1.53%
21	13.92%	6.13%	1.94%	1.17%	1.26%	1.76%	1.07%	0.67%
23	14.32%	6.32%	1.89%	1.43%	1.66%	-	1.32%	0.38%
25	13.92%	6.54%	3.09%	1.74%	1.94%	0.89%	1.76%	1.02%
28	16.92%	11.89%	4.64%	1.37%	1.78%	1.33%	-	1.29%
30	14.10%	7.12%	2.58%	1.71%	1.29%	0.79%	1.12%	0.52%
33	13.30%	4.96%	1.72%	1.61%	1.50%	1.15%	1.96%	-
36	14.60%	6.89%	2.47%	1.95%	1.51%	0.83%	0.78%	1.46%
38	14.36%	5.70%	2.32%	1.66%	2.58%	1.10%	3.23%	0.93%
40	13.76%	5.23%	1.91%	1.88%	2.49%	0.59%	2.58%	1.89%
42	14.42%	8.03%	2.88%	4.66%	1.89%	0.61%	0.55%	0.47%
44	13.81%	7.04%	2.20%	2.99%	1.05%	0.61%	0.54%	4.14%
47	14.08%	6.25%	2.41%	1.63%	1.10%	1.02%	0.69%	4.39%
49	14.24%	6.00%	1.97%	2.18%	2.22%	2.05%	2.09%	9.97%
51	14.24%	7.20%	1.78%	1.62%	1.54%	0.73%	0.85%	2.04%
54	10.37%	4.28%	2.14%	2.07%	1.59%	1.53%	2.05%	2.93%
58	11.26%	2.80%	2.21%	2.39%	1.44%	-	-	1.80%
63	16.06%	-	-	-	-	-	-	9.09%
65	8.87%	2.46%	2.53%	2.35%	2.28%	1.46%	3.78%	3.11%
75	15.42%	-	-	-	-	-	-	1.15%
77	19.51%	17.38%	14.23%	12.57%	11.21%	7.79%	8.94%	
84	19.58%	17.68%	15.84%	13.97%	10.17%	6.57%	8.64%	7.52%
86	13.26%	-	-	-	-	-	-	2.62%
114	18.45%	17.14%	8.76%	1.96%	2.11%	1.36%	1.37%	1.30%
119	18.98%	-	-	-	-	-	-	0.65%
121	19.45%	16.93%	9.82%	2.91%	2.02%	1.85%	1.29%	0.27%
124	18.90%	16.66%	9.17%	3.59%	3.42%	1.91%	2.13%	0.44%
126	19.45%	-	-	-	-	-	-	0.24%
128	20.09%	18.68%	14.04%	5.98%	4.19%	2.98%	2.81%	-
132	19.79%	18.78%	12.74%	5.11%	3.04%	1.97%	1.67%	0.36%
135	19.43%	17.27%	10.08%	3.11%	2.57%	2.22%	2.12%	0.93%
138	20.16%	-	-	-	-	-	-	-
140	21.24%	20.52%	16.36%	8.91%	2.21%	1.54%	1.80%	0.72%
142	17.71%	13.10%	3.76%	2.24%	1.79%	1.14%	1.74%	0.36%
145	17.21%	12.24%	2.35%	2.71%	1.63%	0.98%	0.97%	1.29%
147	17.66%	-	-	-	-	-	-	0.31%
149	17.84%	12.13%	1.89%	4.74%	2.36%	0.61%	1.07%	0.16%
152	18.20%	12.13%	2.10%	2.35%	1.55%	0.57%	1.15%	0.27%

154	17.62%	-	-	-	-	-	-	0.66%
156	17.64%	14.21%	4.32%	2.41%	1.66%	0.71%	1.10%	0.42%
159	17.93%	15.68%	5.54%	4.38%	2.48%	1.16%	1.63%	0.65%
163	14.06%	6.99%	2.78%	3.94%	2.21%	0.55%	1.47%	0.47%
166	12.92%	5.61%	1.62%	2.40%	1.65%	0.46%	1.10%	0.64%
168	17.62%	-	-	-	-	-	-	0.66%
170	14.46%	6.75%	1.49%	1.93%	1.17%	1.16%	1.06%	0.32%
173	12.72%	4.09%	1.89%	3.34%	1.15%	0.43%	1.77%	1.25%
177	14.44%	7.57%	2.01%	2.89%	1.55%	0.71%	1.25%	0.55%
181	17.10%	13.97%	4.64%	2.59%	1.97%	1.62%	3.58%	2.02%
184	14.88%	8.19%	1.87%	3.17%	1.81%	0.93%	1.26%	0.71%
188	14.90%	6.87%	1.65%	2.83%	1.66%	1.25%	1.99%	0.12%
194	13.33%	5.14%	1.49%	2.52%	1.84%	0.93%	2.29%	0.10%
198	16.33%	9.54%	2.10%	4.84%	1.95%	0.80%	1.28%	0.30%
203	13.71%	-	-	-	-	-	-	0.32%
205	14.29%	7.09%	1.77%	4.06%	1.95%	0.78%	2.00%	0.11%
210	14.90%	8.99%	1.51%	2.60%	1.44%	1.09%	1.97%	0.85%
218	15.95%	10.52%	1.70%	2.33%	1.62%	1.21%	2.06%	0.20%
226	13.61%	6.37%	1.57%	2.28%	1.28%	1.04%	2.37%	0.25%
232	15.47%	9.16%	1.72%	2.38%	1.51%	1.02%	3.02%	0.50%
238	16.65%	11.02%	1.98%	1.83%	1.28%	1.36%	0.59%	1.10%

Table E.6. Compost Column Nitrogen Gas Profile Results

Day	Depth / Nitrogen (%, vol. basis)							
	0	5	25	45	65	85	105	157
0	82.94%	85.51%	85.78%	88.35%	88.08%	88.44%	89.22%	78.57%
1	79.96%	78.33%	77.16%	74.71%	69.71%	-	-	-
2	80.37%	82.89%	83.56%	75.11%	-	51.14%	-	13.05%
5	80.57%	83.18%	76.36%	63.02%	-	31.43%	-	7.76%
7	79.01%	81.59%	81.43%	70.34%	58.85%	43.99%	32.55%	11.79%
9	79.68%	79.47%	63.21%	65.68%	54.54%	36.77%	27.76%	4.18%
10	80.35%	81.13%	81.63%	72.48%	55.96%	45.69%	34.41%	5.77%
12	79.83%	81.42%	79.02%	69.35%	59.25%	45.53%	34.46%	5.32%
14	79.90%	78.20%	74.96%	65.76%	51.98%	40.57%	28.29%	1.29%
16	79.57%	78.60%	77.11%	65.55%	53.60%	-	28.93%	4.13%
17	79.53%	81.38%	76.53%	59.49%	52.54%	37.28%	26.75%	2.53%
20	80.08%	81.05%	74.19%	61.56%	47.64%	-	-	5.92%
21	79.96%	80.11%	75.26%	61.89%	49.65%	35.61%	23.48%	2.53%
23	79.93%	80.07%	73.97%	64.53%	52.88%	-	29.98%	5.04%
25	79.94%	81.26%	76.06%	62.53%	52.18%	36.15%	28.05%	4.88%
28	79.40%	80.88%	81.34%	76.22%	68.85%	56.85%	-	8.43%
30	79.89%	81.06%	76.69%	67.03%	54.50%	38.92%	30.32%	2.98%
33	80.67%	80.83%	71.45%	58.28%	45.78%	30.00%	23.39%	-
36	80.25%	81.01%	73.77%	61.44%	48.68%	35.30%	26.10%	5.33%
38	80.55%	81.30%	73.54%	61.29%	50.25%	34.72%	30.48%	3.45%
40	80.74%	81.13%	72.88%	60.60%	49.31%	31.72%	28.25%	6.97%
42	79.94%	79.92%	73.73%	63.98%	54.18%	31.43%	21.54%	1.86%
44	80.70%	74.60%	73.36%	62.20%	50.49%	32.59%	24.64%	15.52%
47	80.54%	81.04%	75.40%	63.12%	47.74%	32.42%	21.65%	16.38%
49	80.61%	81.50%	74.64%	62.18%	52.64%	39.08%	28.70%	37.57%

51	80.61%	80.30%	73.48%	62.58%	50.48%	33.67%	24.81%	7.22%
54	81.05%	82.25%	69.70%	55.90%	48.27%	30.51%	26.68%	11.00%
58	80.37%	80.22%	67.10%	55.11%	42.79%	-	-	6.74%
63	79.24%	-	-	-	-	-	-	33.72%
65	80.82%	76.43%	59.30%	48.17%	37.68%	23.69%	23.78%	13.62%
75	80.24%	-	-	-	-	-	-	4.35%
77	79.94%	78.54%	78.54%	77.62%	77.04%	76.21%	75.83%	-
84	78.72%	78.92%	79.13%	79.18%	80.20%	78.99%	74.82%	28.28%
86	81.39%	-	-	-	-	-	-	9.91%
114	78.93%	80.60%	82.93%	77.67%	63.95%	43.49%	30.58%	7.38%
119	80.20%	-	-					4.01%
121	80.01%	80.56%	82.28%	79.59%	66.88%	46.86%	32.87%	3.30%
124	80.11%	80.31%	81.85%	78.28%	65.83%	43.55%	30.98%	2.69%
126	79.48%	-	-	-	-	-	-	1.59%
128	79.26%	79.49%	80.75%	81.54%	72.77%	52.59%	39.14%	-
132	79.49%	80.89%	80.80%	82.66%	72.21%	52.88%	39.06%	3.57%
135	80.01%	80.84%	82.91%	79.24%	65.09%	42.75%	29.62%	4.28%
138	79.37%	-	-	-	-	-	-	-
140	81.51%	81.34%	80.58%	81.62%	76.19%	52.90%	37.73%	1.72%
142	80.02%	80.12%	80.43%	71.39%	58.37%	38.74%	28.60%	2.38%
145	83.40%	84.04%	80.29%	65.69%	50.60%	31.82%	21.97%	5.38%
147	78.95%	-	-	-	-	-	-	2.46%
149	79.35%	80.91%	78.58%	66.44%	51.37%	31.11%	22.10%	0.96%
152	81.46%	80.82%	80.92%	69.08%	54.85%	35.53%	25.84%	1.98%
154	80.01%	-	-	-	-	-	-	2.28%
156	79.81%	80.48%	81.74%	72.27%	58.87%	39.56%	28.83%	2.96%
159	80.23%	80.55%	82.38%	73.65%	61.45%	41.96%	30.97%	3.98%
163	80.64%	81.13%	74.98%	60.37%	46.97%	29.73%	23.28%	2.61%
166	80.60%	81.03%	70.28%	55.74%	42.34%	25.50%	19.12%	2.91%
168	80.01%	-	-	-	-	-	-	2.28%
170	80.88%	81.05%	73.19%	59.80%	46.62%	32.26%	23.43%	2.11%
173	81.05%	81.50%	67.87%	53.92%	37.75%	21.80%	18.37%	4.48%
177	80.59%	81.09%	74.80%	61.46%	48.30%	32.47%	25.01%	3.19%
181	80.09%	81.83%	81.98%	77.60%	69.10%	57.83%	51.24%	17.52%
184	80.63%	82.02%	74.66%	62.20%	49.35%	33.44%	25.29%	3.88%
188	81.00%	82.26%	73.87%	61.22%	47.43%	31.66%	24.72%	1.34%
194	80.99%	81.78%	69.33%	56.22%	42.49%	26.81%	22.80%	0.75%
198	82.81%	81.40%	75.42%	64.12%	49.12%	31.09%	23.30%	1.73%
203	80.73%	-	-	-	-	-	-	1.53%
205	80.76%	81.38%	71.57%	59.00%	44.23%	27.52%	22.55%	0.91%
210	79.92%	80.25%	73.06%	60.09%	45.87%	29.68%	23.18%	3.24%
218	82.27%	83.88%	82.98%	72.41%	60.73%	43.64%	33.81%	1.86%
226	80.80%	81.11%	69.38%	55.28%	41.80%	27.01%	23.26%	1.44%
232	80.40%	80.80%	73.68%	60.74%	48.11%	32.67%	29.13%	0.50%
238	80.28%	80.80%	75.89%	62.97%	50.01%	35.05%	24.24%	4.98%

Table E.7. Compost Column Carbon Dioxide Gas Profile Result

Day	Depth / Carbon Dioxide (%, vol. basis)							
	0	5	25	45	65	85	105	157
0	3.62%	6.48%	6.71%	7.52%	7.78%	8.09%	7.48%	0.12%
1	1.37%	3.14%	5.50%	7.84%	11.12%	-	-	-
2	2.76%	6.19%	12.11%	15.28%	-	18.72%	-	30.69%
5	5.06%	12.77%	18.20%	21.25%	-	28.36%	-	35.03%
7	4.30%	9.53%	17.23%	20.51%	22.63%	25.02%	29.17%	35.36%
9	4.51%	11.02%	22.87%	22.15%	25.10%	29.69%	31.97%	38.26%
10	3.52%	9.01%	16.75%	20.55%	24.67%	28.12%	31.07%	37.89%
12	4.71%	11.67%	17.56%	20.21%	23.32%	26.74%	29.89%	38.28%
14	5.62%	15.35%	19.12%	23.15%	26.69%	28.17%	33.07%	39.21%
16	4.55%	12.44%	19.21%	23.31%	27.17%	-	33.61%	38.66%
17	5.49%	12.83%	19.80%	24.95%	27.03%	31.24%	34.17%	39.24%
20	5.94%	13.20%	20.34%	24.58%	28.79%	-	-	37.34%
21	6.02%	14.36%	20.16%	25.12%	28.31%	31.46%	34.54%	39.00%
23	5.67%	14.01%	20.36%	24.52%	27.50%	-	33.24%	38.82%
25	5.83%	13.44%	18.42%	23.81%	26.85%	31.71%	33.06%	38.82%
28	3.22%	8.01%	15.41%	20.39%	22.23%	26.82%	-	36.86%
30	4.78%	12.45%	18.27%	22.25%	26.06%	30.64%	32.47%	38.40%
33	6.68%	15.00%	20.95%	25.33%	28.45%	33.02%	33.68%	-
36	5.60%	13.41%	19.79%	24.24%	28.36%	32.55%	34.70%	36.89%
38	5.72%	14.32%	19.98%	24.43%	26.81%	32.17%	31.21%	38.18%
40	6.27%	14.73%	20.47%	24.45%	27.11%	33.39%	32.15%	36.29%
42	5.57%	12.18%	19.38%	20.81%	26.88%	33.27%	35.55%	38.46%
44	6.10%	14.68%	19.86%	23.08%	28.20%	33.01%	35.38%	32.84%
47	5.97%	13.74%	20.30%	24.56%	28.97%	32.95%	35.54%	32.56%
49	5.60%	13.67%	19.86%	23.50%	26.52%	30.26%	32.53%	21.51%
51	5.60%	12.78%	20.18%	24.13%	27.90%	32.89%	34.78%	36.47%
54	9.42%	16.66%	22.57%	26.31%	28.38%	32.58%	33.31%	34.57%
58	7.39%	15.29%	19.38%	22.05%	26.28%	-	-	37.14%
63	4.97%	-	-	-	-	-	-	25.58%
65	9.05%	18.97%	24.19%	27.89%	30.48%	34.46%	32.76%	35.27%
75	4.81%	-	-	-	-	-	-	38.25%
77	1.88%	4.12%	7.70%	10.03%	12.07%	15.96%	15.91%	-
84	1.33%	3.19%	4.97%	6.66%	9.98%	13.09%	12.56%	27.42%
86	5.71%	-	-	-	-	-	-	36.03%
114	1.58%	3.58%	10.43%	18.22%	22.77%	29.58%	33.05%	37.42%
119	1.57%	-	-	-	-	-	-	38.46%
121	1.27%	3.25%	9.52%	17.13%	22.49%	28.48%	32.61%	38.99%
124	1.63%	3.52%	10.58%	17.28%	21.59%	29.49%	32.59%	38.92%
126	1.03%	-	-	-	-	-	-	39.22%
128	0.96%	2.13%	6.27%	13.74%	18.97%	26.84%	30.51%	-
132	1.01%	2.34%	6.94%	15.09%	19.46%	26.97%	30.81%	39.37%
135	1.12%	2.39%	8.12%	16.42%	22.00%	29.39%	32.87%	38.79%
138	0.82%	-	-	-	-	-	-	-
140	0.67%	1.35%	4.06%	11.17%	19.12%	27.73%	31.83%	39.30%
142	2.93%	7.50%	17.11%	21.08%	25.54%	32.43%	33.10%	39.40%
145	3.72%	8.54%	18.63%	22.52%	27.84%	33.55%	35.73%	37.91%
147	2.50%	-	-	-	-	-	-	39.14%
149	3.38%	8.08%	18.97%	20.94%	27.72%	34.13%	36.13%	40.54%

152	2.94%	7.75%	18.06%	22.05%	27.41%	33.64%	35.47%	40.24%
154	2.79%	-	-	-	-	-	-	40.09%
156	2.59%	5.87%	15.54%	20.67%	26.13%	32.36%	34.81%	40.00%
159	2.37%	4.28%	13.82%	18.20%	24.33%	31.46%	33.86%	39.54%
163	6.22%	13.71%	21.57%	23.97%	28.83%	34.15%	35.09%	39.36%
166	7.21%	14.99%	22.42%	26.26%	30.37%	35.37%	36.18%	39.05%
168	4.79%	-	-	-	-	-	-	40.09%
170	5.95%	13.45%	21.53%	25.59%	29.79%	33.73%	35.58%	39.47%
173	7.27%	16.39%	23.35%	25.55%	31.77%	36.07%	35.73%	38.57%
177	5.76%	12.74%	21.27%	24.33%	29.10%	33.98%	35.24%	39.24%
181	3.28%	6.83%	15.14%	19.17%	22.18%	26.52%	26.96%	35.73%
184	5.39%	12.10%	20.81%	23.80%	28.22%	33.11%	34.78%	39.03%
188	4.81%	12.28%	19.78%	23.03%	27.71%	32.46%	33.72%	39.82%
194	6.77%	15.30%	22.47%	25.96%	30.46%	34.83%	34.70%	40.43%
198	4.89%	10.94%	20.36%	22.59%	29.43%	34.70%	35.86%	40.53%
203	6.34%	-	-	-	-	-	-	40.55%
205	5.75%	13.04%	21.58%	24.41%	30.11%	35.53%	35.87%	40.81%
210	5.59%	11.58%	21.62%	25.77%	30.41%	35.14%	35.76%	39.80%
218	2.51%	5.83%	11.85%	13.62%	16.96%	22.94%	26.58%	40.00%
226	6.59%	14.16%	22.57%	26.89%	31.53%	35.28%	35.32%	40.67%
232	4.90%	11.21%	21.25%	25.12%	29.50%	34.33%	33.46%	40.17%
238	3.94%	9.40%	20.46%	25.30%	29.37%	33.69%	36.54%	39.32%

Table E.8 Compost Column Methane Gas Profile Results

Day	Depth / Methane (%, vol. basis)							
	0	5	25	45	65	85	105	157
0	0.00%	0.00%	0.00%	0.00%	0.00%	0.00%	0.00%	0.00%
1	2.27%	2.49%	5.16%	9.40%	16.85%	-	-	-
2	0.27%	0.59%	2.59%	11.86%	-	-	-	58.67%
5	0.00%	0.07%	6.59%	18.98%	-	42.75%	-	60.35%
7	0.50%	0.32%	1.44%	10.28%	19.09%	31.15%	39.96%	54.65%
9	0.12%	1.78%	15.66%	13.87%	21.55%	35.41%	42.18%	57.76%
10	0.14%	0.10%	0.23%	5.17%	15.84%	25.30%	33.67%	56.84%
12	0.00%	0.46%	2.97%	10.64%	18.69%	29.64%	37.97%	57.20%
14	0.26%	2.37%	5.53%	13.48%	22.57%	30.96%	40.95%	60.78%
16	0.03%	2.44%	3.43%	12.30%	26.67%	-	39.85%	58.24%
17	0.29%	0.02%	4.10%	17.42%	21.86%	33.50%	41.42%	59.28%
20	0.06%	0.05%	5.73%	15.14%	25.56%	-	-	56.94%
21	0.08%	1.27%	4.96%	14.81%	23.59%	33.97%	43.43%	59.25%
23	0.03%	1.58%	6.29%	12.48%	20.78%	-	38.31%	57.56%
25	0.08%	0.02%	4.14%	14.64%	21.64%	33.88%	39.70%	57.64%
28	0.07%	0.13%	0.00%	3.93%	8.94%	17.65%	-	55.27%
30	0.03%	0.11%	3.48%	10.89%	20.58%	32.46%	38.60%	61.00%
33	0.00%	0.67%	7.60%	18.35%	26.25%	38.08%	45.60%	-
36	0.00%	0.11%	5.45%	14.69%	24.98%	34.31%	41.44%	58.39%
38	0.00%	0.00%	5.91%	14.86%	23.58%	34.79%	37.85%	59.13%
40	0.05%	0.02%	6.32%	15.24%	23.97%	36.66%	39.71%	57.21%
42	0.00%	0.40%	5.59%	12.63%	19.38%	37.40%	44.84%	59.83%
44	0.00%	5.37%	6.36%	14.29%	23.21%	36.30%	42.30%	50.13%
47	0.00%	0.04%	6.22%	13.47%	25.20%	36.69%	44.60%	49.14%

49	0.00%	0.00%	5.59%	14.46%	21.83%	31.97%	39.12%	33.40%
51	0.00%	0.51%	5.77%	13.84%	23.23%	35.63%	41.94%	56.43%
54	0.05%	1.08%	10.53%	20.67%	24.76%	38.91%	40.49%	53.72%
58	0.48%	2.87%	13.98%	23.56%	34.20%	-	-	56.06%
63	0.01%	-	-	-	-	-	-	36.08%
65	0.05%	3.94%	16.13%	24.18%	32.32%	43.35%	41.84%	50.44%
75	0.16%	-	-	-	-	-	-	57.78%
77		0.00%	0.00%	0.00%	0.00%	0.00%	0.00%	-
84	0.00%	0.00%	0.00%	0.00%	0.22%	2.35%	5.35%	39.05%
86	0.00%	-	-	-	-	-	-	53.30%
114	0.00%	0.00%	0.02%	3.49%	13.18%	27.84%	37.10%	55.07%
119	0.00%	-	-	-	-	-	-	59.08%
121	0.00%	0.00%	0.00%	2.53%	12.20%	26.42%	36.55%	59.05%
124	0.00%	0.00%	0.05%	3.06%	12.18%	28.27%	36.96%	59.77%
126	0.00%	-	-	-	-	-	-	60.82%
128	0.00%	0.00%	0.00%	0.43%	6.80%	21.41%	31.34%	-
132	0.00%	0.00%	0.00%	0.33%	7.70%	21.43%	31.50%	58.04%
135	0.00%	0.00%	0.05%	2.86%	13.36%	29.24%	38.49%	57.17%
138	0.00%	-	-	-	-	-	-	-
140	0.00%	0.00%	0.02%	0.02%	4.42%	20.75%	31.83%	59.72%
142	0.00%	0.00%	0.31%	7.55%	17.04%	31.88%	39.70%	59.66%
145	0.00%	0.00%	2.24%	11.61%	22.74%	36.54%	44.09%	57.14%
147	0.00%	-	-	-	-	-	-	58.60%
149	0.00%	0.00%	2.59%	10.98%	22.84%	37.30%	43.94%	60.50%
152	0.00%	0.00%	0.77%	9.30%	19.42%	33.66%	40.61%	59.78%
154	0.00%	-	-	-	-	-	-	59.87%
156	0.00%	0.00%	0.04%	6.80%	16.56%	30.61%	37.83%	59.03%
159	0.00%	0.00%	0.00%	5.87%	15.35%	30.19%	37.17%	58.66%
163	0.00%	0.00%	6.81%	15.84%	26.10%	39.39%	44.03%	60.02%
166	0.00%	0.04%	8.34%	18.51%	28.80%	41.98%	45.84%	59.87%
168	0.00%	-	-	-	-	-	-	59.87%
170	0.00%	0.00%	6.06%	15.67%	25.45%	36.23%	42.97%	60.35%
173	0.00%	0.24%	10.66%	20.20%	32.65%	44.90%	46.68%	58.19%
177	0.00%	0.00%	5.68%	14.46%	24.15%	36.20%	41.74%	59.51%
181	0.00%	0.00%	0.01%	3.52%	8.92%	18.06%	21.89%	47.98%
184	0.00%	0.00%	5.52%	14.28%	23.96%	36.13%	41.94%	59.05%
188	0.00%	0.00%	6.81%	16.42%	26.84%	38.96%	43.27%	61.16%
194	0.00%	0.07%	9.44%	18.60%	28.97%	40.61%	43.19%	60.58%
198	0.00%	0.00%	4.62%	12.40%	24.30%	36.93%	42.64%	59.95%
203	0.01%	-	-	-	-	-	-	60.31%
205	0.00%	0.00%	7.54%	16.61%	27.88%	40.54%	44.17%	60.81%
210	0.00%	0.00%	5.88%	16.07%	25.67%	37.65%	42.42%	58.70%
218	0.00%	0.00%	4.97%	14.69%	24.39%	36.26%	41.05%	60.29%
226	0.00%	0.05%	8.67%	18.74%	28.72%	40.49%	42.85%	60.67%
232	0.00%	0.00%	5.73%	14.71%	23.93%	36.39%	38.86%	59.67%
238	0.00%	0.00%	4.35%	13.42%	22.80%	33.70%	41.92%	57.38%

Table E.9 Sand-Compost-Perlite Column Temperature Results

Day	Depth / Temperature (°C)						
	0	5	25	45	65	85	105
0	21	20.8	20.7	20.8	20.9	20.9	20.8
1	20.9	20.7	20.5	20.6	20.6	20.7	20.8
2	20.1	20.4	20.9	21.4	21.2	20.7	20.5
5	20	22.7	23.4	21	20.1	19.7	19.6
7	20.5	22.5	23.7	21.2	20.2	19.9	19.7
9	20.3	24.1	23.1	21	20.4	20	19.9
10	20.3	23.1	23.4	21.2	20.3	20	20
12	20.3	22.5	21.1	20.4	19.9	19.6	19.6
14	20.3	23.5	23.1	21.1	20.3	20.1	20
16	19.9	22.8	23.5	21.1	20.3	20	19.9
17	19.8	22.8	23.5	21.1	20.3	20	20
20	20	22.7	23.1	20.9	20.1	19.8	19.7
21	19.9	22.2	23.1	20.8	20	19.7	19.6
23	19.8	22.7	22.8	20.8	20.1	19.8	19.8
25	20.1	22.2	23.1	21.1	20.2	19.8	19.7
28	20.5	21.2	22.8	21.1	20.2	19.8	19.7
30	20.2	22.6	23.2	21	20.2	19.8	19.7
33	19.3	22.5	22.8	20.7	19.9	19.6	19.5
36	19.8	22.7	22.8	20.6	20	19.6	19.3
38	19.9	22.1	22.9	20.9	20	19.6	19.5
42	21.3	22.9	23.3	21.1	20.1	19.8	19.7
44	19.5	22.5	23.2	20.7	19.9	19.6	19.5
47	20.2	22.5	23.3	20.6	19.8	19.6	19.5
49	20.2	23.1	24	21.3	20.4	20	19.9
51	20.2	22.7	23.4	21	20.4	20	19.8
54	20.3	23.2	23.3	20.8	20.1	19.7	19.6
58	20.5	22.2	22.6	20.8	20	19.8	19.6
63	20.2	22.8	22.3	20.2	19.4	19.2	19.1
65	19.8	22.4	22.1	20.3	19.7	19.4	19.2
68	19.8	19.9	19.7	19.5	19.4	19.2	19.2
70	19.8	21	23	21.2	20.2	20	20
86	19.7	19.8	21.6	21.6	22	21.1	20.4
114	21.2	20.5	23.6	21.6	20.7	20.2	19.8
117	21.4	21.7	23.5	21.5	20.5	20.2	20.1
119	20.6	20.8	23.6	21.7	20.7	20.3	20.1
121	21	22.2	23.5	21.5	20.6	20.2	20
124	21.2	23.5	23.2	21	20.2	19.9	19.7
126	20.2	20.8	22.6	20.6	19.9	19.3	19.5
128	20.3	21.3	23.1	21	20	19.6	19.4
132	20.8	20.9	22.9	20.9	20.2	19.7	19.5
135	21	22.9	23	21	20.1	19.7	19.6
138	20.5	21.8	23.3	21.2	20.4	20	19.7
140	20.4	20.7	23.6	21.5	20.5	20.1	20.1

142	20.5	21	23.6	21.8	20.8	20.1	20
145	20.3	20.7	23.5	21.2	20.4	19.9	19.7
147	20.2	20.6	23.4	21.4	20.5	20.1	19.7
149	20.7	20.8	23.2	21.6	20.5	20.2	19.7
152	20.2	20.7	23.2	21.7	20.5	19.7	19.6
154	20.7	21.9		21.6	20.8	20.3	20.1
156	20.9	20.2	23.5	21.5	20.5	20.2	20.1
160	20.8	21.1	23.5	21.5	20.5	20	19.9
163	20.4	21.3	23.5	21.5	20.5	20.1	19.9
166	20.5	21.9	23.5	21.2	20.1	19.7	19.6
168	20.6	20.7	23.4	21.5	20.8	20.1	19.8
170	20.4	21.3	23.5	21.4	20.3	20	19.8
177	20.6	21.5	23.3	21.5	20.6	20.2	20
181	21.7	22.3	23.6	21.3	20.5	20.2	20.1
184	21	22.1	23.1	22.1	20.3	19.9	19.7
188	21.8	22.5	23.7	21.5	20.6	20.3	20.1
194	21.2	21.6	23.2	21.2	20.5	20.1	19.9
198	21	22.1	23.6	21.7	20.6	20.3	20.2
203	20.8	21.9	23	21	20.2	19.9	19.7
205	21	22	23.1	21	20.2	19.8	19.7
210	20.4	21.5	23.4	20.9	20	19.8	19.7
218	20.4	20.5	22.2	21.1	20.5	20.1	20
226	21.9	23.1	24.2	22.4	21.5	21.2	21
232	21.7	21.8	23.6	21.4	20.6	20.5	20.2
238	21	21.8	25	22.2	21	20.1	20

Table E.10. Compost Column Temperature Results

Day	Depth / Temperature (°C)						
	0	5	25	45	65	85	105
0	21	20.9	20.9	21.4	21.5	21.4	21.1
1	20.1	21.3	23.7	23.6	21.7	21.2	20.8
4	20	23.3	27	22.1	20.5	20	20
6	20.5	21.9	25.9	23.4	21.1	20.1	20.1
8	20.3	22.6	27.1	23	20.9	20.5	20.2
9	20.3	21.6	24.1	24.1	21.1	20.3	20.1
11	20.3	21.3	25.3	21.8	20.3	20.2	20
13	20.5	23.9	25.8	22.1	20.6	20.2	20.1
15	19.9	22.3	27	22.5	20.7	20.2	20
16	19.8	22.4	26.6	22.3	20.9	20.2	20.1
19	20	23.5	25.6	21.6	20.5	20	20
20	19.9	23.2	26	22	20.4	20	19.9
22	19.8	23.1	26.7	22	20.4	20	19.9
24	20.1	23.1	25.6	22.1	20.5	20.2	19.9
27	20.5	21.5	23.3	23.5	20.8	20	19.9
30	20.2	22.5	26.2	22.2	20.6	20.1	20
33	19.3	23	25.2	21.5	20.2	19.8	19.8

36	19.8	22.9	26.3	21.6	20.2	19.9	19.9
38	19.9	23.5	25.9	21.6	20.3	19.8	19.7
40	20.2	23.3	26.1	21.7	20.5	20	19.9
42	20.7	23.5	26.1	21.7	20.4	20.1	19.9
44	19.5	23.1	26.8	21.5	20.1	19.8	19.6
47	20.2	23.1	26.6	21.5	20.4	19.8	19.7
49	20.2	22.3	26.1	21.8	20.5	20.2	20
51	20.2	23.1	26	21.7	20.6	20.2	20.1
54	20.3	24.5	24.5	21.1	20.5	20	19.8
58	20.5	23.9	23.6	21.2	20.5	20.2	20
63	20.2	23.1	24	20.7	19.9	19.4	19.2
65	19.8	25.6	23.4	20.6	19.9	19.5	19.5
68	20.2	20.8	22.7	22.6	20.1	19.6	19.6
70	19.8	21.1	25.2	22.8	21.3	20.6	20.3
86	19.9	23.1	24.9	22.3	21.3	20.8	20.8
114	20.3	21	23.2	26.1	22.7	21.1	20.6
117	20.4	21.2	23	26.4	23.4	21.1	20.4
119	20.5	20.9	22.9	26.2	22.8	21.1	20.5
121	20.1	21	22.7	26.3	23.3	21.2	20.5
124	20	20.8	23.1	26.5	22.8	20.8	20.2
126	19.7	20.3	22	26.1	23.2	20.8	20.1
128	20	20.1	22	25.4	23.6	20.8	19.7
132	19.8	20.2	21.3	24.3	23.8	21.1	20.1
135	20	20.5	22.1	26.6	24	21.3	20.2
138	20.2	20.6	22	25.9	24.7	21.6	20.5
140	20.1	21	22.6	24.7	26.1	21.8	20.8
142	19.8	21.6	25.3	23.6	21.7	20.9	20.5
145	20.1	21.4	25.2	23	21.1	20.2	20.1
147	20	21.2	23.6	24.4	21.8	20.6	20.2
149	20	21.3	24.5	23.1	21.5	20.6	20.3
152	19.7	21.1	23.5	23.2	21.1	20.2	20
154	20.2	21.2	24.4	23.9	21.7	20.7	20.4
156	19.5	21.1	23.4	24.3	21.9	20.5	20.3
160	20	21.1	23.1	25	22	20.6	20.1
163	20.6	22.6	25.7	22.6	21	20.3	20.1
166	20.6	23.4	26	22	20.3	20	19.8
168	20.6	22.3	25.5	22.3	20.9	20.4	20.2
170	20.4	22.4	25.7	22.2	20.7	20.2	20.1
177	20.5	22.6	25.9	22.3	20.8	20.3	20.2
181	21	21.1	23	23.6	21.3	20.5	20.4
184	20.7	22.2	25.5	22.3	20.6	20.1	20
188	20.7	22	25.2	22.7	21.4	20.5	20.6
194	21	22.5	25.3	22.4	21.1	20.6	20.4
198	21	23	26.1	22.6	20.9	20.5	20.3
203	20.6	23.1	25.3	22.1	20.6	20.1	19.9
205	20.5	22.7	25.2	21.9	20.4	19.9	19.8
210	20.5	21.6	24.6	21.2	20.2	20	20
218	20.4	20.7	24.1	22.2	21.6	20.7	20.5
226	21.7	23.5	26.2	23.2	22.2	21.5	21.2

232	21.5	22.3	25.6	22.4	21.2	20.8	20.6
238	21	21.8	25	22.2	21	20	20

Table E.11. Column Effluent Flow Results

Day	Outflow ($L \cdot min^{-1}$)	
	Sand-Compost-Perlite	Compost
1	0.38	0.30
2	0.34	0.29
5	0.39	0.3
7	0.40	0.31
9	0.36	0.36
10	0.34	0.3
12	0.40	0.43
14	0.40	0.40
16	0.43	0.40
17	0.38	0.39
20	0.45	0.36
21	0.46	0.36
23	0.42	0.37
25	0.40	0.36
28	0.39	0.34
30	0.39	0.36
36	0.43	0.38
38	0.38	0.26
40	-	0.36
42	0.40	0.30
44	-	0.30
47	0.40	0.28
49	0.44	0.28
51	-	0.40
54	-	0.40
58	0.40	0.40
63	-	0.30
65	-	0.38
38	0.45	-
75	0.31	0.37
84	0.42	0.33
86	0.4	0.32
114	0.30	0.28
119	0.30	0.20
121	0.38	0.26
124	0.32	0.24
126	0.36	0.22
132	0.32	0.15
135	0.30	0.22

138	0.38	0.18
140	0.32	0.14
142	0.30	0.30
145	0.32	0.32
147	0.28	0.24
149	0.26	0.34
152	0.28	0.34
154	0.32	0.32
156	0.3	0.32
159	0.36	0.32
163	0.34	0.36
166	0.35	0.3
168	0.36	0.3
170	0.28	0.36
173	0.36	0.31
177	0.28	0.30
181	0.28	0.36
184	0.32	0.36
188	0.33	0.39
194	0.28	0.3
198	0.28	0.28
203	0.36	0.32
205	0.28	0.3
210	0.40	0.26
218	0.32	0.30
226	0.30	0.28
232	0.30	0.30
238	0.30	0.30

Appendix F Pilot Biofilter Results

Table F.1. Methane Surface Emission Results

Date	Surface Emissions ($gCH_4 \cdot m^{-2} \cdot d^{-1}$)											
	Site 1				Site 2				Site 3			
	A	B	C	D	A	B	C	D	A	B	C	D
25-Oct-05	37.9	121.0	157.9	276.2	57.4	208.7	166.8	365.3	-	-	-	-
28-Nov-05	0.0	0.0	0.0	0.0	0.6	0.2	1.2	0.0	0.0	0.0	-0.1	0.0
14-Dec-05	0.0	0.0	0.0	0.0	0.0	0.0	0.0	0.0	0.0	0.0	0.2	0.0
24-Jan-06	2.5	0.0	0.7	16.0	0.8	0.0	0.6	59.7	0.3	0.4	1.9	0.9
28-Feb-06	0.0	0.0	-3.7	-1.0	0.0	0.0	0.0	0.0	0.0	2.0	0.0	3.1
21-Mar-06	27.1	64.2	0.0	139.5	56.4	0.6	1.8	0.0	4.6	6.9	7.5	0.3
1-May-06	0.8	0.0	0.9	0.2	1.5	2.4	1.8	-0.1	37.1	3.4	5.6	0.2
31-May-06	0.0	7.4	3.4	0.0	9.5	3.1	23.9	0.0	2.3	0.0	0.0	0.0

Table F.2. Carbon Dioxide Surface Emission Results

Date	Surface Emissions ($gCO_2 \cdot m^{-2} \cdot d^{-1}$)											
	Site 1				Site 2				Site 3			
	A	B	C	D	A	B	C	D	A	B	C	D
25-Oct-05	316.4	552.9	576.2	803.7	339.3	658.8	869.2	1262.7	-	-	-	-
28-Nov-05	96.9	117.7	125.5	74.4	258.2	177.2	160.2	0.0	0.0	29.5	0.0	7.2
14-Dec-05	41.4	89.7	116.4	26.1	225.4	48.8	14.8	25.4	0.0	0.0	31.3	0.0
24-Jan-06	77.0	157.8	142.3	175.4	111.1	4.4	7.2	310.9	13.3	0.0	13.4	16.3
28-Feb-06	102.2	107.9	0.0	0.0	0.0	222.1	0.0	0.0	0.0	22.9	22.0	31.5
21-Mar-06	65.5	122.5	0.0	221.4	105.3	0.0	4.7	3.8	10.4	12.9	19.1	0.0
1-May-06	23.8	0.0	165.5	185.3	199.1	206.5	79.8	0.0	51.1	33.3	9.5	0.0
31-May-06	0.0	240.2	306.9	0.0	365.8	204.1	450.3	0.0	63.3	61.2	0.0	44.3

Table F.3. Site 1 Gas Concentration Profile Results

		Gas Profile Concentrations (L^*L^{-1})							
Date	Depth	CH_4	CO_2	O_2	N_2	SE CH_4	SE CO_2	SE O_2	SE N_2
25-Oct-05	-20	0.292	0.298	0.005	0.406	0.056	0.015	0.001	0.071
25-Oct-05	-55	0.474	0.345	0.006	0.175	0.029	0.005	0.001	0.035
25-Oct-05	-90	0.522	0.358	0.007	0.115	0.021	0.003	0.001	0.026
25-Oct-05	-125	0.542	0.362	0.008	0.087	0.019	0.003	0.001	0.024
25-Oct-05	-160	0.554	0.361	0.007	0.078	0.013	0.003	0.001	0.014
28-Nov-05	-20	0.000	0.139	0.070	0.791	0.000	0.012	0.009	0.003
28-Nov-05	-55	0.039	0.235	0.003	0.724	0.016	0.008	0.002	0.022
28-Nov-05	-90	0.087	0.258	0.003	0.652	0.010	0.005	0.001	0.017
28-Nov-05	-125	0.121	0.269	0.005	0.606	0.011	0.005	0.001	0.014
28-Nov-05	-160	0.160	0.281	0.003	0.558	0.008	0.004	0.001	0.013
14-Dec-05	-20	0.000	0.112	0.094	0.793	0.000	0.014	0.011	0.007
14-Dec-05	-55	0.013	0.207	0.009	0.771	0.006	0.020	0.010	0.017
14-Dec-05	-90	0.040	0.231	0.001	0.728	0.012	0.012	0.001	0.023
14-Dec-05	-125	0.063	0.243	0.001	0.694	0.015	0.009	0.001	0.024
14-Dec-05	-160	0.095	0.247	0.000	0.657	0.007	0.005	0.000	0.011
24-Jan-06	-20	0.024	0.164	0.046	0.767	0.012	0.011	0.016	0.010
24-Jan-06	-55	0.115	0.237	0.000	0.648	0.023	0.006	0.000	0.025
24-Jan-06	-90	0.192	0.259	0.000	0.550	0.025	0.008	0.000	0.030
24-Jan-06	-125	0.246	0.274	0.001	0.479	0.031	0.007	0.001	0.037
24-Jan-06	-160	0.304	0.291	0.000	0.403	0.034	0.008	0.000	0.042
28-Feb-06	-20	0.008	0.159	0.077	0.757	0.006	0.017	0.017	0.007
28-Feb-06	-55	0.068	0.271	0.000	0.661	0.023	0.003	0.000	0.026
28-Feb-06	-90	0.139	0.293	0.000	0.568	0.024	0.003	0.000	0.026
28-Feb-06	-125	0.191	0.300	0.001	0.509	0.027	0.004	0.001	0.030
28-Feb-06	-160	0.220	0.269	0.020	0.491	0.042	0.014	0.009	0.052
21-Mar-06	-20	0.223	0.217	0.045	0.515	0.043	0.021	0.014	0.050
21-Mar-06	-90	0.458	0.309	0.000	0.233	0.015	0.003	0.000	0.018
21-Mar-06	-125	0.490	0.317	0.000	0.194	0.011	0.001	0.000	0.012
21-Mar-06	-160	0.447	0.286	0.024	0.243	0.057	0.030	0.017	0.070
1-May-06	-20	0.046	0.197	0.015	0.742	0.023	0.013	0.009	0.032
1-May-06	-55	0.181	0.249	0.000	0.570	0.035	0.013	0.000	0.047
1-May-06	-90	0.267	0.268	0.000	0.465	0.034	0.012	0.000	0.045
1-May-06	-125	0.318	0.279	0.000	0.404	0.036	0.010	0.000	0.044
1-May-06	-160	0.362	0.290	0.001	0.347	0.035	0.007	0.001	0.041
31-May-06	-20	0.041	0.195	0.020	0.743	0.008	0.007	0.006	0.009
31-May-06	-55	0.166	0.265	0.001	0.566	0.018	0.002	0.001	0.019
31-May-06	-90	0.266	0.295	0.002	0.435	0.021	0.004	0.000	0.024
31-May-06	-125	0.321	0.311	0.002	0.364	0.027	0.003	0.000	0.030
31-May-06	-160	0.394	0.327	0.003	0.285	0.034	0.005	0.001	0.040

Table F.4. Site 2 Gas Concentration Profile Results

		Gas Profile Concentrations ($L \cdot L^{-1}$)							
Date	Depth	CH_4	CO_2	O_2	N_2	SE CH_4	SE CO_2	SE O_2	SE N_2
25-Oct-05	-20	0.512	0.408	0.007	0.077	0.044	0.011	0.001	0.054
25-Oct-05	-55	0.586	0.402	0.004	0.009	0.018	0.009	0.002	0.010
25-Oct-05	-90	0.602	0.391	0.006	0.001	0.009	0.009	0.001	0.001
25-Oct-05	-125	0.612	0.381	0.005	0.003	0.008	0.007	0.002	0.002
25-Oct-05	-160	0.585	0.412	0.003	0.001	0.006	0.006	0.001	0.000
25-Oct-05	-195	0.074	0.045	0.178	0.703	0.000	0.000	0.000	0.000
25-Oct-05	-230	0.005	0.003	0.198	0.794	0.000	0.000	0.000	0.000
28-Nov-05	-20	0.022	0.113	0.115	0.751	0.015	0.071	0.071	0.024
28-Nov-05	-55	0.203	0.307	0.004	0.490	0.008	0.013	0.001	0.021
28-Nov-05	-90	0.300	0.352	0.002	0.348	0.015	0.013	0.001	0.028
28-Nov-05	-125	0.358	0.383	0.001	0.259	0.006	0.006	0.000	0.012
28-Nov-05	-160	0.427	0.420	0.000	0.152	0.002	0.001	0.000	0.002
14-Dec-05	-20	0.003	0.158	0.075	0.760	0.003	0.048	0.027	0.025
14-Dec-05	-55	0.021	0.256	0.008	0.705	0.011	0.039	0.007	0.035
14-Dec-05	-90	0.060	0.283	0.000	0.656	0.014	0.029	0.000	0.041
14-Dec-05	-125	0.106	0.371	0.000	0.594	0.009	0.091	0.000	0.024
14-Dec-05	-160	0.193	0.306	0.023	0.475	0.004	0.008	0.008	0.005
24-Jan-06	-20	0.125	0.234	0.000	0.638	0.035	0.020	0.000	0.034
24-Jan-06	-55	0.270	0.289	0.000	0.437	0.045	0.015	0.000	0.044
24-Jan-06	-90	0.386	0.329	0.000	0.285	0.029	0.010	0.000	0.026
24-Jan-06	-125	0.458	0.357	0.000	0.181	0.021	0.004	0.000	0.020
24-Jan-06	-160	0.505	0.397	0.000	0.095	0.040	0.029	0.018	0.055
28-Feb-06	-20	0.000	0.179	0.085	0.736	0.000	0.067	0.053	0.016
28-Feb-06	-55	0.019	0.146	0.113	0.722	0.013	0.095	0.066	0.043
28-Feb-06	-90	0.058	0.187	0.078	0.677	0.023	0.098	0.059	0.055
28-Feb-06	-125	0.080	0.238	0.056	0.627	0.030	0.088	0.062	0.056
28-Feb-06	-160	0.160	0.152	0.139	0.550	0.119	0.083	0.047	0.166
21-Mar-06	-20	0.426	0.345	0.018	0.211	0.072	0.037	0.021	0.089
21-Mar-06	-55	0.556	0.381	0.019	0.045	0.035	0.015	0.013	0.037
21-Mar-06	-90	0.536	0.377	0.023	0.064	0.032	0.014	0.017	0.030
21-Mar-06	-125	0.582	0.385	0.011	0.023	0.014	0.007	0.007	0.015
21-Mar-06	-160	0.516	0.365	0.028	0.090	0.030	0.026	0.017	0.038
1-May-06	-20	0.151	0.267	0.000	0.582	0.052	0.026	0.000	0.076
1-May-06	-55	0.305	0.316	0.000	0.379	0.023	0.016	0.000	0.038
1-May-06	-90	0.446	0.355	0.000	0.200	0.030	0.015	0.000	0.045
1-May-06	-125	0.528	0.376	0.000	0.096	0.009	0.004	0.000	0.013
1-May-06	-160	0.559	0.379	0.008	0.054	0.026	0.019	0.009	0.034
31-May-06	-20	0.115	0.243	0.002	0.641	0.013	0.007	0.000	0.019
31-May-06	-55	0.253	0.291	0.002	0.453	0.014	0.003	0.000	0.017
31-May-06	-90	0.393	0.331	0.003	0.272	0.006	0.004	0.000	0.007
31-May-06	-125	0.494	0.352	0.002	0.152	0.011	0.001	0.000	0.013
31-May-06	-160	0.581	0.376	0.003	0.042	0.014	0.004	0.001	0.009

Table F.5. Site 3 Gas Concentration Profile Results

		Gas Profile Concentrations ($L \cdot L^{-1}$)							
Date	Depth	CH_4	CO_2	O_2	N_2	SE CH_4	SE CO_2	SE O_2	SE N_2
28-Nov-05	-20	0.000	0.035	0.205	0.758	0.000	0.006	0.002	0.005
28-Nov-05	-55	0.001	0.047	0.199	0.753	0.000	0.005	0.002	0.004
28-Nov-05	-90	0.003	0.047	0.197	0.753	0.001	0.004	0.001	0.003
28-Nov-05	-125	0.008	0.048	0.193	0.763	0.005	0.018	0.004	0.003
28-Nov-05	-160	0.044	0.041	0.152	0.763	0.008	0.004	0.008	0.004
14-Dec-05	-20	0.000	0.028	0.208	0.763	0.000	0.007	0.002	0.004
14-Dec-05	-55	0.001	0.032	0.207	0.760	0.000	0.004	0.001	0.003
14-Dec-05	-90	0.001	0.045	0.206	0.763	0.000	0.013	0.001	0.005
14-Dec-05	-125	0.002	0.021	0.207	0.770	0.000	0.004	0.002	0.003
14-Dec-05	-160	0.004	0.013	0.204	0.779	0.001	0.002	0.001	0.002
24-Jan-06	-20	0.002	0.027	0.200	0.771	0.001	0.003	0.001	0.002
24-Jan-06	-55	0.006	0.037	0.192	0.763	0.002	0.000	0.002	0.001
24-Jan-06	-90	0.017	0.037	0.186	0.760	0.004	0.003	0.001	0.003
24-Jan-06	-125	0.037	0.033	0.177	0.751	0.005	0.002	0.001	0.005
24-Jan-06	-160	0.062	0.061	0.160	0.717	0.008	0.004	0.003	0.009
28-Feb-06	-20	0.015	0.056	0.199	0.731	0.000	0.006	0.001	0.005
28-Feb-06	-55	0.025	0.088	0.185	0.702	0.001	0.010	0.002	0.010
28-Feb-06	-90	0.031	0.108	0.174	0.688	0.002	0.011	0.002	0.011
28-Feb-06	-125	0.025	0.082	0.170	0.724	0.010	0.030	0.005	0.035
28-Feb-06	-160	0.018	0.055	0.176	0.751	0.012	0.035	0.015	0.032
21-Mar-06	-20	0.034	0.043	0.194	0.730	0.006	0.007	0.003	0.009
21-Mar-06	-55	0.052	0.078	0.180	0.691	0.009	0.011	0.006	0.014
21-Mar-06	-90	0.054	0.084	0.180	0.682	0.005	0.014	0.006	0.012
21-Mar-06	-125	0.043	0.090	0.182	0.685	0.008	0.013	0.006	0.015
21-Mar-06	-160	0.013	0.021	0.203	0.763	0.006	0.009	0.004	0.011
1-May-06	-20	0.024	0.026	0.179	0.770	0.017	0.007	0.010	0.012
1-May-06	-55	0.060	0.040	0.157	0.743	0.032	0.007	0.015	0.021
1-May-06	-90	0.127	0.052	0.127	0.694	0.059	0.006	0.023	0.041
1-May-06	-125	0.210	0.105	0.088	0.598	0.045	0.031	0.017	0.057
1-May-06	-160	0.271	0.264	0.056	0.410	0.013	0.016	0.004	0.025
31-May-06	-20	0.000	0.103	0.119	0.774	0.000	0.017	0.014	0.003
31-May-06	-55	0.000	0.160	0.069	0.770	0.000	0.013	0.013	0.004
31-May-06	-90	0.016	0.198	0.035	0.750	0.011	0.007	0.009	0.008
31-May-06	-125	0.047	0.213	0.021	0.719	0.016	0.004	0.004	0.015
31-May-06	-160	0.118	0.228	0.021	0.641	0.034	0.012	0.008	0.034

Table F.6. Site 1 Temperature Results

Date	Depth / Temperature (°C)											
	-160	SE	-125	SE	-90	SE	-55	SE	-20	SE	Surface	Ambient
19-Aug-05	26.9	0.8	29.1	0.3	31.3	0.5	32.1	0.2	26.3	1.6	-	-
20-Aug-05	26.9	0.8	29.4	0.3	31.5	0.5	31.9	0.2	29.8	1.3	-	-
21-Aug-05	26.9	0.7	29.3	0.2	30.9	0.5	31.4	0.2	35.0	0.5	-	-
22-Aug-05	26.9	0.7	29.1	0.2	30.4	0.5	31.9	0.6	39.1	0.5	-	-
23-Aug-05	26.9	0.8	29.1	0.3	30.4	0.5	32.9	1.0	40.3	0.3	-	-
24-Aug-05	27.4	1.8	29.1	0.3	30.8	1.4	33.4	-	36.3	1.2	-	-
25-Aug-05	27.5	2.0	29.1	0.3	31.0	1.4	33.2	-	31.9	0.6	-	-
26-Aug-05	27.5	1.8	29.1	0.3	31.0	1.4	32.3	-	32.6	0.3	-	-
27-Aug-05	27.3	1.6	29.0	0.3	30.7	1.4	31.7	-	35.9	0.4	-	-
28-Aug-05	27.1	1.3	28.9	0.3	30.5	1.3	31.9	-	38.2	0.6	-	-
29-Aug-05	26.9	1.1	28.8	0.3	30.4	1.3	32.5	-	40.7	1.1	-	-
30-Aug-05	27.0	1.3	29.0	0.5	30.5	1.3	33.4	-	41.7	0.2	-	-
31-Aug-05	27.0	1.3	29.1	0.7	30.8	1.4	34.1	-	41.3	0.3	-	-
1-Sep-05	27.0	1.2	29.2	0.7	31.2	1.5	34.6	-	40.6	0.5	-	-
2-Sep-05	27.0	1.1	29.3	0.7	31.3	1.5	34.8	-	41.0	0.2	-	-
3-Sep-05	26.9	0.9	29.4	0.7	31.5	1.4	34.9	-	42.6	0.8	-	-
4-Sep-05	27.0	0.9	29.7	0.7	31.7	1.4	35.4	-	40.2	0.4	-	-
5-Sep-05	27.1	0.9	29.8	0.8	31.8	1.3	35.1	-	35.9	1.3	-	-
6-Sep-05	27.2	0.9	30.0	0.8	31.8	1.2	34.3	-	37.1	0.9	-	-
7-Sep-05	27.2	0.8	30.1	0.8	31.7	1.2	34.0	-	38.1	0.7	-	-
8-Sep-05	27.1	0.7	30.1	0.8	31.5	1.1	34.0	-	40.2	0.0	-	-
9-Sep-05	27.2	0.7	30.2	0.8	31.5	1.1	34.4	-	41.8	0.1	-	-
10-Sep-05	27.3	0.8	30.2	0.9	31.5	1.1	34.8	-	39.4	0.7	-	-
11-Sep-05	27.5	1.1	30.5	1.1	31.7	1.1	34.5	-	35.0	1.3	-	-
12-Sep-05	27.6	1.1	30.6	1.1	31.7	1.1	33.8	-	34.5	2.0	-	-
13-Sep-05	27.5	1.1	30.5	1.1	31.3	1.0	33.1	-	35.3	2.1	-	-
14-Sep-05	27.5	1.0	30.4	1.0	31.1	1.0	32.9	-	35.8	1.7	-	-
15-Sep-05	29.0	2.0	30.4	1.2	31.3	0.7	32.5	0.2	33.7	2.1	9.6	-
16-Sep-05	28.7	1.7	30.4	1.2	31.1	0.7	32.1	0.2	29.7	2.1	10.7	-
17-Sep-05	28.4	1.4	30.3	1.1	30.8	0.6	31.1	0.6	25.9	1.8	11.4	-
18-Sep-05	28.1	1.2	30.1	1.0	30.3	0.6	29.9	0.7	27.4	1.0	15.7	-
19-Sep-05	27.9	1.1	29.8	0.9	29.7	0.5	29.2	0.6	31.2	1.0	14.3	-
20-Sep-05	28.1	1.4	29.6	0.9	29.3	0.5	29.3	0.4	34.7	0.8	12.1	-
21-Sep-05	28.1	1.8	29.4	1.0	29.1	0.3	30.0	0.1	36.0	1.0	11.5	8.93
22-Sep-05	27.9	1.6	29.5	1.2	29.2	0.4	30.6	0.2	35.5	1.3	11.7	7.58
23-Sep-05	27.5	1.2	29.3	1.2	29.3	0.4	30.7	0.3	35.5	1.2	11.3	7.78
24-Sep-05	27.2	1.0	29.1	1.1	29.3	0.4	30.8	0.3	36.8	1.1	14.0	8.99
25-Sep-05	26.9	0.9	28.8	1.0	29.2	0.4	30.9	0.2	38.0	1.1	17.3	13.97
26-Sep-05	27.0	1.2	28.7	0.9	29.1	0.4	31.2	0.1	40.0	1.0	15.6	9.69
27-Sep-05	28.1	2.3	28.9	1.2	29.3	0.5	32.1	0.3	40.6	1.5	11.1	7.49
28-Sep-05	27.5	1.7	29.1	1.4	29.6	0.5	32.8	0.4	37.8	1.6	11.2	6.10
29-Sep-05	27.1	1.4	28.9	1.3	29.8	0.6	32.4	0.1	38.2	1.2	17.7	12.70
30-Sep-05	27.1	1.4	28.9	1.3	29.9	0.6	32.3	0.1	41.0	1.0	14.9	10.49

1-Oct-05	27.2	1.5	29.0	1.3	30.0	0.6	32.9	0.2	39.7	1.2	9.3	4.51
2-Oct-05	27.6	1.9	29.1	1.3	30.2	0.6	32.7	0.2	31.6	1.8	5.2	2.23
3-Oct-05	28.1	2.3	29.4	1.5	30.2	0.6	31.5	0.5	27.8	1.8	5.7	2.95
4-Oct-05	27.8	1.8	29.5	1.6	29.9	0.6	30.5	0.5	28.2	2.3	4.9	3.16
5-Oct-05	27.3	1.4	29.4	1.6	29.7	0.6	30.4	1.0	28.3	1.9	6.8	3.70
6-Oct-05	27.1	1.2	29.2	1.4	29.4	0.7	29.9	1.3	29.1	1.6	17.0	4.69
7-Oct-05	26.7	1.0	28.9	1.3	28.9	0.7	29.1	1.3	31.1	1.3	21.4	5.85
8-Oct-05	26.6	1.0	28.6	1.1	28.4	0.7	28.9	1.1	33.9	1.4	18.6	8.43
9-Oct-05	26.4	1.0	28.3	1.1	28.1	0.6	29.1	0.8	35.4	1.7	17.3	7.59
10-Oct-05	26.1	1.1	28.0	1.1	27.9	0.6	29.6	0.8	33.9	1.7	18.5	8.95
11-Oct-05	26.5	1.5	27.8	1.1	27.8	0.7	29.7	0.8	36.4	1.8	20.9	9.77
12-Oct-05	26.2	1.5	27.8	1.2	27.9	0.7	30.3	0.6	35.1	2.0	18.4	8.41
13-Oct-05	26.0	1.3	27.7	1.2	28.0	0.7	30.2	0.8	36.4	1.4	20.6	6.75
14-Oct-05	26.4	1.9	27.7	1.2	28.0	0.7	30.6	0.5	36.9	2.2	16.8	7.09
15-Oct-05	26.0	1.6	27.7	1.3	28.1	0.7	30.9	0.6	35.2	1.6	20.9	6.56
16-Oct-05	25.9	1.6	27.7	1.3	28.2	0.7	30.6	0.7	36.6	1.2	19.8	4.28
17-Oct-05	25.7	1.4	27.6	1.3	28.2	0.7	30.6	0.7	35.7	1.4	20.3	7.65
18-Oct-05	25.7	1.4	27.6	1.2	28.2	0.7	30.5	0.6	35.4	1.1	17.5	6.81
19-Oct-05	25.5	1.4	27.5	1.3	28.1	0.6	30.4	0.6	34.6	1.4	19.0	4.63
20-Oct-05	26.7	2.5	27.6	1.3	28.0	0.6	30.4	0.4	36.0	1.9	16.2	4.69
21-Oct-05	26.8	2.1	28.0	1.6	28.1	0.6	31.4	0.4	32.1	2.4	13.3	2.87
22-Oct-05	26.1	1.7	27.9	1.6	28.4	0.6	31.2	0.6	31.9	2.4	12.5	3.59
23-Oct-05	25.9	1.4	27.9	1.5	28.5	0.6	30.4	0.9	32.9	2.0	21.0	5.62
24-Oct-05	25.7	1.2	27.8	1.3	28.3	0.6	29.9	1.0	35.7	1.5	23.7	7.08
25-Oct-05	25.3	1.1	27.4	1.2	27.9	0.6	29.9	0.8	36.4	1.5	23.6	9.37
26-Oct-05	25.3	1.2	27.2	1.1	27.7	0.6	30.0	0.7	37.7	1.9	23.9	8.37
27-Oct-05	25.4	1.4	27.2	1.1	27.7	0.6	30.8	0.3	37.4	2.4	16.7	5.40
28-Oct-05	25.2	1.2	27.2	1.1	27.9	0.6	31.0	0.7	36.2	2.0	13.9	0.53
29-Oct-05	25.1	1.0	27.2	1.1	28.0	0.6	30.6	0.9	36.9	1.9	16.1	2.07
30-Oct-05	24.9	1.1	27.1	1.0	27.9	0.6	30.6	0.7	38.1	1.9	14.0	3.74
31-Oct-05	24.8	1.2	27.0	1.1	27.9	0.6	30.8	0.7	35.8	1.9	13.1	0.59
1-Nov-05	24.9	1.4	27.0	1.1	27.8	0.6	30.4	0.8	36.4	1.7	13.5	0.71
2-Nov-05	24.9	1.3	27.0	1.2	27.7	0.6	30.0	0.8	35.8	1.9	14.5	0.14
3-Nov-05	24.7	1.1	26.9	1.2	27.6	0.6	29.7	0.8	35.0	1.9	10.5	-1.85
4-Nov-05	24.6	1.1	26.8	1.1	27.4	0.6	29.3	0.9	34.5	1.9	9.0	-3.60
5-Nov-05	24.5	1.1	26.6	1.1	27.1	0.6	29.0	0.8	35.2	1.8	11.0	-2.45
6-Nov-05	24.3	1.0	26.5	1.1	26.9	0.6	28.8	0.8	34.6	2.1	11.9	-3.17
7-Nov-05	24.1	1.0	26.3	1.1	26.7	0.6	28.6	0.8	35.1	2.0	9.1	-3.06
8-Nov-05	24.1	1.0	26.2	1.1	26.6	0.6	28.5	0.9	34.6	2.1	10.3	-2.79
9-Nov-05	23.9	1.0	26.0	1.0	26.4	0.6	28.4	0.9	33.5	2.2	17.2	1.24
10-Nov-05	23.7	1.0	25.7	1.0	26.0	0.6	27.9	1.0	33.5	2.5	26.8	8.50
11-Nov-05	24.1	1.4	25.6	1.0	25.9	0.6	28.1	0.8	35.2	2.9	19.1	1.45
12-Nov-05	24.5	2.0	25.7	1.2	25.8	0.6	28.7	0.6	33.4	2.9	12.9	-3.38
13-Nov-05	24.3	1.8	25.9	1.5	25.9	0.6	29.3	0.7	31.1	2.8	9.5	-4.05
14-Nov-05	25.5	2.6	25.9	1.6	26.1	0.6	29.5	0.3	30.0	2.7	8.7	-6.58
15-Nov-05	25.5	2.2	26.5	2.0	26.5	0.6	30.2	0.5	25.5	2.7	5.8	-9.47

16-Nov-05	24.8	1.8	26.5	1.8	27.0	0.7	29.0	1.0	27.5	2.7	7.6	-0.70
17-Nov-05	24.8	1.9	26.4	1.6	26.6	0.6	28.2	0.9	29.9	2.5	11.4	4.38
18-Nov-05	25.1	2.2	26.1	1.6	26.3	0.5	28.1	0.8	30.2	2.2	17.4	7.36
19-Nov-05	25.4	2.2	26.5	1.9	26.4	0.6	29.1	0.9	28.9	2.2	13.8	7.18
20-Nov-05	24.8	2.0	26.3	1.7	26.3	0.5	28.8	0.8	32.1	2.1	13.6	6.74
21-Nov-05	24.7	2.1	26.2	1.7	26.3	0.4	29.2	0.7	31.0	2.3	12.6	5.61
22-Nov-05	24.2	1.7	26.0	1.5	26.2	0.4	28.5	0.8	32.5	1.8	17.7	11.14
23-Nov-05	23.9	1.6	25.7	1.4	26.0	0.4	28.2	0.7	35.6	1.2	20.3	8.20
24-Nov-05	23.7	1.5	25.7	1.3	25.9	0.4	28.5	0.6	35.9	1.6	21.1	3.76
25-Nov-05	23.5	1.2	25.5	1.2	25.8	0.4	28.5	0.5	36.3	1.7	25.5	1.83
26-Nov-05	23.4	1.2	25.3	1.1	25.8	0.4	28.7	0.5	37.6	1.7	22.5	-1.15
27-Nov-05	24.4	2.4	25.3	1.3	25.8	0.4	29.7	0.6	35.1	2.2	13.2	-2.29
28-Nov-05	24.0	1.8	25.5	1.5	26.0	0.5	30.7	0.7	29.2	2.5	8.0	-6.75
29-Nov-05	23.4	1.5	25.4	1.4	26.4	0.5	29.9	0.6	30.1	2.9	3.9	-12.27
30-Nov-05	23.3	1.4	25.3	1.4	26.3	0.5	28.8	0.8	31.5	2.1	8.1	-12.52
1-Dec-05	23.1	1.3	25.2	1.3	26.0	0.5	28.2	0.7	30.9	1.9	8.5	-14.11
2-Dec-05	22.8	1.1	25.0	1.2	25.6	0.4	27.4	0.8	29.9	1.9	7.7	-14.72
3-Dec-05	22.6	1.1	24.8	1.1	25.2	0.4	26.7	1.0	29.6	1.7	8.0	-17.67
4-Dec-05	22.4	1.0	24.6	1.0	24.8	0.4	26.2	1.0	28.8	1.3	6.9	-18.79
5-Dec-05	22.4	1.0	24.3	1.0	24.3	0.4	25.9	0.7	27.0	1.6	6.3	-16.62
6-Dec-05	22.2	0.9	24.1	1.0	24.1	0.4	26.5	0.5	25.4	2.7	1.5	-21.65
7-Dec-05	21.9	0.9	23.9	0.9	24.0	0.4	25.6	1.0	24.2	2.3	-0.1	-16.82
8-Dec-05	21.9	0.9	23.8	0.8	23.7	0.4	24.7	1.2	23.8	2.1	5.0	0.51
9-Dec-05	22.1	1.2	23.4	0.7	23.1	0.4	24.3	1.1	24.0	1.8	10.6	5.30
10-Dec-05	22.9	1.9	23.7	1.3	23.2	0.5	25.3	1.4	23.4	2.3	9.9	5.21
11-Dec-05	22.6	2.0	23.6	1.2	23.0	0.3	25.0	1.1	25.6	2.6	11.4	4.84
12-Dec-05	22.1	1.6	23.5	1.3	22.9	0.3	24.9	1.3	27.2	2.3	10.4	0.00
13-Dec-05	22.3	2.0	23.2	1.2	22.7	0.2	24.6	1.1	28.2	1.9	11.0	-0.19
14-Dec-05	23.0	2.5	23.3	1.5	23.0	0.6	26.1	1.6	25.0	2.4	8.0	-2.52
15-Dec-05	22.4	2.0	23.2	1.5	23.3	0.6	26.4	1.7	20.6	2.5	1.2	-11.02
16-Dec-05	21.8	1.7	23.1	1.4	23.3	0.4	25.4	1.4	20.3	3.5	-2.3	-17.81
17-Dec-05	21.3	1.4	22.9	1.3	23.1	0.2	24.5	1.4	20.2	3.5	-4.9	-16.64
18-Dec-05	21.0	1.2	22.8	1.1	22.8	0.2	23.7	1.6	18.1	3.6	-4.4	-11.67
19-Dec-05	20.8	1.0	22.5	1.0	22.3	0.2	22.9	1.7	17.2	3.5	-2.7	-9.07
20-Dec-05	20.4	0.9	22.2	0.8	21.8	0.3	22.2	1.7	16.8	3.2	-2.2	-9.15
21-Dec-05	20.2	0.8	21.9	0.7	21.2	0.4	21.5	1.7	16.6	2.9	1.1	2.33
22-Dec-05	19.8	0.7	21.5	0.6	20.7	0.4	20.9	1.7	17.7	2.6	6.8	0.72
23-Dec-05	20.4	1.1	21.2	0.6	20.2	0.4	21.1	1.5	19.5	2.3	9.0	2.53
24-Dec-05	20.1	1.2	21.2	0.8	20.1	0.4	22.1	1.5	19.0	2.4	7.9	1.84
25-Dec-05	19.5	1.0	20.8	0.7	20.1	0.4	21.3	1.6	21.9	2.1	12.0	6.34
26-Dec-05	19.5	0.9	20.6	0.7	19.8	0.4	21.2	1.4	25.7	2.1	12.2	2.41
27-Dec-05	19.1	0.9	20.4	0.6	19.7	0.5	22.0	1.0	25.7	2.6	8.7	-0.53
28-Dec-05	19.0	1.0	20.2	0.6	19.7	0.5	22.4	1.0	26.4	2.6	8.7	0.46
29-Dec-05	18.7	1.0	20.1	0.7	19.8	0.5	22.6	1.0	27.3	2.1	7.9	-3.53
30-Dec-05	18.3	0.9	19.9	0.7	19.8	0.5	22.7	1.0	26.9	1.8	5.6	-5.84
31-Dec-05	18.2	0.8	19.8	0.6	19.8	0.5	22.5	1.1	26.6	1.6	5.5	-4.73

1-Jan-06	18.1	0.8	19.7	0.6	19.7	0.5	22.3	1.2	27.1	1.5	7.8	-3.12
2-Jan-06	17.8	0.7	19.5	0.6	19.6	0.5	22.1	1.2	27.2	1.4	6.5	-6.63
3-Jan-06	17.8	0.8	19.4	0.6	19.5	0.6	22.3	1.2	26.7	1.0	5.1	-6.21
4-Jan-06	18.4	1.3	19.4	0.7	19.5	0.6	23.3	0.7	23.1	2.1	3.4	-5.30
5-Jan-06	18.5	1.3	19.8	1.0	19.9	0.6	24.2	1.2	20.0	2.0	3.6	0.33
6-Jan-06	18.3	1.5	19.8	1.0	20.1	0.6	23.0	1.3	22.8	1.4	8.1	2.22
7-Jan-06	18.0	1.2	19.8	1.0	20.0	0.6	22.6	1.3	24.8	1.0	7.1	-3.44
8-Jan-06	17.9	1.2	19.7	1.0	19.8	0.6	22.5	1.2	25.7	0.8	5.3	-6.18
9-Jan-06	17.7	1.1	19.5	0.9	19.7	0.6	22.5	1.1	24.8	0.9	5.9	-2.78
10-Jan-06	17.5	1.0	19.4	0.9	19.5	0.6	22.3	1.1	24.8	0.9	5.2	-4.09
11-Jan-06	17.4	0.9	19.2	0.8	19.3	0.5	22.0	1.0	25.0	1.0	6.4	-4.54
12-Jan-06	17.6	1.1	19.1	0.8	19.2	0.5	22.1	0.9	25.1	0.9	3.2	-6.35
13-Jan-06	17.4	1.1	19.1	0.8	19.1	0.5	22.5	0.7	23.3	1.2	2.6	-6.54
14-Jan-06	17.1	1.0	18.9	0.8	19.1	0.5	22.1	1.0	23.2	0.9	2.7	-8.67
15-Jan-06	17.1	1.0	18.8	0.8	19.0	0.5	21.9	1.0	23.5	1.0	3.2	-6.97
16-Jan-06	17.1	1.1	18.7	0.8	18.9	0.5	22.0	0.8	22.6	1.0	2.7	-6.37
17-Jan-06	16.8	1.0	18.6	0.8	18.9	0.5	21.9	0.8	21.4	0.9	3.5	-4.98
18-Jan-06	16.8	1.0	18.4	0.7	18.7	0.5	21.3	1.0	21.7	0.9	4.8	-4.36
19-Jan-06	16.9	1.1	18.3	0.8	18.5	0.5	21.6	0.6	20.5	1.4	1.4	-11.21
20-Jan-06	16.5	1.0	18.2	0.8	18.4	0.5	21.4	0.8	20.7	1.2	0.8	-10.26
21-Jan-06	16.4	0.9	18.1	0.8	18.4	0.5	21.1	0.9	20.7	1.1	0.5	-9.69
22-Jan-06	16.3	0.9	18.1	0.7	18.4	0.5	21.1	1.0	19.7	1.0	2.4	-0.34
23-Jan-06	16.5	1.0	17.9	0.7	18.1	0.5	20.8	0.9	19.6	1.0	5.7	0.55
24-Jan-06	17.1	1.4	18.3	1.0	18.2	0.5	21.7	0.9	19.2	1.5	6.4	1.20
25-Jan-06	16.5	1.1	18.2	1.0	18.5	0.6	21.1	1.2	20.8	1.0	7.9	2.13
26-Jan-06	16.4	1.0	18.0	0.9	18.3	0.6	20.7	1.2	22.7	0.6	9.1	1.10
27-Jan-06	16.2	1.0	17.8	0.8	18.1	0.6	20.9	1.0	23.7	0.9	7.1	-4.37
28-Jan-06	15.9	0.9	17.7	0.7	18.0	0.7	21.0	0.9	23.2	0.7	4.5	-6.87
29-Jan-06	16.2	0.9	17.6	0.7	18.0	0.7	21.1	0.9	23.4	0.8	5.5	-4.56
30-Jan-06	15.9	0.9	17.5	0.7	17.9	0.7	21.0	0.9	22.7	0.8	3.4	-6.27
31-Jan-06	16.3	1.1	17.5	0.7	17.9	0.7	21.5	0.4	21.6	0.9	2.0	-6.82
1-Feb-06	16.1	1.0	17.6	0.7	18.1	0.7	21.2	0.7	20.9	0.9	3.3	-3.86
2-Feb-06	16.3	1.0	17.5	0.7	18.0	0.7	21.1	0.8	20.6	1.2	5.1	-1.06
3-Feb-06	16.1	1.1	17.5	0.8	18.0	0.7	22.3	0.5	18.4	1.5	4.5	-1.04
4-Feb-06	15.9	1.1	17.5	0.8	18.4	0.7	22.2	1.0	18.3	1.4	3.7	-2.47
5-Feb-06	17.3	1.3	18.3	1.4	18.8	0.7	22.8	1.4	18.4	1.2	3.9	-3.43
6-Feb-06	18.1	1.3	19.7	1.7	20.4	0.7	23.0	1.8	15.6	1.4	2.2	-4.68
7-Feb-06	17.5	1.1	19.6	1.2	20.6	0.7	22.4	1.7	13.8	1.6	0.3	-4.83
8-Feb-06	17.5	1.1	19.4	1.0	20.1	0.8	21.6	1.6	15.3	1.6	3.1	0.06
9-Feb-06	18.8	1.3	20.5	1.6	20.9	0.6	22.3	1.9	15.4	1.7	3.7	-1.15
10-Feb-06	19.2	1.1	21.8	1.2	21.8	0.9	21.6	2.1	13.6	1.6	1.1	-4.62
11-Feb-06	18.9	1.0	21.4	1.0	21.1	0.9	21.2	1.8	13.6	1.6	4.0	2.25
12-Feb-06	18.3	0.9	20.8	0.9	20.2	1.0	21.0	1.7	15.8	1.7	7.0	5.09
13-Feb-06	18.3	1.0	20.3	0.8	19.8	0.9	21.5	1.3	18.7	1.6	9.0	2.75
14-Feb-06	18.9	1.2	20.1	0.9	19.7	0.8	22.6	0.6	19.9	1.9	4.5	-7.48
15-Feb-06	18.6	1.3	20.0	1.1	19.9	0.7	23.0	0.8	18.0	2.6	-0.8	-12.47

16-Feb-06	19.4	1.2	20.3	1.5	20.5	0.6	22.5	1.4	15.5	3.0	-6.8	-24.31
17-Feb-06	19.1	1.0	20.8	1.4	21.0	0.6	22.2	1.8	11.5	2.8	-8.5	-15.98
18-Feb-06	18.5	1.0	20.4	1.1	20.4	0.7	21.4	1.5	10.6	2.7	-4.7	-7.33
19-Feb-06	18.1	0.9	20.0	0.9	19.7	0.7	20.8	1.4	10.9	2.6	-2.3	-3.49
20-Feb-06	18.1	1.0	19.6	0.8	19.1	0.8	20.5	1.2	11.5	2.5	-1.4	-3.63
21-Feb-06	17.9	1.1	19.4	0.8	18.6	0.9	20.3	1.0	12.7	2.5	-0.4	-2.78
22-Feb-06	17.7	1.0	18.9	0.7	18.1	0.9	19.6	1.0	14.0	2.4	0.5	-9.35
23-Feb-06	17.1	0.9	18.6	0.6	17.8	0.9	19.7	1.0	15.2	2.3	1.6	-11.94
24-Feb-06	16.9	1.0	18.2	0.6	17.6	0.8	19.7	0.9	15.6	2.4	0.1	-12.95
25-Feb-06	16.6	0.9	18.0	0.6	17.5	0.8	20.1	0.8	15.5	2.4	-0.6	-12.66
26-Feb-06	16.0	0.8	17.7	0.6	17.4	0.8	20.0	0.9	15.1	2.3	-1.3	-12.61
27-Feb-06	15.6	0.7	17.4	0.5	17.3	0.8	19.3	1.0	14.5	2.0	-0.7	-10.62
28-Feb-06	16.3	0.8	17.3	0.5	17.1	0.7	19.5	0.6	14.0	2.0	-0.4	-10.09
1-Mar-06	16.4	1.1	17.4	0.7	17.4	0.6	20.5	0.9	13.2	2.3	1.3	-9.60
2-Mar-06	16.4	1.1	17.7	1.0	18.3	0.9	20.4	1.8	11.7	2.1	2.4	-13.98
3-Mar-06	15.7	0.9	17.6	0.9	18.0	0.9	19.4	1.6	12.0	2.0	2.3	-13.96
4-Mar-06	15.5	0.8	17.4	0.8	17.5	0.9	18.7	1.5	13.5	1.8	2.6	-11.10
5-Mar-06	15.1	0.7	17.1	0.7	17.0	0.9	18.3	1.5	14.5	1.6	2.7	-13.28
6-Mar-06	15.0	0.6	16.9	0.6	16.7	0.9	18.0	1.5	14.7	1.3	0.2	-5.62
7-Mar-06	14.8	0.6	16.6	0.5	16.2	1.0	17.5	1.5	14.9	1.1	1.8	-2.20
8-Mar-06	14.4	0.5	16.2	0.4	15.8	1.0	17.2	1.4	14.6	0.9	1.7	-2.23
9-Mar-06	14.4	0.6	15.9	0.4	15.5	0.9	16.8	1.4	13.7	0.9	1.5	-0.69
10-Mar-06	14.9	1.0	16.0	0.7	15.8	0.8	17.6	1.4	13.0	1.5	0.4	-4.32
11-Mar-06	15.8	1.0	16.7	1.1	16.4	0.8	17.6	2.1	11.3	1.6	0.2	-6.42
12-Mar-06	15.8	0.9	17.3	1.0	16.7	1.0	16.7	2.1	9.9	1.4	0.5	-10.28
13-Mar-06	15.1	0.8	17.0	0.9	16.4	0.9	16.2	2.0	9.6	1.3	0.4	-15.03
14-Mar-06	14.8	0.7	16.6	0.7	15.9	0.8	15.8	1.9	10.6	1.1	0.3	-11.31
15-Mar-06	15.1	0.6	16.2	0.6	15.4	0.9	15.5	1.9	11.1	1.0	0.4	-8.46
16-Mar-06	15.0	0.6	16.1	0.6	15.0	0.9	15.5	2.0	11.5	1.0	0.4	-8.96
17-Mar-06	14.5	0.5	15.8	0.5	14.9	1.0	15.4	2.1	11.7	1.0	0.6	-5.34
18-Mar-06	14.7	0.5	15.6	0.5	14.6	1.1	15.1	2.2	12.1	0.8	1.0	-6.57
19-Mar-06	14.6	0.6	15.5	0.6	14.4	1.1	15.5	2.0	12.3	0.9	1.3	-7.08
20-Mar-06	14.0	0.5	15.2	0.6	14.3	1.1	15.2	2.0	12.4	0.9	1.1	-3.67
21-Mar-06	13.6	0.5	15.0	0.6	14.2	1.2	14.9	2.0	12.3	0.8	1.0	-3.44
24-Mar-06	12.7	0.4	14.1	0.5	13.3	1.3	13.4	2.3	10.1	1.3	0.7	-0.23
25-Mar-06	12.5	0.4	13.8	0.5	12.9	1.3	12.6	2.3	9.4	1.4	2.7	0.99
26-Mar-06	12.7	0.4	13.5	0.5	12.5	1.3	12.0	2.1	9.9	1.0	4.0	2.22
27-Mar-06	12.8	0.6	13.4	0.5	12.0	1.2	11.8	1.7	10.7	0.7	4.1	3.55
28-Mar-06	12.4	0.5	13.2	0.5	11.8	1.1	11.7	1.6	11.1	0.7	5.4	1.81
29-Mar-06	11.9	0.5	12.8	0.5	11.5	1.1	11.7	1.5	11.9	0.8	3.5	0.15
30-Mar-06	11.7	0.4	12.5	0.5	11.3	1.0	11.7	1.6	12.4	1.2	5.5	2.51
31-Mar-06	11.6	0.4	12.2	0.5	11.2	1.0	11.9	1.7	13.6	1.6	5.5	-0.13
1-Apr-06	11.5	0.4	12.0	0.5	11.1	1.1	12.1	1.7	14.9	1.7	6.8	1.12
2-Apr-06	11.8	0.6	12.1	0.6	11.2	1.2	13.5	1.7	15.0	1.5	6.5	2.57
3-Apr-06	11.4	0.5	12.1	0.6	11.6	1.3	13.8	1.7	16.4	1.7	9.9	6.96
4-Apr-06	11.1	0.5	12.0	0.6	11.7	1.3	13.8	1.6	19.0	2.1	12.7	6.92

5-Apr-06	10.9	0.4	11.8	0.6	11.7	1.2	14.0	1.4	21.7	2.5	14.1	6.67
6-Apr-06	10.8	0.4	11.7	0.5	11.8	1.2	14.4	1.2	24.2	2.9	12.6	6.00
7-Apr-06	10.9	0.5	11.7	0.5	11.9	1.2	14.9	1.1	25.6	3.1	14.3	7.81
8-Apr-06	10.6	0.4	11.7	0.5	12.2	1.2	15.5	1.2	26.3	2.4	15.5	7.53
9-Apr-06	10.6	0.4	11.7	0.5	12.5	1.2	16.0	1.0	27.5	2.5	15.9	7.25
10-Apr-06	10.5	0.4	11.7	0.5	12.8	1.2	16.4	0.9	29.1	2.6	18.5	9.52
11-Apr-06	10.5	0.4	11.8	0.5	13.0	1.1	17.0	0.8	31.2	2.6	19.4	10.83
12-Apr-06	10.4	0.4	11.8	0.6	13.4	1.1	17.8	0.7	31.4	2.5	18.6	9.20
13-Apr-06	10.7	0.5	12.0	0.6	13.9	1.0	18.4	0.7	31.8	2.4	19.6	7.96
14-Apr-06	10.6	0.5	12.2	0.6	14.2	1.0	18.9	0.6	32.1	2.6	22.1	11.44
15-Apr-06	11.3	0.7	12.5	0.7	14.7	1.0	19.5	0.6	34.7	2.4	18.4	5.20
16-Apr-06	11.7	1.0	13.1	0.9	15.3	0.9	20.6	0.4	34.9	2.7	11.9	1.37
17-Apr-06	12.7	1.3	13.9	1.3	15.9	0.9	21.8	0.3	31.2	3.4	12.1	6.29
18-Apr-06	13.5	1.3	14.8	1.6	16.9	0.7	23.0	0.3	27.0	2.7	15.1	9.66
19-Apr-06	13.1	1.1	15.0	1.4	17.7	0.8	23.4	0.9	25.8	2.0	15.7	9.77
20-Apr-06	13.0	0.9	15.2	1.2	18.1	1.0	22.8	1.2	30.3	2.2	21.3	14.61
21-Apr-06	12.8	0.8	15.2	1.1	18.0	1.0	22.5	1.0	33.8	2.2	25.6	15.12
22-Apr-06	14.3	0.9	16.2	1.2	18.7	0.9	23.8	0.3	36.8	2.9	16.6	3.95
23-Apr-06	15.1	1.0	17.4	1.2	19.7	1.0	25.9	0.7	30.1	1.7	16.3	8.39
24-Apr-06	15.1	0.8	17.7	1.2	20.5	1.1	26.4	0.9	27.6	1.3	11.2	4.13
30-Apr-06	17.2	1.5	19.0	1.3	22.6	0.6	28.6	0.6	38.2	4.2	19.3	-
1-May-06	16.9	1.3	19.3	1.3	23.1	0.5	29.0	0.4	36.6	3.5	20.1	-
2-May-06	18.4	1.7	20.0	1.3	23.9	0.5	29.4	0.6	35.7	4.2	21.5	-
3-May-06	19.9	1.6	21.3	1.6	24.9	0.3	29.7	0.3	31.0	3.6	19.7	7.60
4-May-06	19.0	1.4	21.5	1.5	25.4	0.1	29.5	0.7	30.6	2.7	20.9	12.36
5-May-06	18.5	1.2	21.5	1.4	25.1	0.3	28.6	0.8	35.6	1.8	31.5	18.68
6-May-06	18.4	1.1	21.4	1.3	24.8	0.4	28.4	0.4	40.8	2.1	35.6	10.04
7-May-06	18.4	1.2	21.4	1.2	24.6	0.4	29.0	0.1	39.5	1.6	30.5	13.72
8-May-06	19.5	1.7	21.8	1.3	24.8	0.4	29.7	0.3	39.4	1.2	25.1	4.92
9-May-06	21.0	2.1	22.7	2.0	25.6	0.2	31.3	1.0	34.1	1.6	17.6	6.24
10-May-06	21.5	1.9	23.3	2.0	26.4	0.5	31.9	0.9	29.5	1.4	19.7	12.23
11-May-06	20.5	1.6	23.3	1.7	26.7	0.3	30.9	0.7	30.4	1.0	22.0	13.86
12-May-06	20.4	1.5	23.3	1.5	26.6	0.2	30.1	0.6	34.9	0.6	26.9	11.06
13-May-06	21.5	2.1	23.7	1.5	26.5	0.3	31.0	0.4	33.8	0.7	24.3	11.72
14-May-06	21.2	1.9	23.8	1.6	26.8	0.2	32.1	0.5	31.4	1.2	25.1	16.46
15-May-06	20.7	1.5	23.8	1.4	27.1	0.3	31.8	0.6	32.9	1.3	26.8	19.21
16-May-06	20.5	1.3	23.8	1.3	27.1	0.4	31.5	0.5	36.9	0.8	31.6	21.07
17-May-06	20.2	1.2	23.8	1.1	27.1	0.5	31.5	0.2	41.4	0.7	38.5	25.18
18-May-06	20.2	1.1	23.8	1.1	27.1	0.5	32.0	0.2	45.5	1.1	42.3	21.98
19-May-06	20.0	1.0	23.7	1.0	27.3	0.4	33.0	0.5	46.6	0.8	41.3	18.55
20-May-06	20.1	1.1	23.8	1.0	27.8	0.4	34.1	0.4	45.4	0.4	38.1	12.72
21-May-06	20.4	1.1	24.1	1.0	28.5	0.5	34.8	0.4	41.7	0.6	34.4	15.78
22-May-06	20.4	1.0	24.3	1.0	28.9	0.5	34.4	0.3	44.4	1.3	34.1	18.08
23-May-06	20.6	1.1	24.5	1.0	28.9	0.5	34.6	0.4	44.5	0.8	31.6	15.72
24-May-06	21.6	1.5	25.0	1.1	29.4	0.4	35.6	0.7	41.3	1.2	26.9	13.29
25-May-06	21.6	1.4	25.3	1.2	29.8	0.4	35.7	0.5	35.7	1.5	22.3	10.17

26-May-06	21.8	1.3	25.6	1.2	30.2	0.2	33.9	0.2	31.5	1.2	16.3	7.85
27-May-06	22.0	1.2	25.8	1.2	29.8	0.1	32.1	0.1	31.2	1.4	17.3	10.14
28-May-06	22.0	1.2	25.8	1.1	27.4	2.2	31.0	0.2	35.7	1.9	20.2	9.70
29-May-06	22.1	1.1	25.7	1.1	28.6	0.1	30.7	0.2	37.5	2.0	22.9	11.49
30-May-06	22.3	1.2	25.6	1.0	28.0	0.2	30.6	0.2	35.7	2.3	21.9	13.50
31-May-06	22.6	1.5	25.5	1.0	28.0	0.1	30.8	0.4	36.9	3.0	22.5	14.10

Table F.7. Site 2 Temperature Results

Date	Depth / Temperature (°C)											
	160	SE	125	SE	90	SE	55	SE	20	SE	Surface	Ambient
19-Aug-05	36.7	0.4	29.7	0.2	28.0	0.4	27.0	0.6	24.9	0.5	-	-
20-Aug-05	37.3	0.5	30.7	0.2	28.7	0.3	27.2	0.4	27.3	0.5	-	-
21-Aug-05	37.4	0.4	31.2	0.2	29.1	0.2	27.8	0.2	31.0	0.5	-	-
22-Aug-05	38.1	0.4	31.9	0.3	29.7	0.2	29.4	0.3	34.2	0.5	-	-
23-Aug-05	38.2	0.4	32.5	0.3	30.7	0.2	31.1	0.2	35.3	0.3	-	-
24-Aug-05	38.0	0.3	33.1	0.2	31.5	0.2	32.1	0.2	33.0	1.0	-	-
25-Aug-05	38.0	0.2	33.8	0.2	32.5	0.1	32.4	0.3	30.1	1.4	-	-
26-Aug-05	37.9	0.2	34.3	0.2	33.2	0.2	32.4	0.5	31.4	0.7	-	-
27-Aug-05	37.6	0.1	34.6	0.2	33.4	0.1	32.7	0.3	34.4	0.3	-	-
28-Aug-05	37.7	0.2	34.9	0.2	33.7	0.1	33.6	0.1	36.3	0.2	-	-
29-Aug-05	37.7	0.1	35.2	0.2	34.2	0.1	34.6	0.1	38.1	0.1	-	-
30-Aug-05	38.8	0.2	35.8	0.2	35.2	0.3	36.1	0.3	37.2	0.9	-	-
31-Aug-05	38.8	0.2	36.4	0.4	35.8	0.2	36.6	0.2	37.5	0.9	-	-
1-Sep-05	38.7	0.1	36.9	0.4	36.3	0.2	37.0	0.1	38.3	0.8	-	-
2-Sep-05	38.6	0.1	37.2	0.4	36.7	0.1	37.4	0.3	40.2	0.2	-	-
3-Sep-05	38.5	0.1	37.5	0.3	37.1	0.1	38.2	0.3	41.6	0.2	-	-
4-Sep-05	38.8	0.0	37.9	0.3	37.7	0.1	38.8	0.4	38.2	0.9	-	-
5-Sep-05	38.9	0.1	38.2	0.3	38.0	0.2	38.1	0.2	35.6	1.0	-	-
6-Sep-05	39.0	0.1	38.4	0.2	38.0	0.2	37.6	0.1	36.2	0.9	-	-
7-Sep-05	39.0	0.2	38.6	0.2	38.0	0.3	37.5	0.3	38.2	0.9	-	-
8-Sep-05	38.6	0.2	38.5	0.2	37.9	0.3	37.8	0.4	39.7	0.5	-	-
9-Sep-05	38.5	0.2	38.6	0.2	38.1	0.4	38.4	0.5	40.5	0.5	-	-
10-Sep-05	38.6	0.2	38.5	0.2	38.2	0.4	38.5	0.5	36.9	1.4	-	-
11-Sep-05	38.8	0.2	38.5	0.2	38.2	0.4	37.6	0.4	33.1	2.3	-	-
12-Sep-05	38.7	0.2	38.5	0.2	38.0	0.4	36.9	0.4	35.3	1.3	-	-
13-Sep-05	38.6	0.2	38.3	0.2	37.6	0.4	36.7	0.3	35.6	1.1	-	-
14-Sep-05	38.6	0.1	38.1	0.2	36.5	1.4	36.6	0.3	36.3	0.9	-	-
15-Sep-05	39.5	0.1	38.1	0.1	32.6	5.7	36.6	0.2	33.9	1.7	27.2	7.2
16-Sep-05	39.3	0.1	38.3	0.2	37.5	0.2	35.9	0.3	31.4	1.4	27.0	6.9
17-Sep-05	38.8	0.2	38.1	0.2	37.3	0.1	34.6	0.3	28.6	1.3	27.7	9.3
18-Sep-05	38.4	0.2	37.7	0.1	36.8	0.1	33.4	0.3	29.5	1.1	28.8	12.1
19-Sep-05	37.9	0.2	37.3	0.1	36.2	0.1	33.1	0.3	31.6	1.1	30.3	9.6
20-Sep-05	37.9	0.1	36.9	0.1	35.8	0.0	33.6	0.3	32.1	1.4	26.3	9.5

21-Sep-05	37.9	0.1	36.4	0.1	35.4	0.0	33.8	0.2	31.9	1.9	25.8	8.4
22-Sep-05	37.8	0.2	36.3	0.2	35.4	0.1	33.9	0.4	32.4	2.1	29.0	6.9
23-Sep-05	37.4	0.2	36.1	0.2	35.2	0.1	33.8	0.6	33.7	1.6	29.9	6.5
24-Sep-05	37.1	0.2	35.9	0.2	35.2	0.1	33.9	0.7	33.8	1.7	29.7	8.8
25-Sep-05	36.8	0.2	35.6	0.3	35.0	0.2	33.9	0.7	34.3	1.5	31.8	13.1
26-Sep-05	37.4	0.0	35.5	0.2	34.9	0.2	34.4	0.5	34.3	1.7	31.5	9.6
27-Sep-05	38.6	0.1	35.8	0.2	35.0	0.2	34.6	0.6	34.6	1.9	29.2	5.8
28-Sep-05	38.5	0.0	36.1	0.1	35.3	0.2	34.6	0.6	33.2	2.1	28.8	6.3
29-Sep-05	37.7	0.2	36.0	0.1	35.3	0.2	34.0	0.8	34.0	1.5	34.4	13.0
30-Sep-05	37.4	0.2	35.9	0.2	35.2	0.3	34.2	0.8	35.7	1.4	32.6	10.2
1-Oct-05	37.3	0.1	35.8	0.2	35.3	0.3	34.8	0.8	34.9	2.0	30.7	5.0
2-Oct-05	37.2	0.1	35.7	0.2	35.3	0.3	34.3	0.8	29.8	2.5	28.5	2.6
3-Oct-05	37.5	0.1	35.6	0.3	35.1	0.3	32.8	0.8	26.7	2.4	23.8	3.6
4-Oct-05	38.0	0.3	35.4	0.2	34.7	0.3	31.5	0.8	26.2	2.5	24.0	3.3
5-Oct-05	38.1	0.1	35.3	0.2	34.3	0.3	30.8	0.8	25.8	2.6	25.8	3.4
6-Oct-05	37.3	0.3	35.0	0.3	33.8	0.3	30.1	0.9	25.8	2.7	28.6	4.6
7-Oct-05	36.5	0.3	34.6	0.4	33.4	0.4	29.8	1.1	28.0	2.3	30.0	5.9
8-Oct-05	36.3	0.2	34.2	0.5	33.1	0.5	30.2	1.1	29.4	2.3	28.7	7.5
9-Oct-05	36.3	0.2	33.8	0.5	32.9	0.5	30.5	1.2	30.3	2.3	28.0	6.9
10-Oct-05	36.4	0.2	33.5	0.5	32.7	0.5	30.6	1.2	29.8	2.2	33.1	9.2
11-Oct-05	36.9	0.1	33.4	0.5	32.6	0.5	30.6	1.2	30.7	2.2	31.2	8.9
12-Oct-05	37.1	0.1	33.5	0.5	32.6	0.5	31.0	1.2	30.1	2.6	30.6	8.6
13-Oct-05	36.6	0.2	33.5	0.5	32.7	0.5	31.0	1.3	31.4	2.1	32.8	7.3
14-Oct-05	37.1	0.1	33.5	0.5	32.8	0.5	31.6	1.2	31.4	2.7	25.5	6.9
15-Oct-05	36.8	0.2	33.6	0.5	32.9	0.5	31.5	1.3	30.4	2.6	34.9	6.8
16-Oct-05	36.4	0.2	33.6	0.5	33.0	0.5	31.4	1.3	31.0	2.3	28.9	4.4
17-Oct-05	36.2	0.3	33.6	0.6	33.1	0.5	31.4	1.3	30.5	2.4	29.6	6.8
18-Oct-05	36.1	0.2	33.5	0.6	33.0	0.5	31.2	1.3	29.4	2.2	27.2	6.6
19-Oct-05	36.1	0.2	33.4	0.6	33.0	0.5	30.8	1.2	30.0	2.7	31.3	4.7
20-Oct-05	37.1	0.1	33.4	0.6	32.8	0.5	30.7	1.1	30.6	2.7	24.8	4.1
21-Oct-05	37.7	0.1	33.8	0.5	32.9	0.5	31.0	1.0	27.9	3.2	19.0	2.4
22-Oct-05	37.4	0.0	33.9	0.4	32.9	0.5	30.5	1.1	28.9	2.9	25.9	3.4
23-Oct-05	36.7	0.3	33.9	0.4	32.9	0.5	29.9	1.2	28.6	3.1	34.3	5.4
24-Oct-05	36.2	0.3	33.7	0.5	32.7	0.5	29.8	1.3	30.7	2.7	30.5	6.7
25-Oct-05	36.0	0.3	33.4	0.5	32.6	0.5	30.0	1.4	31.7	2.6	30.3	5.1
21-Nov-05	37.6	0.4	33.9	0.7	32.2	0.8	29.6	1.2	28.0	2.5	24.4	7.7
22-Nov-05	37.1	0.5	34.3	0.5	33.0	0.2	30.0	1.3	29.6	2.2	25.8	11.7
23-Nov-05	36.9	0.4	34.2	0.5	33.0	0.2	30.9	1.3	30.6	2.6	23.6	8.4
24-Nov-05	36.4	0.5	34.1	0.5	33.2	0.2	31.3	1.2	30.8	2.5	23.9	3.6
25-Nov-05	36.1	0.5	34.1	0.5	33.4	0.2	31.4	1.3	31.0	2.4	25.1	1.4
21-Dec-05	33.9	0.3	30.5	0.4	28.4	0.2	22.7	1.0	18.3	1.7	7.4	6.2
22-Dec-05	33.8	0.3	30.3	0.4	28.2	0.2	22.6	1.1	19.5	1.4	9.9	1.8
23-Dec-05	34.6	0.2	29.9	0.4	27.7	0.3	22.8	1.2	20.9	1.5	9.9	3.2
24-Dec-05	35.5	0.2	30.1	0.4	27.5	0.3	23.5	1.3	20.5	1.7	8.6	2.1

25-Dec-05	34.6	0.3	30.0	0.4	27.6	0.3	23.0	1.3	21.8	1.3	14.8	6.7
26-Dec-05	34.7	0.1	29.7	0.5	27.5	0.3	23.3	1.4	24.0	0.9	16.2	2.9
27-Dec-05	34.1	0.1	29.6	0.5	27.5	0.4	23.9	1.4	24.6	1.2	14.7	-0.4
28-Dec-05	33.8	0.1	29.3	0.5	27.5	0.4	24.2	1.4	24.8	1.0	13.9	0.9
29-Dec-05	33.6	0.1	29.2	0.5	27.5	0.4	24.5	1.4	24.7	1.1	12.1	-3.3
30-Dec-05	33.3	0.2	29.0	0.5	27.4	0.4	24.5	1.3	23.9	1.4	10.0	-5.6
31-Dec-05	33.2	0.3	29.0	0.5	27.4	0.4	24.4	1.1	23.3	2.0	11.6	-4.5
1-Jan-06	33.1	0.2	28.8	0.5	27.3	0.3	24.1	1.1	23.5	1.9	13.6	-2.9
2-Jan-06	32.8	0.2	28.7	0.5	27.1	0.3	24.0	1.2	23.5	1.7	13.5	-6.1
3-Jan-06	32.8	0.3	28.5	0.5	27.0	0.3	24.0	1.3	23.4	1.8	10.8	-4.8
4-Jan-06	32.9	0.3	28.5	0.5	27.0	0.3	23.9	1.3	23.5	1.8	9.0	-4.4
5-Jan-06	33.5	0.1	28.6	0.4	26.9	0.3	24.0	1.3	23.0	1.8	9.2	0.5
6-Jan-06	33.2	0.2	28.6	0.4	26.9	0.3	23.9	1.3	23.6	1.6	14.1	2.5
7-Jan-06	32.9	0.2	28.5	0.4	27.0	0.2	24.0	1.2	23.9	1.4	14.4	-3.2
8-Jan-06	32.6	0.1	28.4	0.5	27.0	0.2	24.0	1.2	23.7	1.4	11.7	-5.3
9-Jan-06	32.6	0.2	28.4	0.5	26.9	0.2	24.0	1.1	23.3	1.4	13.5	-2.4
10-Jan-06	32.6	0.2	28.3	0.5	26.8	0.2	24.0	1.1	23.4	1.4	13.8	-3.8
11-Jan-06	32.5	0.2	28.2	0.5	26.7	0.3	23.9	1.1	23.6	1.5	13.6	-4.3
12-Jan-06	32.9	0.2	28.1	0.5	26.7	0.3	23.8	1.1	23.8	1.4	9.7	-5.7
13-Jan-06	32.8	0.2	28.2	0.4	26.6	0.3	23.9	1.1	22.8	2.0	9.6	-5.8
14-Jan-06	32.3	0.2	28.2	0.4	26.6	0.2	23.6	1.0	22.3	2.1	10.7	-8.4
15-Jan-06	32.3	0.2	28.1	0.4	26.6	0.2	23.4	1.0	22.1	1.9	10.5	-6.8
16-Jan-06	32.1	0.2	28.0	0.4	26.4	0.2	23.2	1.0	22.1	1.7	9.8	-5.7
17-Jan-06	31.9	0.2	27.9	0.4	26.3	0.2	23.1	0.9	21.4	1.9	12.2	-4.1
18-Jan-06	32.0	0.2	27.7	0.4	26.2	0.2	22.9	0.9	21.9	1.8	12.8	-4.1
19-Jan-06	33.1	0.2	27.9	0.4	26.0	0.2	22.9	1.0	22.0	1.9	8.0	-11.0
20-Jan-06	32.4	0.2	28.0	0.4	26.1	0.2	22.8	0.9	20.8	1.9	9.3	-9.8
21-Jan-06	32.0	0.2	28.0	0.4	26.1	0.2	22.6	0.9	20.4	1.9	9.6	-9.5
22-Jan-06	32.0	0.2	27.9	0.4	26.1	0.2	22.5	1.0	21.0	2.0	13.8	-0.2
23-Jan-06	32.3	0.2	27.7	0.4	25.9	0.2	22.6	1.0	22.2	1.8	16.9	0.9
24-Jan-06	33.5	0.2	28.0	0.3	26.0	0.2	23.6	1.2	22.4	1.9	14.5	1.6
25-Jan-06	32.8	0.2	28.3	0.4	26.4	0.4	23.4	1.2	22.5	0.9	17.7	2.7
26-Jan-06	32.8	0.2	28.3	0.5	26.5	0.4	23.3	1.2	23.5	0.6	19.2	1.9
27-Jan-06	32.8	0.2	28.4	0.5	26.5	0.4	23.5	1.2	24.3	0.9	18.0	-4.1
28-Jan-06	32.3	0.2	28.3	0.5	26.5	0.4	23.7	1.1	23.6	1.3	15.8	-6.5
29-Jan-06	32.9	0.2	28.2	0.5	26.5	0.4	23.6	1.1	23.3	1.5	15.2	-3.5
30-Jan-06	32.7	0.2	28.2	0.5	26.4	0.3	23.4	1.0	22.9	1.7	13.2	-6.5
31-Jan-06	33.6	0.2	28.3	0.4	26.4	0.3	23.4	0.9	22.6	1.8	10.4	-6.3
1-Feb-06	33.3	0.2	28.6	0.4	26.5	0.3	23.3	0.9	21.6	1.6	11.1	-3.8
2-Feb-06	34.1	0.1	28.6	0.3	26.5	0.3	23.0	1.0	22.3	1.2	11.4	-0.4
3-Feb-06	33.8	0.2	28.7	0.3	26.5	0.3	23.1	1.0	22.2	1.1	11.3	-0.6
4-Feb-06	33.0	0.2	28.7	0.3	26.6	0.3	23.1	1.0	22.0	1.1	12.0	-2.2
5-Feb-06	34.2	0.2	28.7	0.3	26.5	0.2	23.8	1.0	22.0	1.5	10.9	-3.7
6-Feb-06	35.4	0.3	29.8	0.2	27.1	0.4	24.5	0.8	19.4	2.1	6.9	-5.4

7-Feb-06	34.7	0.1	30.3	0.3	27.8	0.4	23.8	0.7	19.7	1.7	5.7	-4.6
8-Feb-06	34.3	0.2	30.2	0.3	27.8	0.4	23.4	0.7	20.5	1.4	10.0	0.2
9-Feb-06	35.4	0.2	30.2	0.3	27.8	0.6	24.2	0.8	20.3	2.4	10.6	-1.2
10-Feb-06	36.2	0.2	31.3	0.5	28.5	0.9	24.5	0.7	18.6	2.4	6.8	-4.6
11-Feb-06	35.2	0.1	31.6	0.5	28.8	0.8	24.0	0.6	20.1	1.5	9.7	1.8
12-Feb-06	34.7	0.3	31.3	0.5	28.6	0.6	23.9	0.6	21.7	0.9	14.4	4.8
13-Feb-06	34.4	0.4	30.8	0.4	28.3	0.5	24.8	0.8	24.0	2.4	17.9	2.8
14-Feb-06	34.8	0.3	30.7	0.5	28.3	0.6	25.8	1.1	24.8	3.4	15.8	-7.3
15-Feb-06	35.1	0.2	30.9	0.6	28.5	0.7	26.0	1.0	24.2	3.6	10.9	-12.8
16-Feb-06	36.2	0.3	31.7	0.7	28.9	0.8	26.2	0.9	21.8	3.8	2.8	-24.5
17-Feb-06	36.4	0.3	32.5	0.8	29.7	0.9	25.8	0.7	19.2	3.6	-1.3	-16.1
18-Feb-06	35.5	0.2	32.4	0.8	29.7	0.9	24.7	0.6	18.6	3.3	2.8	-7.5
19-Feb-06	35.1	0.4	32.0	0.7	29.4	0.8	24.0	0.6	18.8	2.9	10.2	-4.3
20-Feb-06	34.9	0.4	31.5	0.6	29.0	0.7	23.9	0.6	19.9	2.8	14.0	-3.5
21-Feb-06	34.6	0.4	31.2	0.6	28.7	0.7	24.2	0.8	21.1	2.7	16.9	-3.0
22-Feb-06	34.7	0.3	30.8	0.6	28.3	0.8	24.1	0.8	22.2	2.7	16.2	-8.4
23-Feb-06	34.2	0.2	30.5	0.6	28.1	0.7	24.1	0.7	21.9	2.1	12.7	-10.5
24-Feb-06	34.2	0.2	30.3	0.6	27.9	0.7	24.0	0.6	21.5	1.9	9.6	-12.3
25-Feb-06	33.6	0.2	30.0	0.6	27.6	0.6	23.7	0.5	20.6	1.8	7.9	-12.4
26-Feb-06	33.3	0.3	29.8	0.6	27.5	0.5	23.4	0.4	19.4	2.2	6.1	-12.1
27-Feb-06	33.2	0.4	29.4	0.5	27.1	0.4	22.8	0.4	18.7	2.5	6.2	-10.3
28-Feb-06	34.6	0.2	29.3	0.4	26.8	0.4	22.5	0.5	19.5	2.2	5.5	-9.9
1-Mar-06	35.7	0.2	29.6	0.4	26.7	0.3	22.9	0.6	18.4	1.9	6.2	-9.8
2-Mar-06	36.1	0.2	30.1	0.3	27.0	0.4	22.9	0.5	16.9	1.8	5.4	-14.1
3-Mar-06	34.8	0.2	30.3	0.3	27.2	0.3	22.1	0.5	16.9	2.0	2.3	-13.8
4-Mar-06	34.0	0.2	29.9	0.2	27.0	0.2	21.6	0.5	16.7	2.4	2.5	-10.5
5-Mar-06	33.4	0.2	29.4	0.1	26.7	0.1	21.2	0.6	16.2	1.9	3.7	-13.8
6-Mar-06	33.3	0.4	29.0	0.1	26.4	0.1	20.8	0.5	15.7	1.5	4.6	-6.1
7-Mar-06	33.0	0.4	28.6	0.1	25.9	0.1	20.3	0.6	15.3	1.4	5.1	-2.9
8-Mar-06	32.6	0.4	28.1	0.1	25.5	0.1	19.9	0.5	14.8	1.3	4.1	-2.4
9-Mar-06	32.7	0.4	27.7	0.1	25.0	0.1	19.7	0.4	15.0	1.1	4.2	-0.9
10-Mar-06	34.0	0.3	27.5	0.1	24.7	0.1	20.1	0.3	15.1	1.6	3.1	-4.5
11-Mar-06	35.0	0.2	28.3	0.1	25.0	0.2	20.2	0.3	13.3	1.6	3.1	-7.0
12-Mar-06	34.9	0.1	28.9	0.1	25.4	0.3	19.8	0.3	12.9	1.4	3.5	-11.1
13-Mar-06	33.9	0.2	28.9	0.1	25.5	0.2	19.4	0.3	13.4	1.3	3.1	-15.3
14-Mar-06	33.2	0.3	28.6	0.1	25.3	0.2	19.2	0.4	13.4	1.5	2.7	-11.2
15-Mar-06	33.4	0.3	28.1	0.0	25.0	0.2	19.0	0.4	13.6	1.7	2.6	-8.6
16-Mar-06	33.3	0.3	27.8	0.0	24.6	0.2	18.8	0.5	13.9	1.9	2.6	-8.7
17-Mar-06	32.7	0.3	27.5	0.1	24.4	0.2	18.6	0.5	13.7	2.0	3.0	-5.3
18-Mar-06	32.9	0.3	27.1	0.1	24.1	0.2	18.3	0.5	14.3	2.4	3.5	-6.6
19-Mar-06	33.3	0.1	27.0	0.1	23.9	0.2	18.2	0.6	14.1	2.0	3.7	-8.3
20-Mar-06	32.6	0.3	26.9	0.1	23.8	0.1	18.0	0.6	13.0	1.8	3.6	-3.9
21-Mar-06	32.2	0.3	26.6	0.1	23.6	0.1	17.6	0.5	12.5	1.7	3.0	-2.7
22-Mar-06	32.7	0.4	26.3	0.2	23.3	0.1	17.3	0.5	12.2	1.8	2.5	-1.4

23-Mar-06	32.3	0.5	26.1	0.2	23.0	0.2	17.0	0.6	12.1	1.7	2.1	-3.5
24-Mar-06	31.7	0.4	25.9	0.3	22.8	0.2	16.7	0.6	11.2	1.6	2.0	-2.1
25-Mar-06	31.5	0.4	25.5	0.3	22.5	0.2	16.3	0.6	11.1	1.4	5.8	1.0
26-Mar-06	31.3	0.3	25.2	0.3	22.2	0.2	16.0	0.6	11.9	1.3	5.3	1.7
27-Mar-06	31.0	0.3	24.8	0.3	21.9	0.3	16.0	0.5	12.2	0.9	4.9	2.6
28-Mar-06	30.5	0.3	24.5	0.3	21.6	0.3	16.1	0.5	12.5	0.9	5.7	2.1
29-Mar-06	30.1	0.4	24.3	0.3	21.5	0.2	16.1	0.4	13.0	0.8	5.3	0.9
30-Mar-06	29.9	0.4	24.0	0.3	21.2	0.2	16.2	0.4	13.1	0.5	6.7	2.7
31-Mar-06	29.7	0.4	23.8	0.2	21.1	0.3	16.4	0.5	13.7	0.3	7.2	0.6
1-Apr-06	29.7	0.4	23.6	0.2	21.0	0.3	16.6	0.6	14.4	0.4	8.1	1.1
2-Apr-06	30.3	0.3	23.5	0.1	20.9	0.3	16.8	0.6	15.2	0.2	8.5	2.4
3-Apr-06	29.9	0.4	23.6	0.1	20.9	0.4	17.1	0.7	15.6	0.2	11.4	5.8
4-Apr-06	29.6	0.4	23.6	0.1	21.0	0.4	17.4	0.8	16.9	0.2	14.1	7.2
5-Apr-06	29.4	0.4	23.5	0.2	21.1	0.4	17.9	0.8	18.2	0.1	15.6	7.2
6-Apr-06	29.5	0.4	23.5	0.2	21.3	0.5	18.4	0.9	19.3	0.2	15.6	6.2
7-Apr-06	29.5	0.4	23.6	0.2	21.4	0.5	19.0	1.0	19.7	0.4	18.6	8.2
8-Apr-06	29.2	0.4	23.7	0.2	21.7	0.5	19.6	1.1	21.0	0.3	19.8	7.7
9-Apr-06	29.3	0.5	23.8	0.3	22.0	0.5	20.1	1.1	21.8	0.2	20.5	7.5
10-Apr-06	29.1	0.4	24.0	0.3	22.3	0.5	20.6	1.1	22.7	0.2	23.1	8.7
11-Apr-06	29.0	0.4	24.1	0.3	22.5	0.5	21.1	1.1	23.7	0.1	24.2	8.8
12-Apr-06	29.0	0.5	24.3	0.3	22.8	0.5	21.7	1.1	24.2	0.3	25.2	8.8
13-Apr-06	29.5	0.4	24.4	0.4	23.1	0.5	22.3	1.3	25.1	0.3	27.5	7.8
14-Apr-06	29.5	0.4	24.7	0.4	23.4	0.5	22.9	1.4	26.1	0.2	30.1	10.9
15-Apr-06	30.3	0.4	25.0	0.5	23.9	0.6	23.6	1.5	27.8	0.5	24.9	4.9
16-Apr-06	30.5	0.3	25.6	0.5	24.5	0.6	24.4	1.5	27.4	1.2	18.0	1.5
17-Apr-06	30.7	0.3	26.1	0.5	25.0	0.6	24.7	1.4	26.0	1.5	15.3	5.0
18-Apr-06	30.8	0.3	26.5	0.6	25.4	0.6	24.9	1.5	24.8	1.3	16.9	7.8
19-Apr-06	30.5	0.3	26.9	0.6	25.8	0.6	24.6	1.2	25.2	0.7	21.9	9.4
20-Apr-06	30.1	0.3	27.1	0.6	26.1	0.6	24.9	1.3	27.9	0.2	34.0	13.7
21-Apr-06	30.1	0.2	27.1	0.6	26.2	0.5	25.7	1.5	31.1	0.5	36.6	14.7
22-Apr-06	31.5	0.2	27.6	0.6	26.9	0.5	27.9	1.5	33.1	1.7	22.1	3.8
23-Apr-06	32.7	0.3	28.7	0.6	27.9	0.7	29.0	1.3	30.0	1.6	17.9	6.6
24-Apr-06	32.4	0.2	29.5	0.7	28.7	0.7	28.5	1.1	27.9	1.8	21.1	8.2
25-Apr-06	32.0	0.2	29.9	0.7	29.1	0.6	28.6	1.2	30.2	1.9	31.6	11.7
26-Apr-06	32.0	0.2	30.1	0.7	29.5	0.6	29.6	1.4	32.9	2.0	37.9	12.9
27-Apr-06	32.5	0.2	30.2	0.7	29.9	0.6	31.1	1.4	34.8	2.4	29.5	11.7
28-Apr-06	32.8	0.2	30.8	0.8	30.7	0.7	32.3	1.3	33.7	2.1	27.3	14.4
29-Apr-06	32.6	0.2	31.2	0.8	31.2	0.7	32.2	1.2	35.3	1.7	32.9	15.1
30-Apr-06	33.1	0.2	31.7	0.8	31.7	0.7	33.4	1.2	36.8	2.5	22.2	7.9
1-May-06	33.1	0.2	32.2	0.8	32.4	0.7	34.1	1.2	35.1	2.3	24.2	7.7
2-May-06	33.8	0.2	32.7	0.9	32.9	0.7	34.5	1.1	35.4	3.2	21.6	3.6
3-May-06	34.9	0.0	33.4	0.9	33.4	0.8	35.1	1.2	32.9	3.0	20.6	5.1
4-May-06	34.3	0.1	34.1	0.9	34.0	0.8	34.3	1.2	32.8	2.3	31.9	11.6
5-May-06	34.0	0.1	34.2	0.9	34.0	0.7	34.0	1.2	35.0	2.1	40.5	17.3

6-May-06	34.0	0.1	34.2	0.8	34.0	0.5	34.3	1.3	37.0	2.2	37.5	10.4
7-May-06	34.1	0.2	34.2	0.7	34.1	0.5	34.9	1.2	35.6	2.3	32.3	11.8
8-May-06	34.6	0.1	34.3	0.7	34.3	0.4	35.0	1.1	35.8	2.6	26.1	4.9
9-May-06	35.2	0.1	34.4	0.6	34.5	0.5	35.7	1.1	32.3	3.3	16.5	6.2
10-May-06	35.8	0.1	34.8	0.7	34.8	0.6	35.1	0.9	30.1	3.1	19.7	10.6
11-May-06	34.9	0.1	35.0	0.7	34.7	0.5	33.8	0.8	32.1	2.0	29.9	13.2
12-May-06	34.7	0.0	34.9	0.6	34.5	0.4	33.7	1.0	35.4	1.7	32.5	10.4
13-May-06	36.0	0.2	34.8	0.5	34.5	0.4	34.6	1.0	34.5	2.6	26.3	10.7
14-May-06	35.9	0.2	34.9	0.5	34.6	0.5	34.7	1.1	33.4	2.4	27.1	15.1
15-May-06	35.1	0.2	34.9	0.4	34.7	0.5	34.3	1.0	35.1	1.8	36.2	18.2
16-May-06	34.7	0.2	34.8	0.4	34.7	0.4	34.7	1.1	38.2	1.7	43.0	20.6
17-May-06	34.5	0.2	34.8	0.4	34.9	0.4	35.7	1.1	40.4	1.5	45.1	22.7
18-May-06	34.3	0.2	34.6	0.4	35.0	0.4	36.6	1.2	41.5	1.8	44.6	20.8
19-May-06	34.1	0.2	34.6	0.4	35.3	0.4	37.4	1.3	42.1	2.1	41.7	18.8
20-May-06	34.4	0.2	34.7	0.4	35.7	0.5	38.1	1.3	43.1	1.7	35.3	12.6
21-May-06	34.3	0.2	35.1	0.5	36.3	0.6	38.7	1.1	41.5	1.5	33.9	15.9
22-May-06	34.3	0.1	35.5	0.5	36.8	0.7	38.7	1.0	41.6	1.8	36.8	18.8
23-May-06	34.4	0.1	35.7	0.6	36.9	0.8	38.8	1.0	42.1	2.0	34.7	15.6
24-May-06	34.8	0.1	36.1	0.6	37.4	0.9	39.2	1.2	40.7	2.4	28.5	13.1
25-May-06	34.7	0.1	36.4	0.7	37.7	0.9	38.9	1.1	37.3	2.1	26.9	10.3
26-May-06	34.8	0.1	36.7	0.7	37.8	0.8	37.4	0.8	32.9	2.2	21.2	8.1
27-May-06	34.8	0.2	36.7	0.7	37.2	0.7	35.6	0.6	31.1	1.9	21.8	10.2
28-May-06	34.7	0.2	36.4	0.6	36.5	0.6	34.5	0.5	32.5	1.4	25.1	9.9
29-May-06	34.6	0.2	36.0	0.5	35.9	0.5	34.2	0.6	33.8	1.4	27.5	11.5
30-May-06	34.8	0.2	35.6	0.5	35.4	0.5	34.1	0.6	33.0	1.5	25.1	13.5
31-May-06	34.8	0.2	35.4	0.5	35.2	0.5	33.9	0.7	33.3	1.7	26.4	11.6

Table F.8. Site 3 Temperature Results

Date	Depth / Temperature (°C)											
	160	SE	125	SE	90	SE	55	SE	20	SE	Surface	Ambient
18-Nov-05	4.0	0.4	4.4	0.4	2.5	0.4	0.9	0.5	1.0	1.1		
19-Nov-05	3.8	0.2	4.2	0.3	2.4	0.3	0.9	0.4	2.1	1.9		
20-Nov-05	4.4	0.5	4.4	0.1	2.2	0.3	0.9	0.5	2.2	1.8		
21-Nov-05	4.9	0.5	4.1	0.4	2.8	0.3	1.4	0.5	1.4	1.0	6.2	2.4
22-Nov-05	6.1	0.3	4.0	0.3	3.2	0.2	1.8	0.2	0.9	0.1	11.2	3.8
23-Nov-05	6.1	0.3	4.0	0.3	3.1	0.2	1.8	0.2	1.8	0.1	7.8	3.7
24-Nov-05	6.3	0.2	4.2	0.3	3.3	0.2	2.2	0.1	2.0	0.1	4.4	1.1
25-Nov-05	6.5	0.2	4.3	0.3	3.5	0.2	2.5	0.1	1.7	0.1	0.4	
8-Dec-05	3.5	7.5	-2.2	2.8	0.2	4.5	1.7	0.1	4.1	1.1	-19.8	-6.8
9-Dec-05	8.4	0.9	2.2	1.1	2.3	1.5	0.5	0.9	-0.6	0.6	-8.2	-7.5
10-Dec-05	7.4	1.0	5.0	0.4	3.4	0.6	1.1	0.6	-2.2	0.3	2.7	-3.1
11-Dec-05	6.6	1.1	5.6	0.5	3.1	0.4	1.7	0.5	-2.1	0.2	5.3	-1.8
21-Dec-05	7.6	0.2	4.5	0.2	3.0	0.1	0.2	0.1	-3.6	0.2	4.0	-2.2

22-Dec-05	7.8	0.2	4.7	0.2	3.3	0.1	0.5	0.1	-2.9	0.1	1.0	-2.3
23-Dec-05	7.7	0.2	4.7	0.2	3.2	0.1	0.4	0.1	-2.5	0.1	2.7	-1.9
24-Dec-05	7.8	0.2	4.6	0.2	3.2	0.1	0.4	0.1	-2.2	0.1	1.8	-1.7
25-Dec-05	7.7	0.2	4.6	0.2	3.1	0.1	0.3	0.1	-2.0	0.1	6.3	-0.9
26-Dec-05	7.7	0.2	4.5	0.2	3.0	0.1	0.2	0.1	-1.9	0.1	2.6	-0.7
27-Dec-05	7.7	0.2	4.5	0.2	3.0	0.1	0.3	0.1	-1.7	0.1	-0.6	-1.0
28-Dec-05	7.6	0.2	4.4	0.2	2.9	0.1	0.2	0.1	-1.6	0.1	0.7	-1.3
29-Dec-05	7.5	0.2	4.3	0.2	2.9	0.1	0.2	0.1	-1.7	0.1	-3.3	-2.7
30-Dec-05	7.4	0.2	4.3	0.2	2.8	0.1	0.2	0.1	-1.8	0.1	-6.0	-4.3
31-Dec-05	7.6	0.3	4.3	0.2	2.8	0.1	0.2	0.1	-2.0	0.1	-4.8	-4.0
1-Jan-06	7.7	0.3	4.3	0.2	2.8	0.1	0.2	0.1	-2.0	0.1	-3.2	-2.8
2-Jan-06	7.5	0.3	4.2	0.2	2.7	0.1	0.1	0.1	-2.0	0.1	-6.4	-3.9
3-Jan-06	7.5	0.3	4.2	0.2	2.8	0.2	0.2	0.1	-2.3	0.2	-5.6	-5.5
4-Jan-06	7.4	0.3	4.2	0.2	2.8	0.2	0.2	0.1	-2.7	0.2	-4.8	-5.7
5-Jan-06	7.6	0.3	4.3	0.2	2.8	0.2	0.2	0.1	-2.8	0.2	0.2	-4.0
6-Jan-06	7.7	0.3	4.3	0.2	2.8	0.2	0.1	0.1	-2.3	0.1	2.2	-1.8
7-Jan-06	7.7	0.3	4.3	0.2	2.8	0.2	0.1	0.1	-2.2	0.1	-3.4	-2.7
8-Jan-06	7.6	0.3	4.3	0.2	2.8	0.2	0.1	0.1	-2.3	0.1	-5.9	-5.0
9-Jan-06	7.6	0.3	4.3	0.2	2.8	0.2	0.1	0.1	-2.5	0.1	-2.7	-4.1
10-Jan-06	7.7	0.3	4.3	0.2	2.8	0.2	0.1	0.1	-2.6	0.1	-4.2	-4.5
11-Jan-06	7.6	0.3	4.3	0.2	2.7	0.2	0.0	0.1	-2.5	0.1	-4.6	-3.4
12-Jan-06	7.6	0.4	4.3	0.2	2.8	0.2	0.0	0.1	-2.6	0.1	-5.8	-5.2
13-Jan-06	7.6	0.4	4.2	0.2	2.7	0.2	0.0	0.1	-2.9	0.1	-6.7	-5.3
14-Jan-06	7.5	0.4	4.2	0.2	2.7	0.2	-0.1	0.1	-3.1	0.2	-8.7	-5.6
15-Jan-06	7.6	0.4	4.2	0.2	2.7	0.2	-0.1	0.1	-3.1	0.1	-6.9	-5.2
16-Jan-06	7.6	0.4	4.2	0.2	2.7	0.2	-0.1	0.1	-3.2	0.2	-5.8	-6.0
17-Jan-06	7.7	0.4	4.3	0.2	2.7	0.2	-0.1	0.1	-3.4	0.2	-4.7	-5.5
18-Jan-06	7.7	0.4	4.2	0.2	2.7	0.2	-0.2	0.1	-3.3	0.1	-4.3	-4.8
19-Jan-06	7.6	0.4	4.1	0.2	2.6	0.2	-0.3	0.1	-3.4	0.2	-11.2	-7.0
20-Jan-06	7.6	0.4	4.2	0.2	2.6	0.2	-0.3	0.1	-3.8	0.2	-10.3	-7.3
21-Jan-06	7.7	0.4	4.2	0.3	2.6	0.2	-0.3	0.1	-4.0	0.2	-9.8	-7.3
22-Jan-06	8.0	0.5	4.3	0.3	2.8	0.2	-0.2	0.1	-3.8	0.2	-0.6	-4.8
23-Jan-06	7.9	0.4	4.3	0.3	2.6	0.2	-0.4	0.1	-3.2	0.1	0.6	-3.0
24-Jan-06	8.0	0.4	4.3	0.2	2.7	0.2	-0.3	0.1	-2.7	0.1	1.3	-2.2
25-Jan-06	8.0	0.4	4.4	0.2	2.7	0.2	-0.4	0.1	-2.4	0.1	2.1	-1.6
26-Jan-06	8.1	0.4	4.3	0.2	2.7	0.2	-0.5	0.1	-2.2	0.1	1.6	-1.3
27-Jan-06	8.1	0.4	4.3	0.2	2.6	0.2	-0.5	0.1	-2.1	0.1	-4.4	-2.1
28-Jan-06	8.0	0.4	4.2	0.2	2.6	0.2	-0.5	0.1	-2.1	0.1	-6.9	-3.6
29-Jan-06	8.1	0.4	4.3	0.3	2.6	0.2	-0.4	0.1	-2.2	0.1	-3.3	-3.4
30-Jan-06	7.9	0.4	4.2	0.3	2.6	0.2	-0.5	0.1	-2.5	0.2	-6.5	-4.3
31-Jan-06	7.8	0.4	4.2	0.3	2.6	0.2	-0.5	0.1	-2.8	0.2	-6.7	-5.1
1-Feb-06	8.0	0.4	4.3	0.3	2.6	0.2	-0.4	0.1	-2.9	0.2	-3.8	-4.1
2-Feb-06	8.0	0.4	4.3	0.3	2.7	0.2	-0.4	0.1	-2.8	0.1	-0.9	-3.5
3-Feb-06	8.0	0.4	4.3	0.3	2.6	0.2	-0.4	0.1	-2.8	0.2	-0.9	-3.6

4-Feb-06	8.0	0.4	4.3	0.3	2.6	0.2	-0.4	0.1	-2.7	0.1	-2.5	-3.1
5-Feb-06	8.0	0.4	4.3	0.3	2.6	0.2	-0.5	0.1	-2.5	0.1	-3.7	-3.0
6-Feb-06	8.0	0.4	4.2	0.3	2.5	0.2	-0.5	0.1	-2.6	0.2	-4.4	-3.9
7-Feb-06	8.0	0.4	4.3	0.2	2.6	0.2	-0.4	0.1	-3.0	0.2	-4.9	-4.7
8-Feb-06	8.1	0.4	4.3	0.2	2.6	0.2	-0.5	0.1	-2.8	0.1	0.1	-2.6
9-Feb-06	8.0	0.4	4.2	0.2	2.5	0.2	-0.5	0.1	-2.4	0.1	-1.3	-2.2
10-Feb-06	8.0	0.3	4.2	0.2	2.6	0.2	-0.5	0.1	-2.4	0.1	-4.6	-3.8
11-Feb-06	8.2	0.3	4.4	0.2	2.7	0.2	-0.5	0.1	-2.4	0.1	2.5	-2.5
12-Feb-06	6.7	1.9	4.4	0.2	2.7	0.2	-0.4	0.1	-2.3	0.1	4.7	-1.4
13-Feb-06	8.2	0.4	4.3	0.2	2.6	0.2	-0.5	0.1	-2.1	0.0	2.7	-0.7
14-Feb-06	8.0	0.3	4.2	0.2	2.5	0.2	-0.6	0.1	-2.1	0.0	-7.4	-2.5
15-Feb-06	7.9	0.3	4.1	0.1	2.4	0.2	-0.7	0.1	-2.3	0.1	-12.9	-6.6
16-Feb-06	7.8	0.3	4.0	0.1	2.4	0.2	-0.7	0.1	-3.7	0.5	-24.5	-12.9
17-Feb-06	7.9	0.4	4.3	0.1	2.6	0.2	-0.4	0.1	-5.7	0.6	-16.2	-12.7
18-Feb-06	8.2	0.5	4.3	0.1	2.7	0.2	-0.5	0.1	-5.5	0.3	-7.7	-8.0
19-Feb-06	8.3	0.5	4.4	0.1	2.7	0.2	-0.6	0.1	-4.5	0.1	-4.1	-5.2
20-Feb-06	8.2	0.6	4.4	0.1	2.7	0.2	-0.7	0.1	-4.0	0.1	-3.8	-4.6
21-Feb-06	8.2	0.6	4.4	0.1	2.6	0.1	-0.8	0.1	-3.4	0.1	-3.2	-3.3
22-Feb-06	8.1	0.5	4.2	0.1	2.5	0.1	-1.0	0.1	-3.2	0.1	-9.6	-4.8
23-Feb-06	8.0	0.4	4.2	0.1	2.4	0.1	-1.0	0.1	-3.4	0.1	-11.9	-5.8
24-Feb-06	8.0	0.4	4.2	0.1	2.4	0.1	-1.0	0.1	-3.7	0.1	-12.7	-6.6
25-Feb-06	8.1	0.4	4.1	0.1	2.4	0.1	-1.1	0.1	-4.0	0.2	-11.9	-6.9
26-Feb-06	8.0	0.4	4.2	0.1	2.4	0.1	-1.0	0.1	-4.3	0.2	-13.0	-7.0
27-Feb-06	8.1	0.4	4.2	0.1	2.4	0.1	-1.1	0.1	-4.3	0.1	-10.8	-6.2
28-Feb-06	8.0	0.4	4.1	0.1	2.4	0.1	-1.1	0.1	-4.1	0.1	-10.3	-6.0
1-Mar-06	8.0	0.4	4.1	0.1	2.3	0.1	-1.2	0.1	-3.9	0.1	-9.7	-5.0
2-Mar-06	8.0	0.3	4.1	0.1	2.2	0.1	-1.3	0.1	-3.6	0.1	-14.6	-4.3
3-Mar-06	7.9	0.3	4.0	0.1	2.2	0.1	-1.2	0.1	-3.5	0.1	-14.5	-4.3
4-Mar-06	8.0	0.3	4.0	0.1	2.2	0.1	-1.3	0.1	-3.4	0.1	-11.7	-4.0
5-Mar-06	8.1	0.3	4.1	0.1	2.2	0.1	-1.3	0.1	-3.1	0.1	-13.9	-3.8
6-Mar-06	8.2	0.3	4.2	0.1	2.4	0.2	-1.1	0.1	-3.0	0.1	-6.7	-3.5
7-Mar-06	8.2	0.4	4.2	0.1	2.4	0.2	-1.1	0.1	-2.9	0.1	-1.6	-3.0
8-Mar-06	8.1	0.3	4.2	0.2	2.4	0.2	-1.1	0.1	-2.7	0.1	-2.4	-2.8
9-Mar-06	8.0	0.4	4.1	0.2	2.3	0.2	-1.1	0.1	-2.6	0.1	-1.2	-2.4
10-Mar-06	7.8	0.4	3.9	0.2	2.1	0.2	-1.1	0.1	-2.5	0.1	-4.6	-2.5
11-Mar-06	7.7	0.4	3.9	0.2	2.1	0.2	-1.1	0.1	-2.5	0.1	-6.8	-2.7
12-Mar-06	7.6	0.3	3.7	0.2	1.9	0.2	-1.3	0.1	-2.5	0.1	-9.7	-2.6
13-Mar-06	7.6	0.3	3.8	0.2	2.0	0.2	-1.2	0.1	-2.5	0.1	-15.2	-3.2
14-Mar-06	7.6	0.3	3.8	0.2	2.0	0.2	-1.1	0.1	-2.6	0.1	-11.9	-3.5
15-Mar-06	7.7	0.4	3.8	0.2	2.1	0.2	-1.1	0.1	-2.6	0.1	-9.2	-3.9
16-Mar-06	7.7	0.4	3.8	0.2	2.0	0.2	-1.1	0.1	-2.7	0.1	-9.5	-3.9
17-Mar-06	7.8	0.4	3.8	0.2	2.1	0.2	-1.0	0.1	-2.6	0.1	-5.7	-3.4
18-Mar-06	7.7	0.4	3.8	0.2	2.0	0.2	-1.1	0.1	-2.6	0.1	-7.4	-3.0
19-Mar-06	7.6	0.3	3.8	0.2	2.0	0.2	-1.1	0.1	-2.5	0.0	-8.3	-2.9

20-Mar-06	7.9	0.4	3.9	0.2	2.1	0.2	-1.0	0.1	-2.3	0.0	-4.3	-2.5
21-Mar-06	7.8	0.4	3.9	0.2	2.2	0.2	-1.0	0.1	-2.3	0.0	-3.6	-2.4
22-Mar-06	7.6	0.5	3.7	0.2	1.9	0.2	-1.2	0.0	-2.3	0.1	-3.2	-1.1
23-Mar-06	7.7	0.5	3.8	0.2	2.1	0.2	-1.0	0.1	-2.1	0.0	-4.1	-1.8
24-Mar-06	7.8	0.5	3.9	0.2	2.1	0.2	-0.9	0.0	-2.0	0.0	-2.4	-1.6
25-Mar-06	7.8	0.5	3.9	0.2	2.2	0.2	-0.9	0.0	-1.9	0.0	0.6	-0.8
26-Mar-06	7.9	0.4	3.9	0.2	2.2	0.2	-0.9	0.0	-1.8	0.1	2.0	0.0
27-Mar-06	7.7	0.4	4.0	0.2	2.2	0.2	-0.9	0.0	-1.6	0.0	3.1	0.5
28-Mar-06	7.6	0.4	3.9	0.2	2.1	0.2	-0.9	0.0	-1.6	0.1	1.2	1.2
29-Mar-06	7.5	0.3	3.9	0.2	2.1	0.2	-0.9	0.0	-1.6	0.0	-0.2	0.1
30-Mar-06	7.5	0.3	3.8	0.2	2.1	0.2	-0.9	0.0	-1.5	0.0	2.8	2.0
31-Mar-06	7.5	0.3	3.8	0.2	2.1	0.2	-1.0	0.0	-1.5	0.1	0.5	1.6
1-Apr-06	7.5	0.3	3.8	0.2	2.1	0.2	-0.9	0.0	-1.4	0.1	1.0	2.3
2-Apr-06	7.6	0.3	3.9	0.2	2.2	0.2	-0.8	0.0	-1.3	0.1	2.0	1.8
3-Apr-06	7.5	0.3	3.9	0.2	2.2	0.2	-0.8	0.0	-1.2	0.1	6.3	4.7
4-Apr-06	7.5	0.3	3.8	0.2	2.2	0.2	-0.8	0.0	-1.2	0.1	6.1	5.5
5-Apr-06	7.4	0.3	3.8	0.2	2.1	0.2	-0.8	0.0	-1.1	0.0	6.0	5.8
6-Apr-06	7.3	0.2	3.7	0.2	2.1	0.2	-0.8	0.0	-1.1	0.1	5.9	4.7
7-Apr-06	7.3	0.2	3.6	0.2	2.0	0.2	-0.8	0.0	-0.9	0.2	8.1	6.8
8-Apr-06	7.3	0.3	3.7	0.2	2.1	0.2	-0.7	0.0	-0.4	0.4	6.8	6.6
9-Apr-06	7.2	0.3	3.7	0.2	2.0	0.2	-0.8	0.0	-0.1	0.5	7.1	6.8
10-Apr-06	7.3	0.3	3.7	0.2	2.1	0.2	-0.7	0.1	0.3	0.6	9.1	8.2
11-Apr-06	7.4	0.2	3.8	0.2	2.2	0.2	-0.6	0.1	0.8	0.6	9.8	8.3
12-Apr-06	7.3	0.1	3.7	0.2	2.1	0.2	-0.7	0.1	1.1	0.5	9.1	7.7
13-Apr-06	7.0	0.2	3.7	0.2	2.1	0.2	-0.6	0.1	1.3	0.5	8.0	7.8
14-Apr-06	7.1	0.2	3.7	0.2	2.1	0.2	-0.6	0.1	1.7	0.5	11.3	9.4
15-Apr-06	7.0	0.2	3.6	0.2	2.0	0.2	-0.7	0.1	2.0	0.5	5.2	6.9
16-Apr-06	6.6	0.5	3.6	0.2	2.1	0.2	-0.5	0.1	1.7	0.3	1.3	3.0
17-Apr-06	6.9	0.3	3.7	0.2	2.2	0.2	-0.4	0.1	1.1	0.2	5.5	4.9
18-Apr-06	7.0	0.2	3.6	0.2	2.2	0.2	-0.4	0.1	1.4	0.3	9.0	7.8
19-Apr-06	7.0	0.2	3.6	0.2	2.2	0.2	-0.4	0.1	2.0	0.3	10.1	8.7
20-Apr-06	7.0	0.2	3.7	0.2	2.3	0.2	-0.2	0.1	3.1	0.3	15.0	12.6
21-Apr-06	7.0	0.2	3.6	0.2	2.2	0.2	0.3	0.3	4.7	0.4	15.5	14.0
22-Apr-06	7.0	0.2	3.7	0.2	2.4	0.2	1.3	0.4	5.7	0.4	4.0	7.6
23-Apr-06	7.1	0.2	3.9	0.2	2.7	0.2	2.1	0.4	4.9	0.3	8.2	8.9
24-Apr-06	7.3	0.1	4.1	0.2	3.1	0.2	2.8	0.4	5.3	0.3	3.1	5.1
28-Apr-06	7.1	0.2	4.5	0.2	3.8	0.3	4.6	0.3	8.6	0.4	13.2	14.7
29-Apr-06	7.5	0.2	4.9	0.2	4.3	0.3	5.2	0.3	9.3	0.3	15.1	15.5
30-Apr-06	7.7	0.2	5.1	0.2	4.7	0.3	5.9	0.3	9.8	0.2	8.1	10.3
1-May-06	7.9	0.2	5.5	0.2	5.2	0.3	6.6	0.3	9.1	0.2	8.7	9.6
2-May-06	8.0	0.2	5.7	0.2	5.5	0.3	6.8	0.3	8.6	0.2	3.5	7.4
3-May-06	8.3	0.3	6.1	0.2	5.9	0.3	7.0	0.3	7.8	0.2	5.9	8.9
4-May-06	8.5	0.2	6.6	0.2	6.4	0.3	7.2	0.2	7.9	0.1	12.6	10.9
5-May-06	8.8	0.2	7.0	0.2	6.8	0.2	7.3	0.2	9.0	0.2	18.6	15.7

6-May-06	8.9	0.2	7.1	0.2	6.9	0.2	7.5	0.2	10.2	0.2	10.3	12.5
7-May-06	9.2	0.2	7.5	0.2	7.3	0.2	8.1	0.2	10.2	0.1	12.5	12.8
8-May-06	9.3	0.2	7.7	0.2	7.5	0.2	8.4	0.2	10.2	0.1	5.3	8.5
9-May-06	9.4	0.2	7.9	0.2	7.8	0.2	8.6	0.2	9.1	0.2	6.5	6.6
10-May-06	9.8	0.2	8.3	0.2	8.2	0.2	8.7	0.2	8.7	0.1	12.1	12.1
11-May-06	10.1	0.2	8.6	0.2	8.4	0.2	8.7	0.2	9.8	0.1	13.5	13.9
12-May-06	10.3	0.1	8.8	0.2	8.6	0.2	8.9	0.2	10.7	0.1	11.5	12.8
13-May-06	10.4	0.1	9.2	0.2	9.0	0.2	9.4	0.2	10.9	0.1	11.9	13.3
14-May-06	10.7	0.2	9.5	0.2	9.2	0.2	9.7	0.2	11.6	0.1	15.8	14.9
15-May-06	10.9	0.2	9.7	0.2	9.5	0.2	10.1	0.2	12.9	0.2	19.4	17.2
16-May-06	11.3	0.1	10.0	0.2	9.8	0.2	10.7	0.2	14.3	0.2	21.2	19.1
16-May-06	11.5	0.2	10.4	0.2	10.3	0.2	11.5	0.3	15.8	0.3	25.1	21.0
18-May-06	11.5	0.2	10.6	0.2	10.5	0.2	12.1	0.3	17.1	0.4	22.5	21.4
19-May-06	11.7	0.2	10.8	0.2	10.9	0.2	13.0	0.3	18.1	0.4	18.8	19.9
20-May-06	12.0	0.2	11.1	0.2	11.3	0.3	13.8	0.4	18.4	0.6	12.6	17.5
21-May-06	12.4	0.2	11.6	0.3	12.0	0.3	14.7	0.6	18.0	0.9	16.6	17.7
22-May-06	12.6	0.3	12.1	0.3	12.6	0.3	15.4	0.9	18.9	0.9	18.8	20.4
23-May-06	12.7	0.3	12.4	0.3	13.0	0.4	16.1	1.1	19.8	0.7	15.8	18.2
24-May-06	13.2	0.3	13.0	0.3	13.8	0.5	16.9	0.9	19.1	0.5	13.0	15.4
25-May-06	13.7	0.2	13.6	0.4	14.5	0.5	17.3	0.9	18.3	0.5	10.0	11.6
26-May-06	14.2	0.2	14.2	0.4	15.1	0.6	17.7	0.9	17.8	0.5	7.8	8.2
27-May-06	14.6	0.3	14.8	0.5	15.6	0.6	17.7	0.7	17.5	0.5	10.1	10.8
28-May-06	15.0	0.3	15.3	0.5	16.0	0.5	18.3	0.8	17.3	0.3	9.8	10.5
29-May-06	15.3	0.3	15.7	0.5	16.5	0.5	19.0	0.7	17.4	0.3	12.3	12.5
30-May-06	15.7	0.3	16.3	0.5	17.1	0.5	19.3	0.6	17.7	0.3	14.8	14.3
31-May-06	16.4	0.3	17.0	0.5	17.8	0.5	19.4	0.5	17.9	0.2	19.4	17.6

Table F.9. Site 1 Moisture Content Results

Date	Location	Average Vol. MC ($L \cdot L^{-1}$)	SE ($L \cdot L^{-1}$)
21-Nov-05	55	0.30	0.050
21-Nov-05	90	0.27	0.013
21-Nov-05	125	0.36	0.082
25-Nov-05	20	0.15	0.019
25-Nov-05	55	0.29	0.022
25-Nov-05	90	0.26	0.008
25-Nov-05	125	0.34	0.035
9-Dec-05	20	0.16	0.021
9-Dec-05	55	0.27	0.019
9-Dec-05	90	0.26	0.012
9-Dec-05	125	0.33	0.031
24-Jan-06	20	0.21	0.044
24-Jan-06	55	0.22	0.030
24-Jan-06	90	0.25	0.008
24-Jan-06	125	0.32	0.026
6-Mar-06	20	0.22	0.035
6-Mar-06	55	0.26	0.017
6-Mar-06	90	0.26	0.012
6-Mar-06	125	0.32	0.026
21-Mar-06	20	0.29	0.046
21-Mar-06	55	0.24	0.019
21-Mar-06	90	0.26	0.012
21-Mar-06	125	0.31	0.023
24-Apr-06	20	0.24	0.028
24-Apr-06	55	0.27	0.023
24-Apr-06	90	0.27	0.022
24-Apr-06	125	0.33	0.039
31-May-06	20	0.16	0.044
31-May-06	55	0.28	0.034
31-May-06	90	0.33	0.037
31-May-06	125	0.28	0.052

Table F.10. Site 2 Moisture Content Results

Year	Day	Port	Average Vol. MC ($L \cdot L^{-1}$)	SE ($L \cdot L^{-1}$)
2005	238	20	0.695	0.12
2005	238	125	0.501	-
2005	238	55	0.346	0.04
2005	238	90	0.805	0.13
2005	239	20	0.794	0.15
2005	239	125	0.494	0.10
2005	239	55	0.390	0.08
2005	239	90	0.650	0.13
2005	240	20	0.787	0.15
2005	240	125	0.551	-
2005	240	55	0.339	0.03
2005	240	90	0.906	0.12
2005	241	20	0.788	0.15
2005	241	125	0.391	0.27
2005	241	55	0.343	0.03
2005	241	90	0.820	0.16
2005	242	20	0.780	0.14
2005	242	125	0.382	0.26
2005	242	55	0.403	0.05
2005	242	90	0.766	0.17
2005	243	20	0.788	0.14
2005	243	125	0.689	0.06
2005	243	55	0.376	0.03
2005	243	90	0.775	0.14
2005	244	20	0.736	0.14
2005	244	125	0.465	0.29
2005	244	55	0.362	0.04
2005	244	90	0.838	0.11
2005	245	20	0.759	0.13
2005	245	125	0.426	0.32
2005	245	55	0.442	0.07
2005	245	90	0.768	0.11
2005	246	20	0.783	0.13
2005	246	125	0.505	0.08
2005	246	125	0.665	-
2005	246	55	0.422	0.04
2005	246	90	0.487	0.05
2005	247	20	0.747	0.14
2005	247	125	0.563	0.10
2005	247	55	0.434	0.04
2005	247	90	0.485	0.06
2005	249	20	0.654	0.11
2005	250	20	0.658	0.10
2005	251	20	0.725	0.13
2005	257	20	0.609	0.11
2005	258	20	0.599	0.10
2005	258	125	0.535	0.09
2005	258	55	0.404	0.03
2005	258	90	0.463	0.05
2005	259	20	0.539	0.08
2005	259	125	0.526	0.09
2005	259	55	0.408	0.03
2005	259	90	0.456	0.05
2005	260	20	0.554	0.10
2005	260	125	0.501	0.10
2005	260	55	0.416	0.03
2005	260	90	0.457	0.04
2005	261	20	0.565	0.08
2005	261	125	0.541	0.11
2005	261	55	0.402	0.03
2005	261	90	0.448	0.04
2005	262	20	0.597	0.09
2005	262	125	0.494	0.09
2005	262	55	0.403	0.03
2005	262	90	0.450	0.05
2005	263	20	0.595	0.09

2005	263	125	0.515	0.11
2005	263	55	0.403	0.03
2005	263	90	0.452	0.04
2005	264	20	0.613	0.10
2005	264	125	0.526	0.10
2005	264	55	0.410	0.03
2005	264	90	0.456	0.04
2005	265	20	0.604	0.13
2005	265	125	0.542	0.09
2005	265	55	0.409	0.03
2005	265	90	0.461	0.05
2005	266	20	0.603	0.10
2005	266	125	0.588	0.11
2005	266	55	0.432	0.04
2005	266	90	0.469	0.05
2005	267	20	0.627	0.10
2005	267	125	0.552	0.10
2005	267	55	0.429	0.04
2005	267	90	0.488	0.06
2005	268	20	0.603	0.09
2005	268	125	0.568	0.10
2005	268	55	0.422	0.03
2005	268	90	0.480	0.05
2005	269	20	0.568	0.08
2005	269	125	0.546	0.11
2005	269	55	0.415	0.03
2005	269	90	0.471	0.05
2005	270	20	0.637	0.11
2005	270	125	0.584	0.11
2005	270	55	0.427	0.03
2005	270	90	0.483	0.05
2005	271	20	0.597	0.09
2005	271	125	0.575	0.10
2005	271	55	0.450	0.04
2005	271	90	0.494	0.05
2005	272	20	0.585	0.09
2005	272	125	0.561	0.12
2005	272	55	0.438	0.04
2005	272	90	0.495	0.05
2005	273	20	0.607	0.11
2005	273	125	0.554	0.10
2005	273	55	0.433	0.04
2005	273	90	0.489	0.05
2005	274	20	0.590	0.10
2005	274	125	0.544	0.09
2005	274	55	0.442	0.04
2005	274	90	0.502	0.05
2005	275	20	0.549	0.11
2005	275	125	0.577	0.12
2005	275	55	0.440	0.04
2005	275	90	0.496	0.05
2005	276	20	0.510	0.08
2005	276	125	0.539	0.10
2005	276	55	0.426	0.03
2005	276	90	0.476	0.05
2005	277	20	0.497	0.08
2005	277	125	0.501	0.08
2005	277	55	0.414	0.03
2005	277	90	0.458	0.05
2005	278	20	0.501	0.10
2005	278	125	0.516	0.09
2005	278	55	0.409	0.03
2005	278	90	0.443	0.04
2005	279	20	0.506	0.15
2005	279	125	0.501	0.09
2005	279	55	0.393	0.03
2005	279	90	0.453	0.04
2005	280	20	0.503	0.09
2005	280	125	0.508	0.10
2005	280	55	0.393	0.02
2005	280	90	0.449	0.04
2005	281	20	0.493	0.08

2005	281	125	0.492	0.09
2005	281	55	0.391	0.03
2005	281	90	0.451	0.05
2005	282	20	0.465	0.06
2005	282	125	0.492	0.09
2005	282	55	0.394	0.03
2005	282	90	0.449	0.05
2005	283	20	0.489	0.07
2005	283	125	0.488	0.08
2005	283	55	0.387	0.02
2005	283	90	0.439	0.04
2005	284	20	0.492	0.08
2005	284	125	0.497	0.09
2005	284	55	0.385	0.02
2005	284	90	0.451	0.04
2005	285	20	0.498	0.09
2005	285	125	0.488	0.09
2005	285	55	0.384	0.02
2005	285	90	0.446	0.04
2005	286	20	0.473	0.08
2005	286	125	0.478	0.08
2005	286	55	0.380	0.02
2005	286	90	0.438	0.04
2005	287	20	0.462	0.08
2005	287	125	0.470	0.08
2005	287	55	0.377	0.02
2005	287	90	0.436	0.04
2005	288	20	0.455	0.07
2005	288	125	0.474	0.08
2005	288	55	0.378	0.02
2005	288	90	0.438	0.04
2005	289	20	0.437	0.07
2005	289	125	0.476	0.09
2005	289	55	0.377	0.02
2005	289	90	0.435	0.04
2005	290	20	0.427	0.07
2005	290	125	0.477	0.09
2005	290	55	0.377	0.02
2005	290	90	0.441	0.04
2005	291	20	0.416	0.07
2005	291	125	0.491	0.10
2005	291	55	0.379	0.02
2005	291	90	0.437	0.04
2005	292	20	0.403	0.07
2005	292	125	0.470	0.09
2005	292	55	0.372	0.02
2005	292	90	0.429	0.03
2005	293	20	0.391	0.07
2005	293	125	0.459	0.08
2005	293	55	0.370	0.02
2005	293	90	0.423	0.03
2005	294	20	0.371	0.06
2005	294	125	0.463	0.08
2005	294	55	0.370	0.02
2005	294	90	0.423	0.04
2005	295	20	0.377	0.06
2005	295	125	0.470	0.09
2005	295	55	0.373	0.02
2005	295	90	0.421	0.03
2005	296	20	0.379	0.07
2005	296	125	0.472	0.09
2005	296	55	0.373	0.02
2005	296	90	0.428	0.04
2005	297	20	0.378	0.07
2005	297	125	0.466	0.08
2005	297	55	0.373	0.02
2005	297	90	0.427	0.04
2005	298	20	0.370	0.07
2005	298	125	0.471	0.09
2005	298	55	0.372	0.02
2005	298	90	0.429	0.03
2005	326	20	0.567	0.14

2005	326	125	0.800	0.13
2005	326	55	0.374	0.02
2005	326	90	0.406	0.03
2005	327	20	0.587	0.14
2005	327	125	0.858	0.19
2005	327	55	0.384	0.02
2005	327	90	0.422	0.03
2005	328	20	0.581	0.14
2005	328	125	0.861	0.19
2005	328	55	0.383	0.02
2005	328	90	0.416	0.03
2005	329	20	0.423	0.07
2005	329	125	0.593	0.04
2005	329	55	0.395	0.01
2005	329	90	0.434	0.03
2005	330	20	0.250	0.03
2005	330	125	0.427	0.07
2005	330	55	0.442	0.01
2005	330	90	0.667	0.15
2005	331	20	0.233	0.02
2005	331	125	0.419	0.07
2005	331	55	0.420	0.03
2005	331	90	0.550	0.00
2005	332	20	0.230	0.03
2005	332	125	0.434	0.07
2005	332	55	0.445	0.00
2005	332	90	0.534	0.03
2005	333	20	0.245	0.03
2005	333	125	0.416	0.06
2005	333	55	0.408	-
2005	333	90	0.544	0.01
2005	334	20	0.253	0.03
2005	334	125	0.432	0.08
2005	334	55	0.451	0.01
2005	334	90	0.521	0.00
2005	335	20	0.248	0.04
2005	335	125	0.440	0.08
2005	335	55	0.453	0.06
2005	335	90	0.552	0.02
2005	336	20	0.290	0.05
2005	336	125	0.429	0.09
2005	337	20	0.232	0.03
2005	337	125	0.438	0.09
2005	337	55	0.465	0.01
2005	337	90	0.516	0.09
2005	338	20	0.223	0.02
2005	338	125	0.444	0.08
2005	338	55	0.447	0.02
2005	338	90	0.563	0.04
2005	339	20	0.308	0.09
2005	339	55	1.128	-
2005	340	20	0.220	0.02
2005	340	125	0.434	0.08
2005	340	55	0.443	0.01
2005	340	90	0.654	0.14
2005	341	20	0.229	0.03
2005	341	125	0.431	0.07
2005	341	55	0.486	0.03
2005	341	90	0.518	0.03
2005	342	20	0.220	0.02
2005	342	125	0.403	0.06
2005	342	55	0.447	0.00
2005	342	90	0.511	0.00
2005	343	20	0.530	0.13
2005	343	125	0.829	0.20
2005	343	90	0.404	0.04
2005	343	55	0.381	0.04
2005	344	20	0.524	0.13
2005	344	125	0.839	0.18
2005	344	55	0.387	0.03
2005	344	90	0.401	0.05
2005	345	20	0.535	0.13

2005	345	125	0.841	0.20
2005	345	55	0.380	0.02
2005	345	90	0.400	0.03
2005	346	20	0.545	0.13
2005	346	125	0.837	0.19
2005	346	55	0.376	0.02
2005	346	90	0.399	0.05
2005	347	20	0.537	0.13
2005	347	125	0.707	0.19
2005	347	55	0.381	0.02
2005	347	90	0.395	0.03
2005	348	20	0.532	0.13
2005	348	125	0.831	0.18
2005	348	55	0.380	0.02
2005	348	90	0.395	0.03
2005	349	20	0.541	0.14
2005	349	125	0.842	0.20
2005	349	55	0.395	0.02
2005	349	90	0.399	0.03
2005	350	20	0.530	0.13
2005	350	125	0.850	0.20
2005	350	55	0.398	0.02
2005	350	90	0.397	0.04
2005	351	20	0.520	0.14
2005	351	125	0.823	0.19
2005	351	55	0.394	0.02
2005	351	90	0.402	0.04
2005	352	20	0.539	0.13
2005	352	125	0.838	0.19
2005	352	55	0.381	0.02
2005	352	90	0.371	0.03
2005	353	20	0.536	0.13
2005	353	125	0.809	0.19
2005	353	55	0.381	0.02
2005	353	90	0.379	0.03
2005	354	20	0.542	0.13
2005	355	20	0.535	0.12
2005	355	125	0.783	0.18
2005	355	55	0.354	0.02
2005	355	90	0.345	0.02
2005	356	20	0.494	0.16
2005	356	125	0.805	0.17
2005	356	55	0.381	0.02
2005	356	90	0.355	0.02
2005	357	20	0.533	0.13
2005	357	125	0.802	0.18
2005	357	55	0.376	0.02
2005	357	90	0.368	0.03
2005	358	20	0.532	0.13
2005	358	125	0.850	0.21
2005	358	55	0.378	0.02
2005	358	90	0.365	0.03
2005	359	20	0.551	0.13
2005	359	125	0.801	0.18
2005	359	55	0.383	0.01
2005	359	90	0.362	0.02
2005	360	20	0.533	0.14
2005	360	125	0.795	0.17
2005	360	55	0.378	0.02
2005	360	90	0.365	0.02
2005	361	20	0.549	0.13
2005	361	125	0.833	0.21
2005	361	55	0.376	0.02
2005	361	90	0.369	0.03
2005	362	20	0.544	0.14
2005	362	125	0.801	0.17
2005	362	55	0.380	0.02
2005	362	90	0.374	0.03
2005	363	20	0.538	0.13
2005	363	125	0.797	0.18
2005	363	55	0.372	0.02
2005	363	90	0.372	0.03

2005	364	20	0.532	0.13
2005	364	125	0.798	0.18
2005	364	55	0.379	0.02
2005	364	90	0.362	0.03
2005	365	20	0.532	0.13
2005	365	125	0.794	0.18
2005	365	55	0.381	0.02
2005	365	90	0.368	0.03
2006	1	20	0.537	0.13
2006	1	125	0.793	0.18
2006	1	55	0.374	0.02
2006	1	90	0.363	0.02
2006	2	20	0.536	0.13
2006	2	125	0.795	0.18
2006	2	55	0.372	0.02
2006	2	90	0.364	0.03
2006	3	20	0.519	0.13
2006	3	125	0.802	0.18
2006	3	55	0.373	0.02
2006	3	90	0.360	0.02
2006	4	20	0.522	0.13
2006	4	125	0.787	0.17
2006	4	55	0.368	0.02
2006	4	90	0.365	0.03
2006	5	20	0.519	0.13
2006	5	125	0.780	0.17
2006	5	55	0.368	0.01
2006	5	90	0.357	0.03
2006	6	20	0.521	0.12
2006	6	125	0.787	0.18
2006	6	55	0.370	0.02
2006	6	90	0.363	0.02
2006	7	20	0.526	0.12
2006	7	125	0.792	0.18
2006	7	55	0.380	0.02
2006	7	90	0.367	0.02
2006	8	20	0.523	0.13
2006	8	125	0.806	0.18
2006	8	55	0.374	0.02
2006	8	90	0.370	0.03
2006	9	20	0.522	0.13
2006	9	125	0.799	0.18
2006	9	55	0.372	0.02
2006	9	90	0.360	0.02
2006	10	20	0.522	0.12
2006	10	125	0.824	0.19
2006	10	55	0.377	0.02
2006	10	90	0.364	0.03
2006	11	20	0.515	0.12
2006	11	125	0.786	0.18
2006	11	55	0.373	0.02
2006	11	90	0.361	0.02
2006	12	20	0.511	0.12
2006	12	125	0.789	0.18
2006	12	55	0.338	0.02
2006	12	90	0.360	0.02
2006	13	20	0.511	0.12
2006	13	125	0.787	0.17
2006	13	55	0.376	0.02
2006	13	90	0.359	0.02
2006	14	20	0.507	0.12
2006	14	125	0.787	0.18
2006	14	55	0.376	0.02
2006	14	90	0.359	0.03
2006	15	20	0.514	0.12
2006	15	125	0.839	0.23
2006	15	55	0.368	0.02
2006	15	90	0.357	0.02
2006	16	20	0.516	0.12
2006	16	125	0.790	0.18
2006	16	55	0.372	0.02
2006	16	90	0.736	0.19

2006	17	20	0.519	0.12
2006	17	125	0.788	0.18
2006	17	55	0.375	0.02
2006	17	90	0.354	0.02
2006	18	20	0.519	0.12
2006	18	125	0.773	0.17
2006	18	55	0.372	0.02
2006	18	90	0.354	0.02
2006	19	20	0.520	0.12
2006	19	125	0.787	0.18
2006	19	55	0.371	0.02
2006	19	90	0.355	0.02
2006	20	20	0.521	0.12
2006	20	125	0.783	0.18
2006	20	55	0.362	0.02
2006	20	90	0.350	0.02
2006	21	20	0.520	0.12
2006	21	125	0.777	0.17
2006	21	55	0.356	0.02
2006	21	90	0.350	0.02
2006	22	20	0.531	0.13
2006	22	125	0.778	0.18
2006	22	55	0.373	0.02
2006	22	90	0.355	0.02
2006	66	20	0.520	0.13
2006	66	125	0.807	0.21
2006	66	55	0.371	0.01
2006	66	90	0.347	0.02
2006	67	20	0.524	0.13
2006	67	125	0.802	0.20
2006	67	55	0.370	0.01
2006	67	90	0.347	0.02
2006	68	20	0.516	0.13
2006	68	125	0.785	0.20
2006	68	55	0.381	0.01
2006	68	90	0.339	0.02
2006	69	20	0.516	0.13
2006	69	125	0.786	0.20
2006	69	55	0.375	0.02
2006	69	90	0.344	0.02
2006	70	20	0.516	0.13
2006	70	125	0.790	0.20
2006	70	55	0.387	0.02
2006	70	90	0.345	0.02
2006	71	20	0.559	0.16
2006	71	125	0.821	0.22
2006	71	55	0.381	0.02
2006	71	90	0.335	0.03
2006	72	20	0.549	0.15
2006	72	125	0.825	0.18
2006	72	55	0.374	0.02
2006	72	90	0.349	0.02
2006	73	20	0.566	0.16
2006	73	125	0.828	0.21
2006	73	55	0.390	0.02
2006	73	90	0.347	0.02
2006	74	20	0.650	0.07
2006	74	125	0.638	0.24
2006	74	55	0.372	0.02
2006	74	90	0.357	0.03
2006	75	20	0.524	0.13
2006	75	125	0.659	0.18
2006	75	55	0.395	0.02
2006	75	90	0.351	0.02
2006	76	20	0.523	0.13
2006	76	125	0.779	0.19
2006	76	55	0.379	0.02
2006	76	90	0.348	0.02
2006	77	20	0.525	0.14
2006	77	125	0.787	0.20
2006	77	55	0.379	0.02
2006	77	90	0.347	0.03

2006	78	20	0.566	0.17
2006	78	125	0.795	0.20
2006	78	55	0.405	0.03
2006	78	90	0.366	0.03
2006	79	20	0.548	0.16
2006	79	125	0.789	0.19
2006	79	55	0.364	0.03
2006	79	90	0.404	0.03
2006	81	20	0.209	0.02
2006	81	125	0.439	0.12
2006	81	55	0.475	0.06
2006	81	90	0.445	0.04
2006	82	20	0.215	0.03
2006	82	125	0.433	0.12
2006	82	55	0.468	0.06
2006	82	90	0.469	0.05
2006	83	20	0.226	0.04
2006	83	125	0.448	0.11
2006	83	55	0.545	0.19
2006	83	90	0.510	0.06
2006	84	20	0.215	0.03
2006	84	125	0.452	0.12
2006	84	55	0.465	0.07
2006	84	90	0.460	0.04
2006	85	20	0.217	0.03
2006	85	125	0.455	0.12
2006	85	55	0.492	0.09
2006	85	90	0.461	0.04
2006	86	20	0.209	0.02
2006	86	125	0.450	0.12
2006	86	55	0.479	0.06
2006	86	90	0.460	0.03
2006	87	20	0.212	0.02
2006	87	125	0.444	0.10
2006	87	55	0.449	0.03
2006	87	90	0.466	0.03
2006	88	20	0.208	0.02
2006	88	125	0.415	0.09
2006	88	55	0.465	0.08
2006	88	90	0.460	0.06
2006	89	20	0.211	0.02
2006	89	125	0.435	0.10
2006	89	55	0.483	0.07
2006	89	90	0.466	0.06
2006	90	20	0.212	0.02
2006	90	125	0.437	0.10
2006	90	55	0.473	0.05
2006	90	90	0.457	0.04
2006	91	20	0.206	0.02
2006	91	125	0.436	0.09
2006	91	55	0.456	0.03
2006	91	90	0.466	0.04
2006	92	20	0.212	0.02
2006	92	125	0.466	0.12
2006	92	55	0.477	0.06
2006	92	90	0.471	0.04
2006	93	20	0.212	0.02
2006	93	125	0.441	0.09
2006	93	55	0.474	0.04
2006	93	90	0.475	0.06
2006	94	20	0.222	0.03
2006	94	125	0.442	0.10
2006	94	55	0.471	0.11
2006	94	90	0.479	0.03
2006	95	20	0.221	0.02
2006	95	125	0.444	0.10
2006	95	55	0.481	0.07
2006	95	90	0.466	0.03
2006	96	20	0.224	0.02
2006	96	125	0.435	0.11
2006	96	55	0.471	0.06
2006	96	90	0.458	0.06

2006	97	20	0.231	0.02
2006	97	125	0.447	0.10
2006	97	55	0.473	0.07
2006	97	90	0.468	0.04
2006	98	20	0.222	0.02
2006	98	125	0.439	0.10
2006	98	55	0.479	0.06
2006	98	90	0.487	0.02
2006	99	20	0.229	0.02
2006	99	125	0.434	0.09
2006	99	55	0.481	0.04
2006	99	90	0.483	0.03
2006	100	20	0.212	0.03
2006	100	125	0.441	0.08
2006	100	55	0.533	0.12
2006	100	90	0.468	0.02
2006	101	20	0.224	0.02
2006	101	125	0.435	0.09
2006	101	55	0.476	0.05
2006	101	90	0.503	0.04
2006	102	20	0.230	0.02
2006	102	125	0.452	0.11
2006	102	55	0.461	0.03
2006	102	90	0.479	0.04
2006	103	20	0.222	0.01
2006	103	125	0.431	0.09
2006	103	55	0.481	0.05
2006	103	90	0.508	0.06
2006	104	20	0.215	0.01
2006	104	125	0.440	0.09
2006	104	55	0.517	0.08
2006	104	90	0.510	0.04
2006	105	20	0.215	0.02
2006	105	125	0.447	0.09
2006	105	55	0.493	0.10
2006	105	90	0.498	0.04
2006	106	20	0.210	0.02
2006	106	125	0.466	0.09
2006	106	55	0.493	0.08
2006	106	90	0.520	0.02
2006	107	20	0.210	0.02
2006	107	125	0.479	0.11
2006	107	55	0.522	0.09
2006	107	90	0.491	0.04
2006	108	20	0.212	0.02
2006	108	125	0.474	0.10
2006	108	55	0.512	0.07
2006	108	90	0.473	0.00
2006	109	20	0.228	0.03
2006	109	125	0.474	0.10
2006	109	55	0.547	0.14
2006	109	90	0.533	0.05
2006	110	20	0.224	0.02
2006	110	125	0.487	0.13
2006	110	55	0.578	0.16
2006	110	90	0.563	0.08
2006	111	20	0.233	0.03
2006	111	125	0.469	0.09
2006	111	55	0.504	0.05
2006	111	90	0.513	0.02
2006	112	20	0.209	0.03
2006	112	125	0.429	0.08
2006	112	55	0.526	0.11
2006	112	90	0.539	0.08
2006	113	20	0.191	0.02
2006	113	125	0.503	0.12
2006	113	55	0.545	0.17
2006	113	90	0.525	0.03
2006	114	20	0.524	0.13
2006	114	125	0.747	0.25
2006	114	55	0.477	0.04
2006	114	90	0.419	0.02

2006	115	20	0.539	0.13
2006	115	125	0.767	0.21
2006	115	55	0.480	0.04
2006	115	90	0.427	0.03
2006	116	20	0.527	0.12
2006	116	125	0.755	0.22
2006	116	55	0.494	0.05
2006	116	90	0.444	0.04
2006	117	20	0.487	0.12
2006	117	125	0.742	0.23
2006	117	55	0.446	0.03
2006	117	90	0.431	0.03
2006	118	20	0.492	0.12
2006	118	125	0.744	0.22
2006	118	55	0.501	0.05
2006	118	90	0.452	0.04
2006	119	20	0.501	0.12
2006	119	125	0.767	0.23
2006	119	55	0.468	0.03
2006	119	90	0.436	0.03
2006	120	20	0.483	0.11
2006	120	125	0.732	0.25
2006	120	55	0.448	0.04
2006	120	90	0.450	0.03
2006	121	20	0.492	0.12
2006	121	125	0.777	0.22
2006	121	55	0.494	0.04
2006	121	90	0.450	0.04
2006	122	20	0.487	0.12
2006	122	125	0.763	0.23
2006	122	55	0.480	0.04
2006	122	90	0.465	0.04
2006	123	20	0.479	0.11
2006	123	125	0.778	0.21
2006	123	55	0.490	0.04
2006	123	90	0.464	0.03
2006	124	20	0.512	0.12
2006	124	125	0.802	0.21
2006	124	55	0.494	0.06
2006	124	90	0.425	0.03
2006	125	20	0.540	0.10
2006	125	125	0.825	0.17
2006	125	55	0.565	0.10
2006	125	90	0.536	0.07
2006	126	20	0.496	0.12
2006	126	125	0.770	0.22
2006	126	55	0.487	0.04
2006	126	90	0.441	0.03
2006	127	20	0.481	0.12
2006	127	125	0.758	0.23
2006	127	55	0.509	0.05
2006	127	90	0.428	0.02
2006	128	20	0.478	0.12
2006	128	125	0.751	0.21
2006	128	55	0.494	0.05
2006	128	90	0.423	0.03
2006	129	20	0.470	0.12
2006	129	125	0.767	0.22
2006	129	55	0.482	0.04
2006	129	90	0.454	0.04
2006	130	20	0.466	0.12
2006	130	125	0.738	0.21
2006	130	55	0.493	0.04
2006	130	90	0.419	0.03
2006	131	20	0.491	0.12
2006	131	125	0.738	0.23
2006	131	55	0.502	0.04
2006	131	90	0.419	0.03
2006	132	20	0.493	0.12
2006	132	125	0.742	0.21
2006	132	55	0.468	0.04
2006	132	90	0.396	0.02

2006	133	20	0.482	0.12
2006	133	125	0.749	0.21
2006	133	55	0.471	0.03
2006	133	90	0.421	0.03
2006	134	20	0.483	0.12
2006	134	125	0.779	0.21
2006	134	55	0.492	0.04
2006	134	90	0.427	0.04
2006	135	20	0.509	0.12
2006	135	125	0.776	0.18
2006	135	55	0.617	0.08
2006	135	90	0.480	0.05
2006	136	20	0.502	0.12
2006	136	125	0.760	0.19
2006	136	55	0.529	0.05
2006	136	90	0.451	0.05
2006	137	20	0.499	0.13
2006	137	125	0.726	0.20
2006	137	55	0.563	0.08
2006	137	90	0.439	0.03
2006	138	20	0.535	0.11
2006	138	125	0.794	0.18
2006	138	55	0.458	0.04
2006	138	90	0.446	0.03
2006	139	20	0.496	0.13
2006	139	125	0.746	0.19
2006	139	55	0.593	0.07
2006	139	90	0.515	0.06
2006	140	20	0.483	0.12
2006	140	125	0.734	0.21
2006	140	55	0.494	0.03
2006	140	90	0.453	0.04
2006	141	20	0.484	0.12
2006	141	125	0.755	0.18
2006	141	55	0.526	0.05
2006	141	90	0.471	0.04
2006	142	20	0.512	0.07
2006	142	125	0.739	0.22
2006	142	55	0.429	0.04
2006	142	90	0.464	0.03
2006	143	20	0.479	0.12
2006	143	125	0.747	0.20
2006	143	55	0.498	0.04
2006	143	90	0.463	0.03
2006	144	20	0.474	0.11
2006	144	125	0.757	0.19
2006	144	55	0.515	0.05
2006	144	90	0.437	0.03
2006	145	20	0.504	0.12
2006	145	125	0.784	0.23
2006	145	55	0.571	0.07
2006	145	90	0.483	0.03
2006	146	20	0.499	0.12
2006	146	125	0.791	0.24
2006	146	55	0.547	0.07
2006	146	90	0.441	0.02
2006	147	20	0.493	0.12
2006	147	125	0.785	0.23
2006	147	55	0.525	0.05
2006	147	90	0.422	0.02
2006	148	20	0.495	0.12
2006	148	125	0.816	0.20
2006	148	55	0.524	0.04
2006	148	90	0.423	0.03
2006	149	20	0.499	0.12
2006	149	125	0.775	0.20
2006	149	55	0.525	0.05
2006	149	90	0.428	0.03
2006	150	20	0.484	0.12
2006	150	125	0.760	0.22
2006	150	55	0.511	0.04
2006	150	90	0.439	0.03

2006	152	20	0.492	0.13
2006	152	125	0.799	0.17
2006	152	55	0.506	0.05
2006	152	90	0.481	0.04
2006	153	20	0.530	0.10
2006	153	125	0.829	0.21
2006	153	55	0.523	0.06
2006	153	90	0.450	0.03
2006	154	20	0.480	0.13
2006	154	125	0.744	0.20
2006	154	55	0.569	0.09
2006	154	90	0.474	0.04
2006	155	20	0.480	0.13
2006	155	125	0.796	0.21
2006	155	55	0.536	0.06
2006	155	90	0.442	0.02
2006	156	20	0.485	0.12
2006	156	125	0.799	0.18
2006	156	55	0.470	0.04
2006	156	90	0.457	0.04
2006	157	20	0.477	0.12
2006	157	125	0.796	0.18
2006	157	55	0.517	0.04
2006	157	90	0.459	0.05
2006	158	20	0.470	0.12
2006	158	125	0.787	0.19
2006	158	55	0.494	0.06
2006	158	90	0.466	0.04
2006	159	20	0.458	0.18
2006	159	125	0.778	0.20
2006	159	55	0.530	0.05
2006	159	90	0.438	0.03
2006	160	20	0.494	0.12
2006	160	125	0.769	0.20
2006	160	55	0.515	0.05
2006	160	90	0.452	0.03
2006	161	20	0.497	0.12
2006	161	125	0.789	0.20
2006	161	55	0.526	0.05
2006	161	90	0.439	0.04
2006	162	20	0.485	0.12
2006	162	125	0.806	0.15
2006	162	55	0.519	0.06
2006	162	90	0.420	0.03
2006	163	20	0.491	0.12
2006	163	125	0.827	0.16
2006	163	55	0.498	0.04
2006	163	90	0.436	0.03
2006	164	20	0.532	0.13
2006	164	125	0.980	0.10
2006	164	55	0.539	0.07
2006	164	90	0.455	0.04
2006	165	20	0.493	0.12
2006	165	125	0.824	0.20
2006	165	55	0.529	0.06
2006	165	90	0.449	0.04
2006	166	20	0.503	0.12
2006	166	125	0.798	0.20
2006	166	55	0.527	0.07
2006	166	90	0.434	0.03
2006	167	20	0.530	0.14
2006	167	125	0.833	0.20
2006	167	55	0.653	0.08
2006	167	90	0.456	0.04
2006	168	20	0.522	0.14
2006	168	125	0.854	0.15
2006	168	55	0.635	0.08
2006	168	90	0.449	0.03
2006	169	20	0.539	0.15
2006	169	125	0.882	0.15
2006	169	55	0.649	0.08
2006	169	90	0.449	0.04

2006	170	20	0.589	0.14
2006	170	125	1.119	-
2006	170	55	0.663	0.08
2006	170	90	0.452	0.04
2006	171	20	0.538	0.14
2006	171	125	0.841	0.15
2006	171	55	0.640	0.08
2006	171	90	0.441	0.03
2006	172	20	0.519	0.13
2006	172	125	0.870	0.21
2006	172	55	0.592	0.06
2006	172	90	0.439	0.04
2006	173	20	0.515	0.13
2006	173	125	0.919	0.18
2006	173	55	0.512	0.05
2006	173	90	0.435	0.04
2006	174	20	0.501	0.13
2006	174	125	0.811	0.21
2006	174	55	0.615	0.08
2006	174	90	0.422	0.04
2006	175	20	0.500	0.14
2006	175	125	0.884	0.19
2006	175	55	0.551	0.06
2006	175	90	0.424	0.03
2006	176	20	0.491	0.13
2006	176	125	0.867	0.17
2006	176	55	0.620	0.08
2006	176	90	0.416	0.04
2006	177	20	0.508	0.10
2006	177	125	0.909	0.19
2006	177	55	0.560	0.05
2006	177	90	0.454	0.05
2006	178	20	0.507	0.10
2006	178	125	0.886	0.15
2006	178	55	0.598	0.07
2006	178	90	0.465	0.05
2006	179	20	0.515	0.08
2006	179	125	0.947	0.12
2006	179	55	0.628	0.07
2006	179	90	0.438	0.03
2006	180	20	0.515	0.08
2006	180	125	0.999	0.06
2006	180	55	0.608	0.06
2006	180	90	0.440	0.05
2006	181	20	0.507	0.09
2006	181	125	0.970	0.20
2006	181	55	0.662	0.09
2006	181	90	0.467	0.05
2006	182	20	0.463	0.13
2006	182	125	0.949	0.16
2006	182	55	0.609	0.07
2006	182	90	0.444	0.04
2006	183	20	0.497	0.08
2006	183	125	0.919	0.18
2006	183	55	0.621	0.07
2006	183	90	0.451	0.05
2006	184	20	0.458	0.12
2006	184	125	0.879	0.20
2006	184	55	0.634	0.08
2006	184	90	0.427	0.03
2006	185	20	0.492	0.08
2006	185	125	0.849	0.17
2006	185	55	0.604	0.06
2006	185	90	0.418	0.03
2006	186	20	0.504	0.09
2006	186	125	0.840	0.20
2006	186	55	0.640	0.06
2006	186	90	0.433	0.04

Table F.11. Site 3 Moisture Content Results

Date	Quadrant	Depth /Vol. MC ($L \cdot L^{-1}$)			
		15	30	45	60
21-Nov-05	AB	0.33	0.26	0.32	0.37
21-Nov-05	AC	0.31	0.24	0.28	0.34
21-Nov-05	CD	0.32	0.26	0.31	0.37
21-Nov-05	BD	0.29	0.30	0.30	0.38
25-Nov-05	AB	0.31	0.26	0.32	0.36
25-Nov-05	AC	0.29	0.24	0.28	0.34
25-Nov-05	CD	0.31	0.26	0.33	0.34
25-Nov-05	BD	0.30	0.29	0.30	0.36
9-Dec-05	AB	0.17	0.20	0.32	0.37
9-Dec-05	AC	0.19	0.21	0.27	0.36
9-Dec-05	CD	0.20	0.23	0.33	0.39
9-Dec-05	BD	0.18	0.24	0.31	0.36
24-Jan-06	AB	0.16	0.16	0.25	0.32
24-Jan-06	AC	0.16	0.16	0.24	0.31
24-Jan-06	CD	0.18	0.16	0.25	0.27
24-Jan-06	BD	0.15	0.17	0.24	0.31
28-Feb-06	AB	0.15	0.14	0.22	0.29
28-Feb-06	AC	0.18	0.14	0.21	0.30
28-Feb-06	CD	0.16	0.14	0.24	0.27
28-Feb-06	BD	0.15	0.16	0.21	0.29
21-Mar-06	AB	0.17	0.16	0.24	0.29
21-Mar-06	AC	0.17	0.15	0.21	0.28
21-Mar-06	CD	0.18	0.17	0.26	0.29
21-Mar-06	BD	0.15	0.23	0.23	0.29